



Agenzia Nazionale per le Nuove Tecnologie,  
l'Energia e lo Sviluppo Economico Sostenibile



*Ministero dello Sviluppo Economico*

## RICERCA DI SISTEMA ELETTRICO

Valutazione delle caratteristiche di codici di termoidraulica di nocciolo ai fini delle analisi di sicurezza: Stato dell'arte dei codici di termoidraulica di nocciolo

*M. Adorni, W. Ambrosini, D. Araneo, M. Cherubini, E. Coscarelli, F. D'Auria,  
E. Molfese, F. Terzuoli*



VALUTAZIONE DELLE CARATTERISTICHE DI CODICI DI TERMOIDRAULICA DI NOCCIOLO AI  
FILI DELLE ANALISI DI SICUREZZA: STATO DELL'ARTE DEI CODICI DI TERMOIDRAULICA DI  
NOCCIOLO

M. Adorni, W. Ambrosini, D. Araneo, M. Cherubini, E. Coscarelli, F. D'Auria, E. Molfese, F.  
Terzuoli (Università di Pisa)

Novembre 2011

Report Ricerca di Sistema Elettrico

Accordo di Programma Ministero dello Sviluppo Economico – ENEA

Area: Governo, gestione e sviluppo del sistema elettrico nazionale

Progetto: Fissione nucleare: metodi di analisi e verifica di progetti nucleari di generazione  
evolutiva ad acqua pressurizzata

Responsabile Progetto: Massimo Sepielli, ENEA

**Titolo**

**Valutazione delle caratteristiche di codici di termoidraulica di nocciolo ai fini delle analisi di sicurezza:**  
**Stato dell'arte dei codici di termoidraulica di nocciolo**

**Ente emittente** CIRTEN – Università di Pisa - GRNSPG

## PAGINA DI GUARDIA

**Descrittori**
**Tipologia del documento:**

**Collocazione contrattuale:** ACCORDO DI PROGRAMMA Ministero dello Sviluppo Economico – ENEA sulla Ricerca di Sistema Elettrico PIANO ANNUALE DI REALIZZAZIONE 2010 Progetto 1.3.2.a: Fissione nucleare: Metodi di analisi e verifica di progetti nucleari di generazione evolutiva ad acqua pressurizzata.

**Argomenti trattati:** Termoidraulica del nocciolo, Reattori nucleari ad acqua, Software

**Sommario**

Questo report è stato preparato al fine di documentare le attività realizzate nell'ambito della sezione D1 del PAR2010. Esso contiene un esame dello stato dell'arte dei più importanti codici per l'analisi di sicurezza delle centrali nucleari. La rassegna include una descrizione generale di diversi tipi di codici di termoidraulica: codici di sistema, codici di sottocanale e codici di CFD, e anche dei più comuni codici di cinetica neutronica tridimensionale.

Particolare attenzione è stata data nel presentare diversi esempi di attività svolte sull'accoppiamento tra codici, aspetto cruciale per un'analisi di sicurezza delle centrali nucleari completa e accurata. Negli ultimi decenni, è stato compiuto a livello mondiale un notevole sforzo di ricerca sulle problematiche dell'accoppiamento. Nessun codice, può infatti, da solo, trattare tutti i fenomeni inerenti al campo della sicurezza nucleare. Per questo motivo, codici differenti, ciascuno applicabile in un diverso ambito tecnologico, sono necessari per realizzare l'analisi di sicurezza.

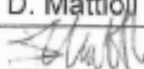
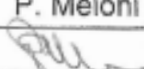
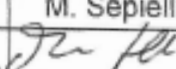
**Note**

Allegato C al Deliverable PAR2010-CIRTEN-LD1-028

Riferimento: CERSE-UNUPI RL 1503/2011

Autori: E. Molfese, M. Adorni, D. Araneo, M. Cherubini, E. Coscarelli, F. Terzuoli, F. D'Auria, W. Ambrosini

**Copia n.**
**In carico a:**

2			NOME			
			FIRMA			
1			NOME			
			FIRMA			
0	EMISSIONE	05/12/11	NOME	D. Mattioli	P. Meloni	M. Sepielli
			FIRMA			
REV.	DESCRIZIONE	DATA	CONVALIDA	VISTO	APPROVAZIONE	





**CIRTEN**

**Consorzio Interuniversitario per la Ricerca TEcnologica Nucleare**

**UNIVERSITÀ DI PISA**

**Gruppo di Ricerca Nucleare San Piero a Grado**

**Dipartimento di Ingegneria Meccanica Nucleare e della Produzione**

**VALUTAZIONE DELLE CARATTERISTICHE DI  
CODICI DI TERMOIDRAULICA DI NOCCIOLO AI FINI  
DELLE ANALISI DI SICUREZZA:  
Stato dell'arte dei codici di termoidraulica di nocciolo**

**Autori**

**Eugenio Molfese  
Martina Adorni  
Dino Araneo  
Marco Cherubini  
Eugenio Coscarelli  
Fulvio Terzuoli  
Francesco D'Auria  
Walter Ambrosini**

**CERSE-UNIPI RL 1503/2011**

**PISA, Novembre 2011**

Lavoro svolto in esecuzione dell'Obiettivo 4.1 Attività D1  
AdP MSE-ENEA sulla Ricerca di Sistema Elettrico- Piano Annuale di Realizzazione 2010  
Progetto 1.3.2.a "Fissione nucleare: Metodi di analisi e verifica di progetti nucleari di  
generazione evolutiva alimentati ad acqua pressurizzata"



## Sommario

Questo report è stato preparato al fine di documentare le attività realizzate nell'ambito della sezione D1 del PAR2010. Esso contiene un esame dello stato dell'arte dei più importanti codici per l'analisi di sicurezza delle centrali nucleari. La rassegna include una descrizione generale di diversi tipi di codici di termoidraulica: codici di sistema, codici di sottocanale e codici di CFD, e anche dei più comuni codici di cinetica neutronica tridimensionale.

Particolare attenzione è stata data nel presentare diversi esempi di attività svolte sull'accoppiamento tra codici, aspetto cruciale per un'analisi di sicurezza delle centrali nucleari completa e accurata. Negli ultimi decenni, è stato compiuto a livello mondiale un notevole sforzo di ricerca sulle problematiche dell'accoppiamento. Nessun codice, può infatti, da solo, trattare tutti i fenomeni inerenti al campo della sicurezza nucleare. Per questo motivo, codici differenti, ciascuno applicabile in un diverso ambito tecnologico, sono necessari per realizzare l'analisi di sicurezza.

## **Abstract**

The report is prepared to document the activities performed in the framework of the PAR2010 section D1. It consists in a review on the state-of-the-art of the most important codes used for the safety analysis of nuclear power plants. The report includes a general description of several kinds of thermal-hydraulics codes, system codes, sub-channel codes and CFD codes, and also the most common 3D neutron kinetic codes.

Special attention is devoted to present different examples of activities performed on the coupling of codes, crucial issue for a complete and accurate safety analysis of the nuclear power plants. In the last decades, a considerable worldwide effort was spent on coupling issues. No single code is capable of covering all phenomena involved in the nuclear safety field. Therefore, different codes for different technological fields are required to perform the safety analysis.



# Table of content

<b>LIST OF FIGURES .....</b>	<b>9</b>
<b>LIST OF TABLES .....</b>	<b>11</b>
<b>LIST OF ABBREVIATIONS.....</b>	<b>12</b>
<b>1. INTRODUCTION.....</b>	<b>13</b>
<b>2. SHORT REVIEW OF THE STATE-OF-THE-ART OF THE THERMAL-HYDRAULIC CODES .....</b>	<b>15</b>
2.1 Introduction .....	15
2.2 Physical Modeling in present nuclear thermal-hydraulic codes.....	16
2.3 System codes .....	17
2.3.1 RELAP5/MOD3 .....	20
2.3.1.1 Generalities.....	20
2.3.1.2 Hydrodynamic model.....	22
2.3.2 TRACE v5 .....	32
2.3.3 ATHLET Mod 2.2 Cycle A.....	39
2.3.3.1 Overview.....	39
2.3.3.2 Code structure .....	39
2.3.3.3 Fluid-dynamics .....	40
2.3.3.4 Code handling.....	44
2.3.4 CATHARE-2 V2.5 .....	46
2.3.4.1 Code structure and models .....	46
2.3.5 MARS.....	50
2.3.5.1 Development of MARS3.0.....	50
2.4 Sub-channel codes .....	53
2.4.1 COBRA-EN.....	53
2.4.2 VIPRE-W.....	56
2.4.3 FLICA-OVAP .....	57
2.5 Computational Fluid-Dynamics (CFD) codes.....	59
2.5.1 The Role of CFD Codes in Nuclear Reactor Safety Analyses .....	59
2.5.1.1 Identification of NRS issues requiring CFD.....	59
2.5.1.2 State-of-the-art in CFD Quality Assurance.....	61
2.5.2 Introduction to CFD Techniques .....	63
2.5.2.1 Numerical Models.....	63
2.5.2.2 Examples of Reynolds-Averaged Navier-Stokes equations .....	64

2.5.2.3	<i>Discretization</i> .....	66
2.5.3	ANSYS CFX Code.....	67
2.5.4	ANSYS FLUENT Code .....	69
2.5.5	Cd-Adapco STAR-CCM+ .....	71
2.5.6	NEPTUNE CFD Code.....	73
2.5.7	Code_Saturne.....	74
2.5.8	OpenFoam Code .....	75
<b>3.</b>	<b>COUPLING WITH NEUTRONIC AND THERMAL-MECHANIC CODES .....</b>	<b>77</b>
3.1	Some considerations related to the coupling between thermal-hydraulic and neutronic nodes	79
3.2	Neutron kinetics codes .....	83
3.2.1	DYN3D.....	83
3.2.2	NEM .....	84
3.2.3	NESTLE .....	84
3.2.4	PARCS.....	84
3.2.5	QUABOX .....	85
3.2.6	Transport codes.....	85
3.2.7	Monte Carlo Method .....	86
3.3	Results and experiences of coupled neutronic/T-H codes.....	87
3.3.1	ATHLET-QUABOX/CUBBOX [93].....	90
3.3.2	RELAP5/PANBOX [97] .....	92
3.3.3	Code-to-code comparison for the PWR MSLB Benchmark [90].....	96
3.3.4	TRAC-PF1/NEM [94] .....	98
3.3.5	HELIOS-NESTLE.....	101
3.3.6	CFX – Relap5/3D (Nestle) .....	102
3.3.7	Relap5/3D – ANSYS.....	105
3.3.8	Relap5/3D – CFX – Ansys .....	106
3.3.9	Relap5/3D – TRANSURANUS .....	107
<b>4.</b>	<b>CONCLUDING REMARKS .....</b>	<b>111</b>
	<b>REFERENCES .....</b>	<b>113</b>

# List of Figures

Figure 2-1. Diagram showing the logic of the thermal-hydraulic system codes [16]..... 18

Figure 2-2. RELAP5 top level structure..... 20

Figure 2-3. Modular structures of transient calculations in RELAP5..... 21

Figure 2-4. Transient/steady-state block structure ..... 21

Figure 2-5. Schematic of difference equation nodalization [8]..... 26

Figure 2-6. RELAP5 boiling and condensing curves..... 30

Figure 2-7. Scheme of a sub-channel and fuel rod [37] ..... 53

Figure 2-8. Fuel rod mesh [37]..... 55

Figure 2-9. Heat flux as function of superheat [37] ..... 55

Figure 2-10. Types of elements..... 66

Figure 2-11. Definition of finite control volumes from nodes and elements (2D example)..... 67

Figure 3-1. CASL Virtual Reactor vision [79]..... 78

Figure 3-2. Scheme of the coupling between PARCS and RELAP5 [3] ..... 79

Figure 3-3. Exchange of parameters for internal, external and parallel coupling [91] ..... 81

Figure 3-4. ATHLET nodalization scheme for MSLB Benchmark [93] ..... 89

Figure 3-5. Comparison of maximum fuel temperature for different mapping schemes [93] ..... 91

Figure 3-6. Comparison of ATHLET-QUABBOX/CUBBOX calculation with respect to point kinetics transient [93] ..... 92

Figure 3-7. Flow logic for coupling of RELAP5 with PANBOX using EUMOD[97]..... 93

Figure 3-8. Core average moderator temperature (BE and RP case) 117[97] ..... 94

Figure 3-9. Predicted total core power (BE and RP case) 117[97] ..... 94

Figure 3-10. 2D coolant temperature distribution at plane z=3.14 m for BE case [97]..... 94

Figure 3-11. 2D coolant temperature distribution at plane z=3.14 (node=27) for RP-case [97] ..... 95

Figure 3-12. Comparison of total power as predicted by point kinetic of RELAP5 and the coupled code RELAP5/PANBOX [97]..... 95

Figure 3-13. Code-to-code comparison for the average coolant temperature for BE scenario [90] .. 97

Figure 3-14. Code-to-code comparison for the broken loop hot leg temperature for BE scenario [90] ..... 97

Figure 3-15. Code-to-code comparison for the broken cold leg temperature for BE scenario [90] .. 98

Figure 3-16. Radial thermal-hydraulic/heat structure coupling scheme for TRAC-PF1/NEM core model with 67 rods [94] ..... 99

Figure 3-17. Power evolution during REA transient for HFP at EOC predicted by TRAC-PF1/NEM [94]..... 100

Figure 3-18. Text file containing CFD results for a given instant [104]..... 103

Figure 3-19. GUI of the VB routine [104] ..... 103

Figure 3-20. Output file from CFD data processing, containing time history of boron mass in each macro-cell [104]..... 104

Figure 3-21. RELAP/3D to ANSYS temperature transfer[104] .....	105
Figure 3-22. Temperature transfer in FE model [104] .....	106
Figure 3-23. RELAP5/3D - CFX coupling technique [104] .....	106
Figure 3-24. Temperature distribution at the wall-fluid interface at t = 200 s [104] .....	107
Figure 3-25. Roadmap of code connections for the TRANSURANUS code [106] .....	108

# List of Tables

Table 2-1. NRS issues needing CFD [52] ..... 60

Table 3-1. Overview of 3-D coupled neutronics/thermal-hydraulics calculations available from the literature [33] ..... 87

Table 3-2. List of participants in Phase III of the PWR MSLB Benchmark [87] ..... 96

Table 3-3. Comparison of the ejected rod worth predicted by the three models [91] ..... 100

## List of abbreviations

ATWS	Anticipated transient without scram
BE	Best-estimate
BWR	Boiling water reactor
CHF	Critical heat flux
CL	Cold leg
ECCS	Emergency core cooling system
GRSNPG	San Piero a Grado Nuclear Research Group
GRS	Gesellschaft für Anlagen- und Reaktorsicherheit mbH
IET	Integral Effect Test (facility)
OECD	Organization for Economic Co-operation and Development
LBLOCA	Large break loss of coolant accident
MSLB	Main steam line break
NEA	Nuclear Energy Agency
NK	Neutron kinetics
NPP	Nuclear power plant
OTSG	Once-through steam generator
PTS	Pressurized thermal shock
PWR	Pressurized water reactor
RANS	Reynolds averaged Navier-Stokes equations
REA	Rod ejection accident
RMBK	Boiling water cooled/graphite moderated (Russian reactor)
SBLOCA	Small break loss of coolant accident
SET	Separate Effect Test (facility)
SG	Steam generator
SGTR	Steam generator tube rupture
T-H	Thermal-hydraulics
THC	Thermal-hydraulic channel
UNIPI	University of Pisa
VVER	<i>See</i> WWER
WWER	Water-cooled Water-moderated Energy Reactor

# 1. Introduction

Reactor core thermal-hydraulics had a considerable development in the last decades, owing to the increasing interest assigned by the scientific community to the development of better qualified and more accurate models for nuclear reactor safety applications.

In addition to the classical system codes, whose role is quite relevant in deterministic analyses of reactor behavior, especially in connection with the evaluation of code uncertainties, present trends in model development include multi-scale and multi-physics approaches. These approaches imply an increasing role of computational fluid-dynamic tools and of multidisciplinary competences in coupling codes which tackle different physical problems at different scales.

Indeed, the evaluation of core dynamics represents a field of active development and application aimed at setting up and assessing tools capable to integrate capabilities for coupled analysis of thermal-hydraulic, neutronic and stress-and-strain phenomena. A considerable effort in this aim was spent in the framework of international projects as ECORA [2], CRISSUE-S [3], NURESIM [4] and NURISP [5], to mention just a few of the important initiatives that took recently place in the field. Different research institutions have been involved in such studies and, in particular, the Nuclear Research Group in San Piero a Grado of the University of Pisa (GRNSPG) is actively involved in validating and applying different codes to safety analysis of nuclear power plants.

This report is aimed at providing a short overview of the state-of-the-art in the field, highlighting relevant upcoming trends, without the pretence to be exhaustive. Indeed, a comprehensive review of the matter would require a broader and more in depth analysis of code capabilities; it is anyway believed that the material reported herein provides a general perspective about the most widespread modeling techniques, ranging from system codes, through sub-channel programs, to the more recent CFD applications. Attention is also devoted to the work performed in the coupling of codes conceived for different physical phenomena (e.g., thermal-hydraulic and neutronic analyses) or different scales of detail (e.g., system codes and CFD codes).

The list of relevant literature works included at the end of the report will provide the reader with suggestions for a more in depth analysis of the material produced worldwide in this field.





## **2. Short review of the state-of-the-art of the thermal-hydraulic codes**

### **2.1 Introduction**

There is probably no other field of engineering which depends so strongly on “numerical process simulation” as nuclear technology. This is mainly due to the difficulties of executing full-scale safety related experiments and to the absence of simplified scaling laws for the governing processes which would allow a direct transfer of results from small scale test facilities to the full size plant [6].

For this reason, the development of more and more reliable codes able to assess the safety of nuclear power plants (NPPs) is a key goal. In fact, the evaluation of the safety of NPPs is closely related to the ability to determine the temporal and spatial distributions of the flow field T-H conditions along with associated effects from heat sources and heat sinks throughout the reactor coolant system and especially in the core region. On the basis of different objectives and levels of sophistication, the T-H analyses are performed with either a conservative or a best-estimate (BE) approach.

The conservative approach has traditionally been used for the licensing analyses, being part of a NPP’s commissioning activities and has to be submitted to and approved by the regulatory authority. However, in those analyses the safety margins obtained are expected to be conservatively large, as certain T-H phenomena as well as certain plant and system features are not credited, and besides, it should be noted that the conservative approach does not provide any indications as to the true safety margins nor does it provide a true simulation of a specified scenario[7].

In the BE analyses the T-H phenomena are simulated as accurately as possible (according to present knowledge) and the safety margins obtained more closely reflect the real margins in the plant. This type of analyses also provides more realistic simulations of the NPP behavior during the course of the transient scenarios and can consequently reveal detailed system information that can be relevant for the understanding of T-H phenomena interaction. If BE analyses are used for licensing purposes, they must be accompanied by uncertainty analyses to quantify the uncertainty of calculated parameters. The uncertainty includes contributions from simplifications introduced both into the governing equations and to the constitutive relationships and models, but also from using such models outside their original ranges of validity.

In order to meet high-priority needs related to flow analysis (fuel performance, DNB evaluation, T/H related to interactions with metallic structures, thermal shocks due to safety coolant injection, etc.), calculations of the steady state and transient single-phase and two-phase flow and heat transfer behavior are required around the whole circuit and especially in the core. The fundamental requirement for such calculations is a knowledge of the local flows and qualities, and this can only be achieved by using codes (“system codes”) , which describe the

whole system. In specific parts of the circuit, more detailed calculations are required using component or CFD codes (these codes use output information from the system code as external input data).

## 2.2 Physical Modeling in present nuclear thermal-hydraulic codes

Nearly all current two-phase flow models used in present “best estimate” thermal hydraulic system codes are based on the “two-fluid model”. Phases are treated as interpenetrating continua and “macroscopic” separate balance equations for each phase are obtained by a space and/or time or ensemble averaging of the local instantaneous basic flow equations, with source terms representing the interfacial transfers for mass, momentum and energy. Due to the averaging, information on local flow processes, in particular at the interface separating the two phases or at the region near the walls, is lost and has to be compensated by additional modeling. All thermal-hydraulic codes can be partitioned into three categories: system codes, component codes and CFD codes.

**System codes** have demonstrated the capability to adequately predict a large variety of off-normal and accidental transients, as has been shown by exhaustive code verification and assessment programs as conducted in the last decades. Nevertheless, one should not forget that good agreement with experimental integral test facilities is not always free of specific code tuning and compensating errors.

Several **sub-channel codes** exist for a more detailed description of some component such as a Core, a Steam-Generator or a Heat Exchanger (condenser). They use 3-D two-phase models for porous medium with an homogenization technique. Compared to system codes, sub-channel, or component, codes aim at a finer 3-D description of the component in a smaller range of flow conditions. When used in such a smaller range of flow conditions, a simplified set of equations may be used (3-equations or 4 equation models) but more effort was put to the modeling of turbulence, of spacer grids effects, and to the formulation of wall friction and interfacial friction (or drift flux model) able to take into account the non-isotropy of the porous medium.

Just recently, **CFD codes** have been used for nuclear design and safety analyses. CFD codes are currently used for single-phase turbulent flows and for some two-phase flows (mainly for dispersed flows), as they are able to provide detailed three-dimensional flow simulations for general purpose applications. Although they can provide a high spatial resolution of local two-phase flow processes it must be emphasized that also CFD codes require some empirical closure relations (however, the degree of empiricism is lower than for more macroscopic models).

## 2.3 System codes

Originally based on different assumptions and equation formulations, the T-H system computer codes generally used, e.g. RELAP5, TRAC, TRACE, ATHLET, CATHARE, are today being developed to have rather similar bases and capabilities. They are now based on governing equations representing the transient, non-homogeneous, non-equilibrium, two-phase flow including heat transfer processes from present solid heat structures like the fuel rods, piping and RPV wall structures, as well as internal support structure components. The associated two-fluid, two-phase flow model is formulated from the spatial and time-averaged conservation equations for mass, energy and momentum of the two basic phases (liquid, vapor) with allowances for soluble components in the liquid phase and non-condensable components in the vapor phase.

Due to the averaging process, all information concerning the local flow processes is lost, like the time fluctuating turbulence contributions. Thus, these effects have to be re-established by means of proper models based on the available averaged properties of the two-fluid model. However, such re-established models can only approximately simulate true behavior; especially when considering the two-phase flow with a large variation in the distribution of interfacial area and its volumetric concentration.

Constitutive relationships, usually in the form of empirical algebraic expressions, are used to describe wall friction, heat transfer and inter-phase drag and mass transfer with interfacial area concentration based on the rather static flow regime maps. As these models are based on direct or indirect information emerging from various types of experiments, they also have implicitly incorporated allowances for the turbulence and other micro-scale conditions that prevailed in the performed experiments.

The codes' two-phase models are essentially 1-D, although most codes have various capabilities to, at least in an approximate way, simulate basic 3-D flow field conditions. In this context it is also realized that, although applying the available 3-D capabilities of the codes, the T-H phenomena are still modeled using basically 1-D assumptions. Thus the multi-dimensionality of the flow field can possibly be simulated only to a certain degree and even then the influence of this multi-dimensionality on predicted phenomena is not taken into account when applying the empirical models, apart from adjustments of pertinent flow velocities.

Despite all codes use a similar set of basic governing differential equations to describe the two-fluid, two-phase model, differences among them exist and can affect the solution strategy. For instance, RELAP5 uses a single pressure for the liquid, vapor, and interface, resulting in elliptic characteristics (i.e. the characteristic equations have imaginary roots) while CATHARE uses a slightly different approach, in which interfacial pressure is systematically different from the pressure of the two phases, so that the equation system always has hyperbolic characteristics (i.e. the characteristic equations always have positive roots).

The numerical models used when solving the governing equations are based on first order finite volume donor cell schemes with "staggered meshes", meaning that the momentum computational cells are displaced half a cell length relative to the mass and energy cells. Various degrees of implicitness in the time domain can be introduced to mitigate the need of using a

sound speed (pressure pulse propagative) based Courant limit for numerical stability. In fact, RELAP5 makes mainly use of a semi-implicit method which requires a material-based Courant limit for stability, i.e. a bulk velocity limit [9][1], but implicitness can also be carried further as is done with TRAC's Stability Enhanced Two-step (SETS) method, which requires no such restrictions for stability. In similarity, anyway, RELAP5 is equipped with a nearly-implicit numerical scheme, introducing a sufficient degree of implicitness to allow for the use of Courant numbers much greater than unity. To mention a further approach, CATHARE is using a fully implicit technique that is intrinsically unconditionally stable.

Due to the numerical approximations and the empirical nature of the models included in the T-H system codes, extensive activities related to validation of the code models have been pursued over the years. At present, a fairly well-based experience has been established as concerns the codes' capability to simulate the T-H conditions prevailing during various time windows in specified transient scenarios. This experience has been collected in the codes' manual sets, for instance the User's Guide [10] and the User's Guidelines [11] of the RELAP5 manuals and the User's Manual [13] of the ATHLET code, resulting in recommendations about how adequately nodalize various parts of the reactor coolant system to get acceptable simulations.

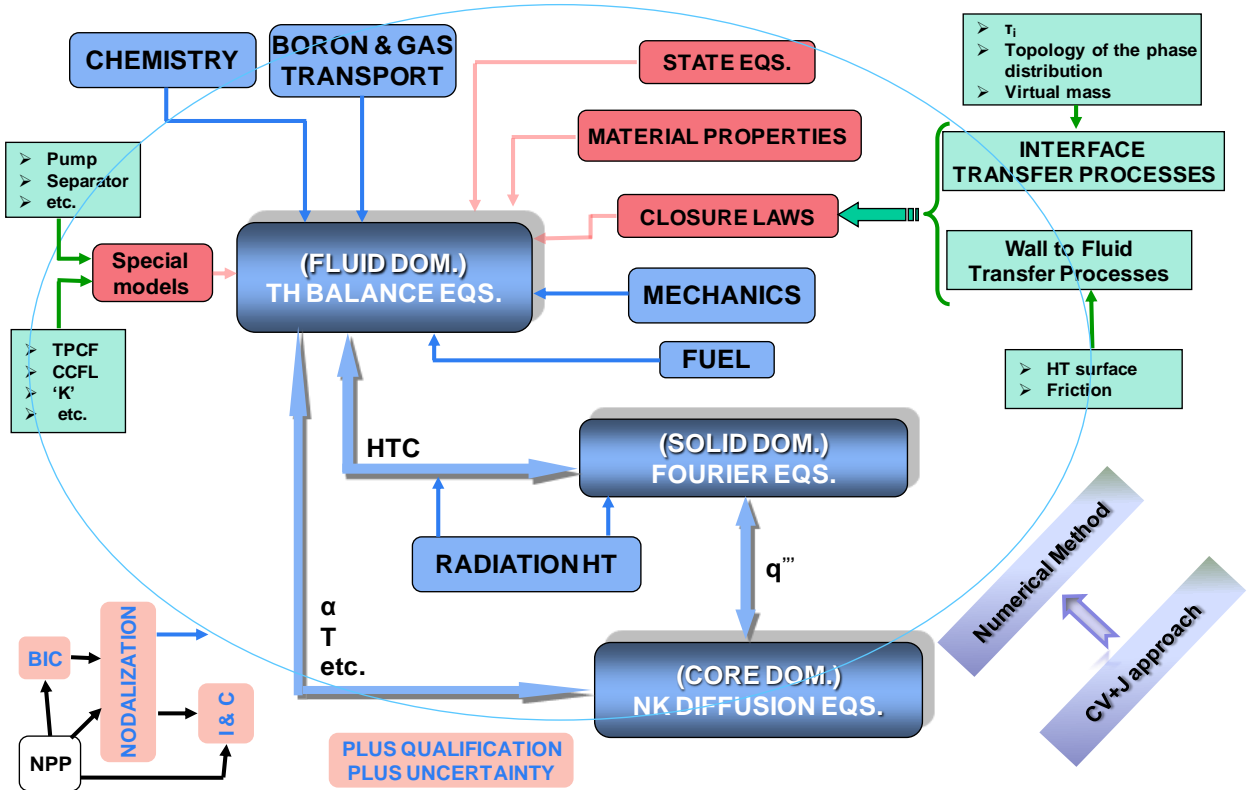


Figure 2-1. Diagram showing the logic of the thermal-hydraulic system codes [16]

Validation has partly been accomplished using experimental data from specially-designed, scaled-down test facilities simulating major components of a complete reactor system. From these integral effect tests (IETs) [17] information can be found regarding the interaction between different parts of the system and their associated influences on the T-H condition and distribution. Another stage of the validation was constituted by the separate effect tests (SETs)

[18], which are conducted at full- or close-to-full-scale with well-defined boundary conditions. These tests are devoted to investigating specific T-H phenomena or to the behavior of single components (pumps, valves, tee junctions, etc.), and provide additional validation information. Transient data from real NPPs were also important due to the full scale and true geometry, although such data could only reveal conditions for fairly mild transients (operational transients, start-up and commissioning tests). Notwithstanding the considerable validation efforts pursued over the years, there are still areas of code applications that reveal limited experiences, e.g. transients for which pressure wave propagation effects are important and for which profound 3-D and recirculating flow formations occur in certain parts of a system.

Hereafter, the T-H system codes that are commonly used within the nuclear safety community are presented.

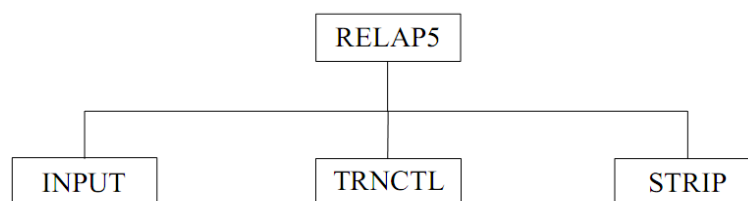
## 2.3.1 RELAP5/MOD3

### 2.3.1.1 Generalities

RELAP5 (Reactor Excursion and Leak Analysis Program) is a light water reactor transient analysis code developed for the U.S. Nuclear Regulatory Commission (NRC) for use in rulemaking, licensing audit calculations, evaluation of operator guidelines, and as a basis for a nuclear plant analyzer. A specific field of its application includes simulations of transients in LWR systems, such as loss of coolant, anticipated transients without scram (ATWS), and operational transients such as loss of feed water, loss of offsite power, station blackout, and turbine trip. Nevertheless, RELAP5 is a highly generic code that, in addition to calculating the behavior of a reactor coolant system during a transient, can be used for simulation of a wide variety of hydraulic and thermal transients in both nuclear and nonnuclear systems involving mixtures of steam, water, non-condensable, and solute [8].

RELAP5 is coded in a modular fashion using top-down structuring. The various models and procedures are isolated in separate subroutines. The top level structure, shown in Figure 2-2, consists of input (INPUT), transient/steady-state (TRNCTL), and stripping (STRIP) blocks. The input block (INPUT) processes input, checks input data, and prepares required data blocks for all program options. The transient/steady-state block (TRNCTL) handles both transient and the steady-state options. The steady-state option determines the steady-state conditions by running an accelerated transient (it artificially accelerates heat conduction by reducing the thermal capacity of the conductors) until the time derivatives approach zero. Instead, if the transient technique alone is used, approach to steady state from an initial condition would be identical to a plant transient from that initial condition. Pressures, densities, and flow distributions would adjust quickly, but thermal effects would occur more slowly.

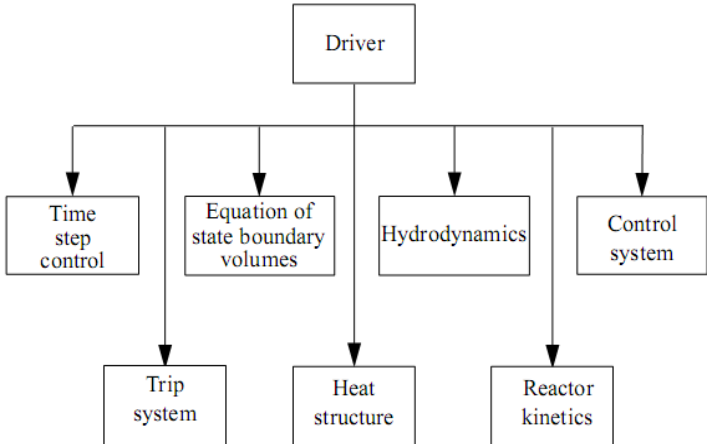
Finally, the strip block (STRIP) extracts simulation data from a restart plot file for convenient passing of RELAP5 simulation results to other computer programs.



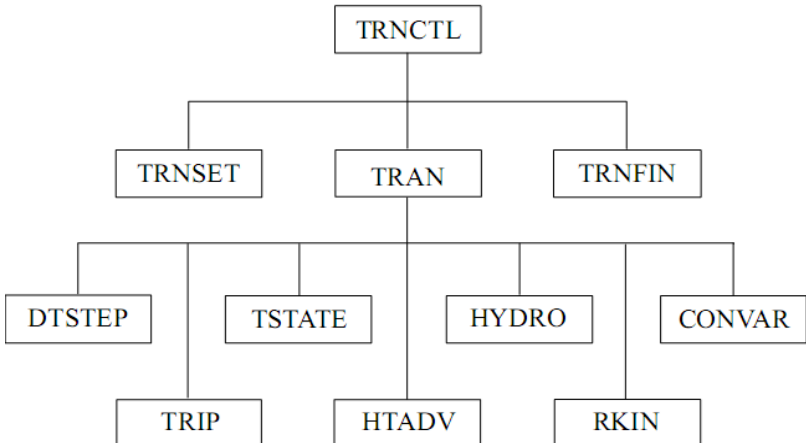
**Figure 2-2. RELAP5 top level structure**

Figure 2-3 and Figure 2-4, instead, show respectively the functional modular structure for the transient calculations and the second-level structures (subroutines) for the transient/steady-state blocks. In particular, subroutine TRNSET performs final cross-linking of information between data blocks. Subroutine TRAN controls the transient advancement of the solution. This block is the most time-consuming and memory-demanding. Finally, when transient advances are terminated, the subroutine TRNFIN releases space for the dynamic data blocks that are no longer needed. In greater detail, the time step control module (DTSTEP) determines the time step size,

controls output editing, and determines whether the transient advancements should be terminated. The trip system module (TRIP) evaluates logical statements, which have a true or false result. The equation of state boundary volume model (TSTATE) calculates the thermodynamic state of the fluid in each hydrodynamic boundary volume (time-dependent volume). The heat structure model (HTADV) advances heat conduction/transfer solutions. The hydrodynamics module (HYDRO) advances the hydrodynamic solution. The reactor kinetics module (RKIN) advances the reactor kinetics of the code with the point kinetics assumption, which hypothesizes that power can be separated into space and time functions. Finally, the control system module (CONVAR) provides the capability of simulating control systems typically used in hydrodynamic systems.



**Figure 2-3. Modular structures of transient calculations in RELAP5**



**Figure 2-4. Transient/steady-state block structure**

### 2.3.1.2 Hydrodynamic model

The RELAP5 hydrodynamic model is a one-dimensional, transient, two-fluid model for flow of a two-phase steam-water mixture that can contain non-condensable components in the steam phase and/or a soluble component in the water phase. The hydrodynamic model of the RELAP5 code contains several options for invoking simpler hydrodynamic models: homogeneous flow, thermal equilibrium, and frictionless flow models, which can be used independently or in combination.

The two-fluid equations of motion that are used as the basis for the RELAP5 hydrodynamic model are formulated in terms of volume and time-averaged parameters of the flow. Phenomena that depend upon transverse gradients, such as friction and heat transfer, are formulated in terms of the bulk properties using empirical transfer coefficient formulations. In situations where transverse gradients cannot be represented within the framework of empirical transfer coefficients, such as subcooled boiling, additional models specially developed for the particular situation are employed. The system model is solved numerically using a semi-implicit finite-difference technique. Whereas, the option for solving the system model using a nearly-implicit finite-difference technique, which allows violation of the material Courant limit, is suitable only for steady-state calculations and for slowly varying transient calculations.

The basic two-fluid differential equations possess complex characteristic roots that give the system a partially elliptic character and thus constitute an ill-posed initial boundary value problem. In RELAP5, the numerical problem is rendered well-posed by the introduction of artificial viscosity terms in the difference equation formulation that damp the high frequency spatial components of the solution. The ill-posed character of the two-fluid model is a result of the spatial averaging process and neglect of higher-order physical effects in the momentum formulation. Ransom and Hicks [19] have studied several formulations in which two pressures (one for each fluid) are included in the model. These models are totally hyperbolic and thus constitute well-posed problems. However, limited numerical studies by Ransom and Scofield [20] have shown that solutions for the two-pressure model compare very well to that for the single-pressure model with damping, and having significant differences only for short wavelength components of the solution where numerical truncation error is dominant.

The RELAP5 thermal-hydraulic model solves eight field equations for eight primary dependent variables. The primary dependent variables are pressure ( $P$ ), phasic specific internal energies ( $U_g$ ,  $U_f$ ), vapor volume fraction (void fraction) ( $\alpha_g$ ), phasic velocities ( $v_g$ ,  $v_f$ ), non-condensable quality ( $X_n$ ), and boron density ( $\rho_b$ ), being time ( $t$ ) and distance ( $x$ ) the independent variables. The secondary dependent variables used in the equations are phasic densities ( $\rho_g$ ,  $\rho_f$ ), phasic temperatures ( $T_g$ ,  $T_f$ ), saturation temperature ( $T^s$ ), and non-condensable mass fraction in non-condensable gas phase ( $X_{ni}$ ) for the  $i$ -th non-condensable species.

Hereafter, the basic two-fluid differential equations that form the basis for the hydrodynamic model are presented. They consist of two phasic continuity equations, two phasic momentum equations, and two phasic energy equations.



### **Mass continuity**

The phasic continuity equations are

$$\frac{\partial}{\partial t}(\alpha_g \rho_g) + \frac{1}{A} \frac{\partial}{\partial x}(\alpha_g \rho_g v_g A) = \Gamma_g \quad (1)$$

$$\frac{\partial}{\partial t}(\alpha_f \rho_f) + \frac{1}{A} \frac{\partial}{\partial x}(\alpha_f \rho_f v_f A) = \Gamma_f \quad (2)$$

Generally, the flow does not include mass sources or sinks, thus resulting that the liquid generation term be the negative of the vapor generation. The interfacial mass transfer model assumes that total mass transfer can be partitioned into mass transfer at the vapor/liquid interface in the bulk fluid ( $\Gamma_{ig}$ ) and mass transfer at the vapor/liquid interface in the boundary layer near the walls ( $\Gamma_w$ ).

### **Momentum conservation**

The momentum equations for vapor and liquid phase are

$$\begin{aligned} \alpha_g \rho_g A \frac{\partial v_g}{\partial t} + \frac{1}{2} \alpha_g \rho_g A \frac{\partial v_g^2}{\partial x} = & -\alpha_g A \frac{\partial P}{\partial x} + \alpha_g \rho_g B_x A - (\alpha_g \rho_g A) \text{FWG}(v_g) \\ & + \Gamma_g A (v_{gl} - v_g) - (\alpha_g \rho_g A) \text{FIG}(v_g - v_f) \\ & - C \alpha_g \alpha_f \rho_m A \left[ \frac{\partial (v_g - v_f)}{\partial t} + v_f \frac{\partial v_g}{\partial x} - v_g \frac{\partial v_f}{\partial x} \right] \end{aligned} \quad (3)$$

$$\begin{aligned} \alpha_f \rho_f A \frac{\partial v_f}{\partial t} + \frac{1}{2} \alpha_f \rho_f A \frac{\partial v_f^2}{\partial x} = & -\alpha_f A \frac{\partial P}{\partial x} + \alpha_f \rho_f B_x A - (\alpha_f \rho_f A) \text{FWF}(v_f) \\ & - \Gamma_g A (v_{fl} - v_f) - (\alpha_f \rho_f A) \text{FIF}(v_f - v_g) \\ & - C \alpha_f \alpha_g \rho_m A \left[ \frac{\partial (v_f - v_g)}{\partial t} + v_g \frac{\partial v_f}{\partial x} - v_f \frac{\partial v_g}{\partial x} \right]. \end{aligned} \quad (4)$$

These equations come from the one-dimensional phasic momentum equations with the following simplifications: the Reynolds stresses are neglected, the phasic pressures are assumed equal, the interfacial pressures are assumed equal to the phasic pressures (except for stratified flow), the covariance terms are universally neglected (unity assumed for covariance multipliers), interfacial momentum storage is neglected, phasic viscous stresses are neglected, the interface force terms consist of both pressure and viscous stresses, and the normal wall forces are assumed adequately modeled by the variable area momentum flux formulation.

The force terms on the right sides of Equations (3) and (4) are, respectively, the pressure gradient, the body force (i.e., gravity and pump head), wall friction, momentum transfer due to

interface mass transfer, interface frictional drag, and force due to virtual mass. The terms FWG and FWF are part of the wall frictional drag, which are linear in velocity, and are products of the friction coefficient, the frictional reference area per unit volume, and the magnitude of the fluid bulk velocity. The interfacial velocity in the interface momentum transfer term is the unit momentum with which phase appearance or disappearance occurs. The coefficients FIG and FIF are parts of the interface frictional drag, which is linear in relative velocity, and are products of the interface friction coefficients, the frictional reference area per unit volume, and the magnitude of interface relative velocity. The coefficient of virtual mass is the same as that used by Anderson [21] in the RISQUE code, where the value for C depends on the flow regime.

### ***Energy conservation***

The phasic thermal energy equations are

$$\begin{aligned} \frac{\partial}{\partial t} (\alpha_g \rho_g U_g) + \frac{1}{A} \frac{\partial}{\partial X} (\alpha_g \rho_g U_g v_g A) = -P \frac{\partial \alpha_g}{\partial t} - \frac{P}{A} \frac{\partial}{\partial X} (\alpha_g v_g A) \quad (5) \\ + Q_{wg} + Q_{ig} + \Gamma_{ig} h_g^* + \Gamma_w h_g' + DISS_g \end{aligned}$$

$$\begin{aligned} \frac{\partial}{\partial t} (\alpha_f \rho_f U_f) + \frac{1}{A} \frac{\partial}{\partial X} (\alpha_f \rho_f U_f v_f A) = -P \frac{\partial \alpha_f}{\partial t} - \frac{P}{A} \frac{\partial}{\partial X} (\alpha_f v_f A) \quad (6) \\ + Q_{wf} + Q_{if} - \Gamma_{ig} h_f^* - \Gamma_w h_f' + DISS_f . \end{aligned}$$

These equations come from the one-dimensional phasic thermal energy equations with the following simplifications: the Reynolds heat flux is neglected, the covariance terms are universally neglected (unity assumed for covariance multipliers), interfacial energy storage is neglected, and internal phasic heat transfer is neglected.

In the phasic energy equations,  $Q_{wg}$  and  $Q_{wf}$  are the phasic wall heat transfer rates per unit volume. The phasic enthalpies ( $h_g^*$ ,  $h_f^*$ ) associated with bulk interface mass transfer are chosen to be  $h_g^s$  and  $h_f$ , respectively, for the case of vaporization and  $h_g$  and  $h_f^s$ , respectively, for the case of condensation. The same is true for the phasic enthalpies ( $h_g'$ ,  $h_f'$ ) associated with wall (thermal boundary layer) interface mass transfer.

The phasic energy dissipation terms,  $DISS_g$  and  $DISS_f$ , are the sums of wall friction and pump effects. The dissipation effects due to interface mass transfer, interface friction, and virtual mass are neglected. The wall friction dissipation for both phases is defined as:

$$DISS_f = \alpha_f \rho_f FWF v_f^2 \quad DISS_g = \alpha_g \rho_g FWG v_g^2 \quad (7)$$

### ***Non condensables in gas-phase***

The non-condensable component is assumed to be in mechanical and thermal equilibrium with the vapor phase, and the additional mass conservation equation for the total non-condensable component, is given by

$$\frac{\partial(\alpha_g \rho_g X_n)}{\partial t} + \frac{1}{A} \frac{\partial}{\partial x} (\alpha_g \rho_g X_n v_g A) = 0 \quad (8)$$

where  $X_n$  is the non-condensable mass fraction in the gas phase. The mass conservation equation, for each non-condensable specie, is used when more than one of them is present.

The energy equations are modified by including the sensible interface (direct) heating term  $Q_{gf}$ , and modifying the interfacial heat transfer and mass transfer terms taking into account the partial pressure of steam component.

### ***Boron Concentration in the Liquid Field***

An Eulerian boron tracking model is used to simulate the transport of a dissolved component in the liquid phase. The solution is assumed to be sufficiently dilute that the following assumptions are valid:

- liquid properties are not altered by the presence of the solute;
- the solute is transported only in the liquid phase and at the velocity of the liquid phase;
- energy transported by the solute is negligible;
- inertia of the solute is negligible.

Under these assumptions, only an additional field equation for the conservation of the solute is required:

$$\frac{\partial \rho_b}{\partial t} + \frac{1}{A} \frac{\partial (\alpha_f \rho_f C_b v_f A)}{\partial x} = 0 \quad (9)$$

where  $C_b$  is the boron concentration defined as:

$$C_b = \frac{\rho_b}{\rho_m (1 - X)} = \frac{\rho_b}{\alpha_f \rho_f} \quad (10)$$

### ***Numerical schemes***

In the following, the two numerical schemes, semi-implicit and nearly implicit scheme, adopted in RELAP5 are presented. Generally speaking, the finite volume numerical solution scheme are based on replacing the system of differential equations with a system of finite-difference equations in time expressing the balances of finite regions in space (volumes). The achieved degree of implicitness determines the type of scheme adopted: semi-implicit or nearly-implicit scheme (in case of a greater level).

Nevertheless, the difference equations of both numerical schemes are based on the concept of a control volume in which mass and energy are conserved by considering the rates of influx through the cell boundaries. This model results in defining mass and energy volume averaged properties and in requiring knowledge of velocities at the volume boundaries. The

velocities at the boundaries are most conveniently defined through the use of momentum control volumes centered on the mass and energy cell boundaries. This approach results in a numerical scheme having a staggered spatial mesh: the scalar properties (pressure and energy) of the flow are defined at cell centers while the vector quantities (velocity) are defined on the cell boundaries. The resulting one-dimensional spatial nodalization is illustrated in Figure 2-5.

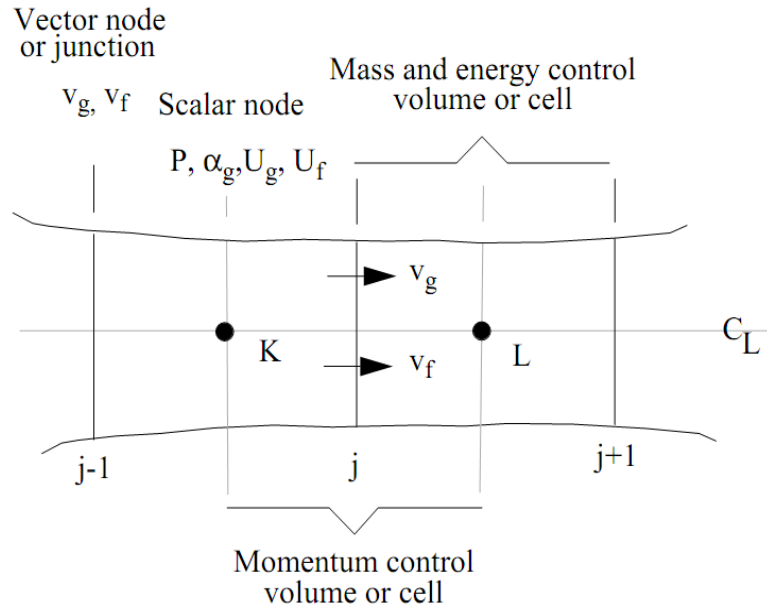


**Figure 2-5. Schematic of difference equation nodalization [8]**

The difference equations for each cell are obtained by integrating the mass and energy equations (actually, the sum and difference equations for mass, momentum and energy) along the spatial variable,  $x$ , from the junction at  $x_j$  to the one at  $x_{j+1}$ . and the momentum equations along the spatial variable from cell center to adjoining cell center ( $x_K$  to  $x_L$ ).

### ***Semi-Implicit Scheme***

After spatial discretization, the time integration is applied. By indicating the time level by the superscripts  $n, n+1$ , the spatial nodding subscripts for volumes and for junctions respectively with  $K, L$  and  $j, j+1$ , the intermediate time variables with a tilde ( $\tilde{\cdot}$ ), and the donored (i.e., upwind) quantities with a dot overscore, for instance, the sum continuity equation results:

$$\begin{aligned}
 V_L [ \dot{\alpha}_{g,L}^n ( \tilde{\rho}_{g,L}^{n+1} - \rho_{g,L}^n ) + \dot{\alpha}_{f,L}^n ( \tilde{\rho}_{f,L}^{n+1} - \rho_{f,L}^n ) + ( \rho_{g,L}^n - \rho_{f,L}^n ) ( \tilde{\alpha}_{g,L}^{n+1} - \alpha_{g,L}^n ) ] \\
 + \left( \dot{\alpha}_{g,j+1}^n \dot{\rho}_{g,j+1}^n V_{g,j+1}^{n+1} A_{j+1} - \dot{\alpha}_{g,j}^n \dot{\rho}_{g,j}^n V_{g,j}^{n+1} A_j \right) \Delta t \\
 + \left( \dot{\alpha}_{f,j+1}^n \dot{\rho}_{f,j+1}^n V_{f,j+1}^{n+1} A_{j+1} - \dot{\alpha}_{f,j}^n \dot{\rho}_{f,j}^n V_{f,j}^{n+1} A_j \right) \Delta t = 0 \quad .
 \end{aligned} \quad (11)$$

In particular, the provisional advanced time phasic densities ( $\tilde{\rho}$ ) appearing in (11) are obtained by linearizing the phasic state relations about the old time values

$$\tilde{\rho}_{g,L}^{n+1} = \rho_{g,L}^n + \left( \frac{\partial \rho_g}{\partial P} \right)_L^n ( P_L^{n+1} - P_L^n ) + \left( \frac{\partial \rho_g}{\partial X_n} \right)_L^n ( \tilde{X}_{n,L}^{n+1} - X_{n,L}^n ) + \left( \frac{\partial \rho_g}{\partial U_g} \right)_L^n ( \tilde{U}_{g,L}^{n+1} - U_{g,L}^n ) \quad (12)$$

whereas, for the donored quantities it results:

$$\dot{\Phi}_j^n = \begin{cases} \Phi_K^n & \text{if } w_j^n > 0 \\ \Phi_L^n & \text{if } w_j^n < 0 \end{cases} \quad (13)$$

Hereafter, a synthesis of the semi-implicit scheme (without boron tracking) is provided.

1. The equations are ordered in this way: first the non-condensable density equation, second the vapor energy equation, third the liquid energy equation, fourth the difference density equation, fifth the sum density equation. In this way, the following five difference variables are obtained:

$$(\tilde{X}_{n,L}^{n+1} - X_{n,L}^n), (\tilde{U}_{g,L}^{n+1} - U_{g,L}^n), (\tilde{U}_{f,L}^{n+1} - U_{f,L}^n), (\tilde{\alpha}_{g,L}^{n+1} - \alpha_{g,L}^n), \text{ and } (P_L^{n+1} - P_L^n) \quad (14)$$

2. Keeping in mind that the tilde quantities ( $\tilde{\cdot}$ ) are provisional new time variables and not new time variables, the following system results:

$$\tilde{\mathbf{A}}\tilde{\mathbf{x}} = \tilde{\mathbf{b}} + \tilde{\mathbf{g}}^1 v_{g,j+1}^{n+1} + \tilde{\mathbf{g}}^2 v_{g,j}^{n+1} + \tilde{\mathbf{f}}^1 v_{f,j+1}^{n+1} + \tilde{\mathbf{f}}^2 v_{f,j}^{n+1} \quad (15)$$

where the matrix  $\tilde{\mathbf{A}}$  and the vectors  $\tilde{\mathbf{b}}, \tilde{\mathbf{g}}^1, \tilde{\mathbf{g}}^2, \tilde{\mathbf{f}}^1, \tilde{\mathbf{f}}^2$  contain only old-time variables, and  $\tilde{\mathbf{x}}$  the previous five difference variables.

3. Multiplying Eq. (15) by  $\tilde{\mathbf{A}}^{-1}$  (actually using an elimination process), it is obtained as last row an equation that involves  $(P_L^{n+1} - P_L^n), v_{g,j+1}^{n+1}, v_{g,j}^{n+1}, v_{f,j+1}^{n+1}$  and  $v_{f,j}^{n+1}$ .
4. Solving the momentum equations and substituting, a single 3-point equation in terms of pressures is obtained. Repeating this operation for each volume, a  $N \times N$  system of linear equations for new time pressures is obtained (for a model with  $N$  volumes).
5. A sparse matrix solver calculates  $(P_L^{n+1} - P_L^n)$  for each volume.
6. The pressure differences are substituted into the momentum equations to obtain new time velocities.
7. Substituting the new time velocities in eq. (15) and using a LU factorization, the provisional time variables  $\tilde{X}_{n,L}^{n+1}, \tilde{U}_{g,L}^{n+1}, \tilde{U}_{f,L}^{n+1}$ , and  $\tilde{\alpha}_{g,L}^{n+1}$  are obtained.
8. Then, the mixture density equation  $\rho_{m,L}^{n+1}$  (from a mixture density equation) and  $\rho_L^{n+1}$  (calculated from the state relations) are compared. On the basis of this mass error, a reduction or an increase in the adopted time-step and the possible repetition of the time advancement is decided.
9. Next, the provisional new time volumetric mass exchange rate  $\tilde{\Gamma}_{g,L}^{n+1}$ , is calculated.
10. Finally, the new time variables  $X_{n,L}^{n+1}, U_{g,L}^{n+1}, U_{f,L}^{n+1}$ , and  $\alpha_{g,L}^{n+1}$  are calculated from vapor, non-condensable and liquid density equations as well as vapor and liquid energy equations.

### ***Nearly-Implicit scheme***

For problems where the flow is expected to change very slowly with time, it is useful to adopt a numerical scheme with a greater time step. This feature is assured by the nearly-implicit scheme through removing the Courant limit typical of the semi-implicit scheme ( $w \leq \Delta x/\Delta t$ ).

In fact, the nearly-implicit scheme, at the price of an increased computational effort, succeeds to remove the Courant limitation as a result of:

- the adoption of an implicit treatment for the convective terms in the momentum equations
- the adoption, in the second step, of implicit values of the donored quantities in the advection terms of mass and energy equations

The whole scheme can be subdivided into two steps:

1. In the first step, a similar formulation to the semi-implicit scheme is obtained with new time pressure and velocities (see eq. 16). Next, because of the implicit momentum terms in the momentum equations, the new time velocities cannot be locally solved, and therefore, also the single 3-point pressure equation cannot be achieved as in the semi-implicit scheme.

$$P_L^{n+1} = A v_{g,j+1}^{n+1} + B v_{g,j}^{n+1} + C v_{f,j+1}^{n+1} + D v_{f,j}^{n+1} + E \quad (16)$$

Differently, eq.(16) is used to eliminate the  $n+1$  level pressure terms from the sum and difference momentum and obtain a coupled pair of momentum equations involving only  $n+1$  level junction velocities. Then, the achieved system  $(2N) \times (2N)$  with  $2 \times 2$  block (for a model with  $N$  junctions) can be solved to get the next time velocities.

After, the  $n+1$  level pressures are obtained again by back-substitution in eq.(16), while substitution into the mass and energy equations provides provisional values of void fraction and specific energy of the two phases.

2. In the second step, the new time velocities,  $v_g^{n+1}$  and  $v_f^{n+1}$ , and the provisional  $n+1$  values, known from step one, are used in the phasic density and energy equations having the convected variables now evaluated implicitly. Each resulting equation involves only one unknown variable, and therefore can be solved independently in order to obtain  $X_{n,L}^{n+1}$ ,  $U_{g,L}^{n+1}$ ,  $U_{f,L}^{n+1}$ , and  $\alpha_{g,L}^{n+1}$ .

Hereafter, for the sake of completeness, a concise explanation of the wall friction and heat transfer models is provided.

### ***Wall friction model***

The wall friction model is based on a two-phase multiplier approach in which the two-phase multipliers are calculated from the Heat Transfer and Fluid Flow Service (HTFS)-modified

Baroczy correlation[22]. It consists in computing the pressure drop of the mixture (see eq.17) through liquid-alone wall friction pressure drop or vapor-alone, and their two-phase friction multipliers ( $\Phi_f$ ,  $\Phi_g$ ).

$$\left(\frac{dP}{dx}\right)_{2\phi} = \phi_f^2 \left(\frac{dP}{dx}\right)_f \quad \text{and} \quad \left(\frac{dP}{dx}\right)_{2\phi} = \phi_g^2 \left(\frac{dP}{dx}\right)_g \quad (17)$$

As a consequence, the multipliers result to be related as

$$\chi^2 = \frac{\phi_g^2}{\phi_f^2} = \frac{\left(\frac{dP}{dx}\right)_f}{\left(\frac{dP}{dx}\right)_g} \quad (18)$$

where  $\chi$  is the Lockhart-Martinelli ratio. Then, by using the Heat Transfer and Fluid Flow Service (HTFS) correlation is possible to calculate the two-phase friction multipliers as

$$\phi_f^2 = 1 + \frac{C}{\chi} + \frac{1}{\chi^2} \quad \text{and} \quad \phi_g^2 = \chi^2 + C\chi + 1 \quad (19)$$

respectively for the liquid-alone and vapor-alone multiplier (C is a correlation coefficient).

Next, substituting one of the two relations for the individual phasic friction multiplier into eq.(17), it is obtained:

$$\left(\frac{dP}{dx}\right)_{2\phi} = \frac{1}{2D} \left\{ \lambda'_f \rho_f (\alpha_f v_f)^2 + C \left[ \lambda'_f \rho_f (\alpha_f v_f)^2 \lambda'_g \rho_g (\alpha_g v_g)^2 \right]^{1/2} + \lambda'_g \rho_g (\alpha_g v_g)^2 \right\} \quad (20)$$

where  $\lambda'_f$  and  $\lambda'_g$  indicate the liquid-alone and vapor-alone Darcy-Weisbach friction factors.

Finally, the two-phase pressure drop is partitioned for obtaining the individual phasic wall shear stress using the Chisholm technique [23], as

$$\tau_f P_f = \alpha_f \frac{dP}{dx} \Big|_{2\phi} \left( \frac{Z^2}{\alpha_g + \alpha_f Z^2} \right) \quad \text{and} \quad \tau_g P_g = \alpha_g \frac{dP}{dx} \Big|_{2\phi} \left( \frac{1}{\alpha_g + \alpha_f Z^2} \right) \quad (21)$$

where

$$Z^2 = \frac{\lambda_f (Re_f) \rho_f v_f^2 \frac{\alpha_{fw}}{\alpha_f}}{\lambda_g (Re_g) \rho_g v_g^2 \frac{\alpha_{gw}}{\alpha_g}} \quad (22)$$

Regarding the Darcy-Weisbach friction factor for unheated surfaces, RELAP5 computes it according to the flow regime (laminar, transition, turbulent) as follows:

$$\lambda_L = \frac{64}{Re\Phi_s} \quad 0 \leq Re \leq 2200 \quad (23)$$

$$\lambda_{L,T} = \left( \frac{Re - 2200}{3000 - 2200} \right) (\lambda_{T,3000} - \lambda_{L,2200}) + \lambda_{L,2200} \quad 2200 < Re < 3000 \quad (24)$$

$$\frac{1}{\sqrt{\lambda_T}} = -2\log_{10} \left\{ \frac{\varepsilon/D}{3.7} + \frac{2.51}{\text{Re}} \left[ 1.14 - 2\log_{10} \left( \frac{\varepsilon}{D} - \frac{21.25}{\text{Re}^{0.9}} \right) \right] \right\} \quad (25)$$

This value is corrected in case of heated surface as

$$\frac{f}{f_{\text{iso}}} = 1 + \frac{P_H}{P_W} \left( \left( \frac{\mu_{\text{wall}}}{\mu_{\text{bulk}}} \right)^D - 1 \right) \quad (26)$$

### Wall heat transfer model

In RELAP5/MOD3 the total wall heat flux ( $q''$ ) is the heat flux to vapor plus the heat flux to liquid:

$$q'' = h_g (T_w - T_{\text{refg}}) + h_f (T_w - T_{\text{reff}}) \quad (27)$$

where the reference temperatures can be the local gas or liquid temperature or the saturation temperature, depending on the heat transfer coefficient correlation being used.

In fact, as illustrated in Figure 2-6, mainly upon the difference between the wall temperature and the saturation temperature (based on total pressure for boiling case and steam partial pressure for condensation) RELAP5 selects the wall heat transfer correlations to be adopted.

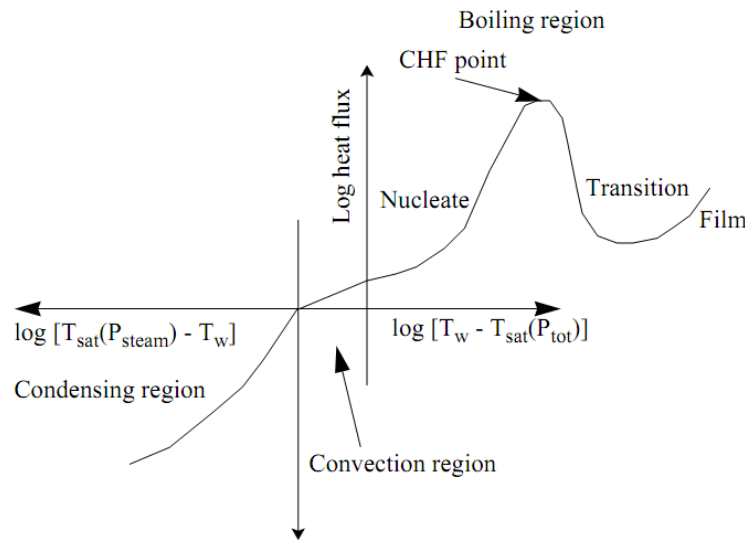


Figure 2-6. RELAP5 boiling and condensing curves

Others factors that RELAP5 accounts for the wall heat transfer correlation are: whether the pressure is above the critical pressure, non-condensable gases are present, the fluid state (liquid, two-phase, or vapor), whether the heat flux is above the critical heat flux (CHF), and if the film boiling heat flux is greater than the transition boiling heat flux.

For instance, the boiling curve uses the Chen boiling correlation [24] up to the critical heat flux point, the Chen-Sundaram-Ozkaynak correlation [25] for transition boiling and a modified Bromley correlation [26] for film boiling. Instead, convection mode calculations rely on evaluating forced convection, laminar convection, and natural convection and selecting the



maximum from these three correlations: Dittus-Boelter [27], Kays [28], and Churchill-Chu [29], respectively.

### ***RELAP5 Components***

RELAP5 is equipped with a variety of component models. The ones in which the hydrodynamic model equations are directly applied are:

- single volumes and junctions,
- time dependent volumes and junctions (for prescribed thermodynamic conditions or flow rates assigned);
- pipes and annuli.

However, there are also other particular components in which specific models have been introduced to perform functions needed in plant simulation:

- o Branch, i.e. a single volume with many junctions;
- o Separator: a special volume for simulating phase separation;
- o Jetmixer: for simulating the dynamic merging of two streams (e.g., jet-pumps);
- o Pump: a quasi-static model superimposed to a volume-junction flow path;
- o Turbine: lumped parameter model for multi-stage turbines;
- o Valves: quasi-steady models for instantaneous or gradual opening covering: trip valves, check valves, motor valves, servo valves, relief valves;
- o Accumulator: model for simulating the hydrodynamic and thermal behavior of ECCS accumulator systems;
- o ECC Mixer: special component for simulating the mixing of ECC water.

### 2.3.2 TRACE v5

TRACE, formerly called TRAC-M, is the latest in a series of advanced, best-estimate reactor system codes developed by the U.S. Nuclear Regulatory Commission (with the involvement of Los Alamos National Laboratory, Integrated Systems Laboratory (ISL), the Pennsylvania State University (PSU) and Purdue University) with the aim of analyzing the neutronic/thermal-hydraulic behavior of light water reactors during operational transients and accident scenarios as the loss of coolant accident (LOCA) in light water reactors[12]. The code is the result of merging the capabilities of many USNRC supported codes, such as TRAC-PF1, TRAC-BF1, RELAP-5 and RAMONA.

TRACE code takes a component-based approach to modeling a reactor system. Each physical piece of equipment in a flow loop can be represented as some type of component and each component can be further nodalized into some number of physical volumes over which the fluid, conduction, and kinetics equations are averaged.

Models for multidimensional two-phase flow, non-equilibrium thermo-dynamics, heat transfer, reflood, level tracking and reactor kinetics are included. The partial differential equations that describe two-phase flow and heat transfer are solved using finite volume numerical methods, where the conservation equations are formulated in terms of volume and time-averaged parameters of the flow and based on first order finite volume donor cell schemes with “staggered meshes”. The set of equations used by TRACE are basically identical to those of RELAP (a little exception is, for example, the absence of the virtual mass term in momentum equation): a full two-fluid (six-equation) hydrodynamic model is adopted to evaluate gas-liquid flow, a seventh field equation (mass balance) describes a non-condensable gas field, and an eighth field equation tracks dissolved solute. TRACE field equations assume that viscous shear stresses are negligible (to a first order approximation) as well as the viscous heating terms, while the two independent thermodynamic variables employed in state relationships are pressure and temperature (instead of internal energy as in RELAP5). An explicit turbulence modeling is not coupled to the conservation equations (although turbulence effects can be accounted for with specialized engineering models for specific situations), and the heat flux through walls is computed using flow-regime-dependent heat transfer coefficients (HTC) obtained from a generalized boiling curve based on a combination of local conditions and history effects.

The numerical schemes adopted in TRACE are mainly two: a semi-implicit time-differencing technique, which is needed for the heat-transfer equations, and, by default, the Stability Enhancing Two-Step (SETS) method for the fluid-dynamics equations. The SETS method has the advantage of avoiding Courant stability limits on time-step size, but the disadvantage of relatively high numerical diffusion; on the other hand, also the semi-implicit method, that can have substantially less numerical diffusion but has time-step sizes restricted by a material Courant limit, can be selected. The finite-difference equations for hydrodynamic phenomena form a system of coupled, non-linear equations that are solved by the Newton-Raphson iteration method, while the resulting linearized equations are solved by direct matrix inversion.

It should be pointed out that TRACE code is not appropriate for transients in which there are large changing asymmetries in the reactor-core power such as would occur in a control-rod-ejection transient unless it is used in conjunction with the PARCS spatial kinetics module. In TRACE, neutronics is evaluated on a core-wide basis by a point-reactor kinetics model with reactivity feedback and the spatially local neutronic response associated with the ejection of a single control rod cannot be modeled.

The TRACE code, as mentioned above, uses a two fluid, two-phase time and volume averaging flow conservation equations. In this flow model, each fluid domain (gas and liquid) is represented by one complete set of partial differential equations: for mass, momentum and energy. Besides the model considers:

1. heat transfer from the interface to gas and to liquid, and heat transfer from surfaces of structures to the fluid;
2. contributions from the stress tensor due to shear at metal surfaces or phase interfaces within the averaging volume.

The time and volume averaged mass equations are:

$$\frac{\partial(1-\alpha)\rho_l}{\partial t} + \nabla \cdot [(1-\alpha)\rho_l \mathbf{v}_l] = -\Gamma \quad (28)$$

$$\frac{\partial\alpha\rho_g}{\partial t} + \nabla \cdot [\alpha\rho_g \mathbf{v}_g] = \Gamma \quad (29)$$

The time and volume averaged energy (internal + kinetic energy) equations are:

$$\begin{aligned} & \frac{\partial(1-\alpha)\rho_l(e_l + v_l^2/2)}{\partial t} + \nabla \cdot \left[ (1-\alpha)\rho_l \left( e_l + \frac{P}{\rho_l} + v_l^2/2 \right) \mathbf{v}_l \right] \\ & = q_{il} + q_{wl} + q_{dl} + (1-\alpha)\rho_l \mathbf{g} \cdot \mathbf{v}_l - \Gamma h'_l + (\mathbf{f}_i + \mathbf{f}_{wl}) \cdot \mathbf{v}_l \end{aligned} \quad (30)$$

$$\begin{aligned} & \frac{\partial\alpha\rho_g(e_g + v_g^2/2)}{\partial t} + \nabla \cdot \left[ \alpha\rho_g \left( e_g + \frac{P}{\rho_l} + v_g^2/2 \right) \mathbf{v}_g \right] \\ & = q_{ig} + q_{wg} + q_{dg} + \alpha\rho_g \mathbf{g} \cdot \mathbf{v}_g - \Gamma h'_l + (-\mathbf{f}_i + \mathbf{f}_{wg}) \cdot \mathbf{v}_g \end{aligned} \quad (31)$$

The time and volume averaged momentum equations are

$$\frac{\partial(1-\alpha)\rho_l \mathbf{v}_l}{\partial t} + \nabla \cdot (1-\alpha)\rho_l \mathbf{v}_l \mathbf{v}_l + (1-\alpha)\nabla P = (\mathbf{f}_i + \mathbf{f}_{wl}) + (1-\alpha)\rho_l \mathbf{g} - \Gamma \mathbf{v}_l \quad (32)$$

$$\frac{\partial\alpha\rho_g \mathbf{v}_g}{\partial t} + \nabla \cdot \alpha\rho_g \mathbf{v}_g \mathbf{v}_g + (1-\alpha)\nabla P = (\mathbf{f}_i + \mathbf{f}_{wg}) + \alpha\rho_g \mathbf{g} - \Gamma \mathbf{v}_g \quad (33)$$

Anyway, for reducing the calculation time, the balance equations are not written in conservation form and, in place of two separate energy equations, one mixture energy and one gas energy equation are solved. The internal energy and motion equations are rearranged from the fully conservative forms of the energy and momentum equations (from Eq. (30) to Eq.(33)). In particular, the internal energy ( $e$ ) conservation equation for the gas phase is obtained by taking

the dot product of the corresponding momentum equation with its velocity and subtracting the results from the fully conservative energy equation:

$$\frac{\partial(\alpha\rho_g e_g)}{\partial t} + \nabla \cdot (\alpha\rho_g e_g \mathbf{v}_g) = -P \frac{\partial\alpha}{\partial t} - P\nabla \cdot (\alpha\mathbf{v}_g) + q_{wg} + q_{dg} + q_{ig} + \Gamma h'_w \quad (34)$$

A similar operation is performed on the liquid energy equation, but rather than using it in that form, the result is added to the gas energy equation to produce a mixture energy conservation equation, namely:

$$\begin{aligned} & \frac{\partial[(1-\alpha)\rho_l e_l + \alpha\rho_g e_g]}{\partial t} + \nabla \cdot [(1-\alpha)\rho_l e_l \mathbf{v}_l + \alpha\rho_g e_g \mathbf{v}_g] \\ & = -P\nabla \cdot [(1-\alpha)\mathbf{v}_l + \alpha\mathbf{v}_g] + q_{wg} + q_{wl} + q_{dg} + q_{dl} \end{aligned} \quad (35)$$

When included in the finite volume equation solution, the mixture energy equation makes it easier to deal with transitions from two-phase to single-phase flow during a step in the time integration. To fully achieve this advantage during a transition, a similar pair of gas and mixture mass equations (see below) must be used in the actual solution.

$$\frac{\partial\alpha\rho_g}{\partial t} + \nabla \cdot [\alpha\rho_g \mathbf{v}_g] = \Gamma \quad (36)$$

$$\frac{\partial[(1-\alpha)\rho_l + \alpha\rho_g]}{\partial t} + \nabla \cdot [(1-\alpha)\rho_l \mathbf{v}_l + \alpha\rho_g \mathbf{v}_g] = 0 \quad (37)$$

Motion equations are obtained by the standard means of multiplying the mass conservation equation for a phase by the related phase velocity, subtracting it from the corresponding momentum conservation equation, and dividing the result by the appropriate macroscopic density.

$$\frac{\partial\mathbf{v}_l}{\partial t} + \mathbf{v}_l \cdot \nabla \mathbf{v}_l = -\frac{1}{\rho_l} \nabla P + \frac{[\mathbf{f}_i + \mathbf{f}_{wl} - \Gamma(\mathbf{v}_i - \mathbf{v}_l)]}{(1-\alpha)\rho_l} + \mathbf{g} \quad (38)$$

$$\frac{\partial\mathbf{v}_g}{\partial t} + \mathbf{v}_g \cdot \nabla \mathbf{v}_g = -\frac{1}{\rho_g} \nabla P + \frac{[\mathbf{f}_{wg} - \mathbf{f}_i - \Gamma(\mathbf{v}_g - \mathbf{v}_i)]}{\alpha\rho_g} + \mathbf{g} \quad (39)$$

The above equations are generally referred to as the non-conservative form of the momentum equations because it is not possible to write a finite volume method that guarantees that some numerical integral of momentum over a system does not change from one time step to the next in the absence of force terms. Use of this form permits simpler numerical solution strategies particularly for a semi-implicit method and can generally be justified because of the presence of wall friction makes the fully conservative form of the momentum equation far less useful. When sharp flow-area changes exist, however, numerical solution of the non-conservative motion

equations can produce significant errors. For these situations, the motion equations have been modified to force Bernoulli flow.

### ***Interfacial drag force***

The transfer of mass, energy and momentum between gas-liquid phases are modeled by the flow regime dependent thermal-hydraulic equations. In TRACE, there are three categories of flow regimes:

- *Pre-CHF*: these consist of the bubbly/slug and the annular/mist regimes;
- *Stratified*: the horizontal stratified flow regime is available for 1-D components that are either horizontal or inclined;
- *Post-CHF*: this encompasses the "inverted" flow regimes that occur when the wall is too hot for liquid-wall contact.

### ***Wall drag force***

TRACE models the fluid-wall shear force using a friction factor approach. Regarding the Pre-CHF regime, wall drag force is only applied to the liquid phase.

### ***Wall condensation and boiling***

When the wall temperature above the liquid level is lower than the saturation temperature, condensation of vapor on the wall is calculated. If the wall temperature above the liquid level is higher than the saturation temperature, natural convection in the vapor region occurs. Natural convection in the liquid region is considered when the wall temperature below the liquid level is lower than the saturation temperature. When the wall temperature below the liquid level is higher than the saturation temperature, heat transfer occurs by boiling.

### ***Heat conduction***

The thermal history of the reactor structure is obtained from a solution of the heat-conduction equation Eq. (40)(40) applied to different geometries.

$$\frac{\partial(\rho c_p T)}{\partial t} + \nabla \cdot \mathbf{q} = q''' \quad (40)$$

The equation above represents the general form that describes the heat conduction process. In practice, the product  $\rho c_p$  is assumed to be constant for purposes of taking the time derivative. In turn, the heat flux  $\mathbf{q}$  can be expressed in terms of the temperature gradient by Fourier's law:

$$\mathbf{q} = -k\nabla T \quad (41)$$

Therefore, the following equation is obtained:

$$\rho c_p \frac{\partial T}{\partial t} - \nabla \cdot (k\nabla T) = q''' \quad (42)$$

Hereafter, the basics of the SETS method are presented. It consists in adding one step more in calculations with respect to the semi-implicit method mentioned in the paragraph 2.3.1.2. This outcome is achieved by devising a “correction” step, from now on “stabilizer” step, for each conservation equations and adding it to the semi-implicit method.

Details of the solution within a given step in time are broken into three stages - a pre-pass, outer iteration (i.e., the semi-implicit step), and post-pass. The outer iteration step involves equations basically identical to those of the semi-implicit method and is accomplished by the same coding. However, this semi-implicit step is preceded by a solution of motion equations for “stabilizer” velocities (calculated during the pre-pass). In addition, stabilizer mass and energy equations are solved after the semi-implicit step, during the post-pass. As a result, SETS involves the solution of flow equations at all three stages of a time step.

For simplicity reasons, the example reported hereafter refers to a special 1D single-phase flow (no source terms and heat transfer). By keeping TRACE notation, scalar nodes are indicated with integer subscripts (e.g.  $j$ ,  $j+1$ ), and vector nodes with a half-integer subscripts (e.g.  $j-1/2$ ,  $j+1/2$ ). As usual, a tilde indicates a provisional new time variable, while actual new-time variables have a superscript “ $n+1$ ” without tilde.

#### Stabilizer Motion Equation

$$\frac{(\tilde{v}_{j+1/2}^{n+1} - v_{j+1/2}^n)}{\Delta t} + v_{j+1/2}^n \frac{\partial \tilde{v}^{n+1}}{\partial x} \Big|_{j+1/2} + \frac{1}{\langle \rho \rangle_{j+1/2}^n} \frac{P_{j+1}^n - P_j^n}{\Delta x} + K_{j+1/2}^n (2\tilde{v}_{j+1/2}^{n+1} - v_{j+1/2}^n) \cdot |v_{j+1/2}^n| = 0 \quad (43)$$

#### Semi-Implicit Equation Step

$$\frac{(\tilde{\rho}_j^{n+1} - \rho_j^n)}{\Delta t} + \frac{\partial (\rho^n v^{n+1})}{\partial x_j} = 0 \quad (44)$$

$$\frac{(v_{j+1/2}^{n+1} - v_{j+1/2}^n)}{\Delta t} + v_{j+1/2}^n \frac{\partial \tilde{v}^{n+1}}{\partial x} \Big|_{j+1/2} + \frac{1}{\langle \rho \rangle_{j+1/2}^n} \frac{\tilde{P}_{j+1}^{n+1} - \tilde{P}_j^{n+1}}{\Delta x} + K_{j+1/2}^n (2v_{j+1/2}^{n+1} - v_{j+1/2}^n) \cdot |v_{j+1/2}^n| = 0 \quad (45)$$

$$\frac{(\tilde{\rho}_j^{n+1} \tilde{u}_j^{n+1} - (\rho u)_j^n)}{\Delta t} + \frac{\partial (\rho^n u^n v^{n+1})}{\partial x_j} + \tilde{P}_j^{n+1} \frac{v_{j+1/2}^{n+1} - v_{j-1/2}^{n+1}}{\Delta x} = 0 \quad (46)$$

#### Stabilizer Mass and Energy Equations

$$\frac{(\rho_j^{n+1} - \rho_j^n)}{\Delta t} + \frac{\partial (\rho^{n+1} v^{n+1})}{\partial x_j} = 0 \quad (47)$$

$$\frac{((\rho u)_j^{n+1} - (\rho u)_j^n)}{\Delta t} + \frac{\partial [(\rho u)^{n+1} v^{n+1}]}{\partial x_j} + \tilde{P}_j^{n+1} \frac{v_{j+1/2}^{n+1} - v_{j-1/2}^{n+1}}{\Delta x} = 0 \quad (48)$$

First, it is worth to highlight the differences in each equation with respect to the semi-implicit set of equations described in RELAP section:

- in the stabilizer momentum equation the basic difference is the explicit formulation for the pressure gradient, which turns the equation as purely linear in the unknown stabilizer velocities;
- the balance equations of the semi-implicit step are the same used in RELAP except for the momentum flux terms, in which the corrected velocity replaces the old time velocity;
- instead, the stabilizer mass and energy equations vary from the mass and energy equations of the semi-implicit step only in that the densities and energies in flux terms are now evaluated at the new time.

Next, the solution method adopted can be concisely investigated:

1. by solving the linear stabilizer momentum equations system, the provisional velocities are obtained;
2. the semi-implicit step is solved, as in RELAP, to get provisional pressures and internal energies, and the new time velocities;
3. the post-pass stage is devoted to achieve new time density and internal energy.

Then, if by means of the semi-implicit method in RELAP all new time variables (for single-phase flow, provisional for two-phase flow) are obtained, in SETS, the semi-implicit step aims only to determine new time velocities, giving to the stabilizer mass and energy equations the task to update the state variables.

Actually, in SETS the stabilizer mass and energy equations are not directly solved, but for computational time-saving reason (especially with two-phase flows where the source terms are canceled out of the equations), the equations solved are those from the difference between the semi-implicit equations and the stabilizer ones. However, a disadvantage of the latter is that the rigorous mass conservation is lost.

Finally, it should be considered that even if the material Courant stability limit actually is eliminated, this does not imply unconditional stability for the method. The time step control is based on convergence criteria for user-specified threshold values for local pressure and void fraction increments.

Hereafter, a brief description of the EXTERIOR component, which gives the ability to run multiple TRACE processes and to couple it with other codes, is provided.

### ***EXTERIOR component***

The EXTERIOR component is a key element of the Exterior Communications Interface (ECI) and running TRACE in a multi-tasking (parallel) mode. It provides the linkage between different pieces of a simulation model that have been separated for running in different processes across one or more physical

processors. It may help to conceptualize the EXTERIOR component as basically just abbreviated information for a "component" that is modeled on an exterior process with which one or more components in this process must communicate. While the most straightforward use of the EXTERIOR component is to break an existing TRACE simulation into separate pieces by running multiple instances of TRACE across multiple processes, it is by no means the only application.

The EXTERIOR component provides the ability to connect TRACE to more detailed models or programs designed to focus on one particular aspect of simulation. Examples would include containment models, a CFD code, a core make-up tank model (like REMIX), or any other computer program which may require data from TRACE. The only prerequisite is that the external program has been modified to allow it to communicate with TRACE. One point worth noting here, however, is that EXTERIOR components are not a necessary prerequisite for initiating a multi-process run. It is, in fact, possible to have TRACE communicating with other programs or processes without needing to define EXTERIOR components in the input model.



## 2.3.3 ATHLET Mod 2.2 Cycle A

### 2.3.3.1 Overview

The thermal-hydraulic computer code ATHLET (Analysis of THERmal-hydraulics of LEaks and Transients) is being developed by the Gesellschaft für Anlagen- und Reaktorsicherheit (GRS) for the analysis of anticipated and abnormal plant transients, small and intermediate leaks as well as large breaks in light water reactors [14].

The aim of the code development is to cover the whole spectrum of design basis and beyond design basis accidents (without core degradation) for PWRs and BWRs with only one code. The main code features are:

- advanced thermal-hydraulics;
- modular code architecture;
- separation between physical models and numerical methods;
- pre- and post-processing tools;
- portability.

ATHLET is being applied by numerous institutions in Germany and abroad, and its development and validation is sponsored by the German Federal Ministry of Economics and Technology.

ATHLET can be applied for accidental scenario simulations (without core damage) in light water reactors, like PWR, BWR, VVER, and RBMK. For accidents with core damage ATHLET-CD has been developed providing extensions for the simulation of the mechanical fuel behavior, core melting and relocation, debris bed formation as well as fission product release and transport. Recently, its range of applicability has been extended to supercritical coolant including the transition from super- to subcritical fluid states (R&D version only).

### 2.3.3.2 Code structure

The ATHLET structure is highly modular, and allows an easy implementation of different physical models. The code is composed of several basic modules for the calculation of the different phenomena involved in the operation of a light water reactor:

- thermo-fluid dynamics (TFD);
- Heat Transfer and Heat Conduction (HECU);
- Neutron Kinetics (NEUKIN);
- General Control Simulation Module (GCSM);

together with the numerical integration method FEBE.

Modules can be partitioned into sub-modules. Each module and sub-module has its own identification (ID) letters (one for a module, two for a sub-module). Each subprogram name starts with the identification letter of that module to which the program is assigned to. The same applies to the names of modules, where the first letter always is a 'C' and the second (and third, respectively) are the (sub-)module identification. This allows a lexical ordering of the program

parts and is very useful for the management of the source code and helpful for a better understanding of the print out.

Other independent modules (e.g., large models with own time advancement procedure) can be coupled without structural changes in ATHLET by means of a general interface. ATHLET provides a modular network approach for the representation of a thermal-hydraulic system. A given system configuration can be simulated by just connecting basic fluid dynamic elements, called thermo-fluid dynamic objects (TFOs). There are several TFO types, each of them applying for a certain fluid-dynamic model. All object types are classified into three basic categories:

- Pipe objects: apply for a one-dimensional TFD Model with partial differential equations describing the transport of fluid. The nodalization (number of nodes or volumes) is defined by input data. After nodalization, a pipe object can be taken as a number of consecutive volumes (control volumes) connected by flow paths (junctions). The mass flow rates at the volume boundaries are calculated by the solution of momentum differential equations (local momentum balance) or by algebraic equations when the integrated momentum balance option is chosen. The calculation of the mass flows at the inlet and at the outlet of a pipe object is included in the pipe object model. A special application of a pipe object, called single junction pipe, consists of only one junction, without any control volumes.
- Branch objects: apply for any TFD Model described by an arbitrary system of non-linear ordinary differential equations or even algebraic equations.
- Special objects: used for components with complex geometry (e.g. the cross connection of pipes within a multi-channel representation).

Each fluid-dynamic object supports a subset of the entire ordinary differential equation (ODE) system of the fluid-dynamics, which is integrated simultaneously (time advancement) by the ODE-solver FEBE. Within the pipe objects, the ODEs are obtained from the partial differential equations by applying a spatial approximation method.

This object structure has been developed in order to allow the coupling of models of different physical formulation and spatial discretization techniques. The inclusion of new models (new object types) is facilitated by a standard implementation procedure, independently of the physical assumptions contained in the model.

### **2.3.3.3 Fluid-dynamics**

ATHLET offers the possibility of choosing between different models for fluid-dynamics simulation:

1. 5-equation model, with separate conservation equations for liquid and vapor mass and energy, and a mixture momentum equation, accounting for thermal and mechanical non-equilibrium, and including a mixture level tracking capability;

2. two-fluid model, with separate conservation equations for liquid and vapor mass, energy, and momentum (without mixture level tracking capability).

The spatial discretization is performed on the basis of a finite volume approach. It means, that the mass and energy equations are solved within control volumes, and the momentum equations are solved over flow paths - or junctions - connecting the centers of the control volumes. The solution variables are the pressure, vapor temperature, liquid temperature and mass quality within a control volume, as well as the mass flow rate (5-eq. model) or the phase mass velocities(6-eq. model) at a junction, respectively.

Two types of control volumes are available. Within the so-called “ordinary” control volume a homogeneous mass and energy distribution is assumed. Within the “non-homogeneous” control volume a mixture level is modeled. Above the mixture level steam with water droplets, below the mixture level liquid with vapor bubbles may exist. The combination of ordinary and non-homogeneous control volumes provides the option to simulate the motion of a mixture level through vertical components.

A full-range drift flux model is available for the calculation of the relative velocity between phases. The model comprises all flow patterns from homogeneous to separated flow occurring in vertical and horizontal two-phase flow. It also takes into account countercurrent flow limitations in different geometries. Moreover, both fluid-dynamic options allow for the simulation of non-condensable gases, on the basis of the ideal gas formulation, and additional mass conservation equations can be included for the description of boron transport within a coolant system as well of the transport and release of nitrogen dissolved in the liquid phase of the coolant. For pipe objects applying the 5-equation model, there is also the possibility to use the method of integrated mass and momentum balances (EIMMB-Method), an option for fast running calculations, mainly in the frame of a nuclear plant analyzer.

With the application of the EIMMB Method, the solution variables are now the average object pressure, the mass flows at pipe inlet and outlet, and the local qualities and temperatures. The local pressures and mass flow rates are obtained from algebraic equations as a function of the solution variables.

Another fluid-dynamic option, applied exclusively for the steady state calculation, consists of a 4-equation model, with balance equations for liquid mass, vapor mass, mixture energy and mixture momentum. The solution variables are the pressure, mass quality and enthalpy of the dominant phase within a control volume, and the mass flow rate at a junction. The entire range of fluid conditions, from subcooled liquid to superheated vapor, including thermal non-equilibrium, is taken into account, assuming the non-dominant phase to be at saturation.

### ***Numerical Methods***

The time integration of the thermo-fluid dynamics is performed with the general purpose ODE Solver called FEBE (Forward - Euler, Backward - Euler). It provides the solution of a general non linear system of differential equations of first order, splitting it into two subsystems,

the first being integrated explicitly, the second implicitly. Generally, the fully implicit option is used in ATHLET. The linearization of the implicit system is done numerically by calculation of the Jacobian matrix. A block sparse matrix package (FTRIX) is available to handle in an efficient way the repeated evaluation of the Jacobian matrix and the solution of the resulting system of linear equations. A rigorous error control is performed based on an extrapolation technique. According to the error bound specified by the user, the time step size and the order of the method ( greater than 2) are determined for every integration step.

### ***Heat Conduction and Heat Transfer***

The simulation of the heat conduction in structures, fuel rods and electrical heaters is performed within the basic module HECU. It permits the user to assign heat conduction objects (HCOs) to all thermal-fluid dynamic objects of a given network.

The one-dimensional heat conductor module HECU provides the simulation of the temperature profile and the energy transport in solid materials. The model has the following characteristics:

- the geometry of a HCO is constant in time;
- the model can simulate the one-dimensional temperature profile and heat conduction in plates, hollow and full cylinders in the radial direction;
- in each HCO up to three material zones can be modeled; a material zone is simulated by a problem dependent number of layers; the material zones can be separated by a geometrical gap and a corresponding heat transfer coefficient;
- the subdivision of material zones into layers can be performed on the basis of equal layer thicknesses, or equal layer volumes, as well as with layer thicknesses specified by input data;
- the HCOs can be coupled on left and/or right side to TFOs by consideration of the energy transport between heat conductor surface and the surrounding fluid; it is also possible to simulate a fluid temperature as boundary condition for the HCO by means of GCSM signals;
- the HCOs decompose into heat conduction volumes (HCVs) according to the nodalization of the adjacent TFOs and to user input;
- heat generation can be considered in material zones; the specific heat generation rate per volume unit is assumed to be distributed uniformly either within a material zone or a material layer.

The heat transfer package covers a wide range of single phase and two-phase flow conditions. Correlations for critical heat flux and minimum film boiling temperature are included. Evaporation and condensation directly at heating or cooling surfaces are calculated. A quench front model for bottom and top reflooding is also available.

## ***Nuclear Heat Generation***

The nuclear heat generation is generally modeled by means of the neutron kinetics module NEUKIN. For the simulation of electrically heated rods or for a simplified, straight-forward representation of a reactor core the total generated power as a function of time can be optionally given.

The generated nuclear reactor power consists of two parts: the prompt power from fission and decay of short-lived fission products, and the decay heat power from the long-lived fission products. The steady state part of the decay heat and its time-dependent reduction after a reactor scram are provided in form of a GCSM signal. The time-dependent behavior of the prompt power generation is calculated either by a point-kinetics model or by a one-dimensional neutron dynamics model. An input-specified fraction of the total power is assumed to be produced directly in the coolant. The remaining power determines the temperature distribution in the fuel rod, and the heat flux through the cladding surface.

The point-kinetics model is based on the application of the well-known kinetics equations for one group of prompt and for six groups of delayed neutrons. The reactivity changes due to control rod movement or reactor scram are given by a GCSM signal, where the GCSM (General Control Simulation Module) is a block-oriented simulation language for the description of control, protection and auxiliary systems. The reactivity feedback effects for fuel temperature, moderator density and moderator temperature are calculated either from dependencies given by input tables or with reference reactivity coefficients. If the boron tracking model is switched on, the reactivity feedback due to changes in the boron concentration will be also taken into account.

The one-dimensional model solves the time-dependent neutron diffusion equations with two energy groups of prompt neutrons and six of delayed neutrons. The active core zone can be subdivided into zones with different materials and a reflector zone can also be considered. The model includes the coarse-mesh spatial approximation of the neutron flux by means of second order polynomials. It also accounts for moderator and Doppler reactivity feedback by temperature and density dependent cross sections. Control rod movement and reactor scram are simulated by means of local changes of group cross sections as a function of rod position. Libraries of effective cross sections for several types of light water reactors are also available.

The module NEUKIN offers also a general interface for coupling of three-dimensional neutronic models. Several 3D codes (DYN3D[88], QUABOX[89]) have been successfully coupled to ATHLET (especially, for BWR analyses) with this interface.

## ***Simulation of Components***

In general, major plant components (e.g., pressurizer and steam generators) can be modeled by connecting thermo-fluid dynamic objects (TFOs) and heat conduction objects (HCOs) via input data. Simplified, compact models for those components are also available as special objects. Additional models are provided for the simulation of valves, pumps, accumulators, steam separators, single ended breaks, double ended breaks, fills, leaks and boundary conditions for pressure and enthalpy. Except for the separator model, they are comparable to the corresponding

models in other advanced codes. In fact, the steam separator model is an empirical approach for the calculation of carry-over and carry-under by means of input functions of the inlet mass flow rates, of the void fraction in the separator region, and of the mixture level outside the separator. Anomalous separator conditions, like flow reversal or flooding, can be simulated.

Critical discharge flow is calculated by a one-dimensional thermodynamic non-equilibrium model, with consideration of the current geometry of the discharge flow path. A pre-processing tool, called CDR1D, generates automatically the input tables needed in ATHLET for interpolation of the critical mass flow rates. Optionally, a homogeneous equilibrium model and the MOODY discharge model is available.

### ***Simulation of Control and Balance of Plant (BOP)***

The simulation of balance-of-plants systems within ATHLET is performed by the basic module GCSM

The user can model control circuits or even simplified fluid systems just by connecting basic functional blocks (e.g. switch, adder, integrator). Most of the system variables calculated within the fluid-dynamics, neutron kinetics or within other ATHLET modules (process variables) can be selected as input to these functional blocks. The output of such control blocks can be fed back to the thermo-fluid dynamics in form of hardware actions (e.g. valve cross sectional area, control rod position) or boundary conditions (e.g. temperature, heat and mass addition).

This simulation module allows for the representation of fluid-dynamic systems (e.g. steam line, condensate system) in a very simplified way (quasi stationary approach) with the advantage of requiring very little computation time in comparison with the fluid-dynamics module.

GCSM also provides a general interface to an external library of BOP models. This library contains detailed models with fixed structure and own input data for plant components (e.g. turbine, or even a containment model) or for control systems (e.g. power control, feed water control or pressurizer pressure control for typical power plants). The GRS containment codes CONDRU and COCOSYS have been coupled to ATHLET by means of this interface.

#### **2.3.3.4 Code handling**

ATHLET provides a free-format hierarchically structured input. Both the generation and the maintenance of the ATHLET input decks are facilitated by several copy functions and by the use of a flexible parameter technique during input data processing, which helps to avoid the repeated typing of identical or similar input data. An extended checking of both the input data and the program processing helps the user to discover input errors or modeling weaknesses affecting the code performance. Moreover, ATHLET provides a restart capability, and the program execution can be parallelized on computers with shared memory architecture using the Fortran OpenMP standard.

The ATHLET Program Package comprises also a series of auxiliary programs to support both the ATHLET users and developers in the application and development of ATHLET:

- G2: Generates GCSM input data from control diagrams (proprietary, license required);
- AIG: Graphical representation of the thermo-fluid and heat conduction objects of the input model;
- GIG: Graphical representation of the structure of GCSM controllers;
- Several programs for the post-processing of plot data (concatenation, merging, algebraic operations, etc.);
- JSPLIT: Generates time and locus diagrams exploiting the structure of the input model;
- ATLAS - DyVis: Dynamic visualization of the simulation results on the basis of AIG and GIG pictures;
- Several programs for the analysis of the Jacobian matrix (interdependencies, Eigenvalues, etc.).

Furthermore, ATHLET can be applied as process model of the ATLAS plant simulator providing full interaction and extended data visualization.

Finally, ATHLET runs under different computer operational systems (Windows, Unix, Linux). All supporting programs run under Windows, some of them also on other platforms.

### ***Validation***

The development of ATHLET was and is accompanied by a systematic and comprehensive validation program. The validation is mainly based on pre- and post-test calculations of separate effects tests, integral system tests, including the major International Standard Problems, as well as on real plant transients. A well balanced set of tests has been derived from the CSNI Validation Matrix, emphasizing the German combined ECC injection system. The tests cover phenomena which are expected to be relevant for all types of events of the envisaged ATHLET range of application in all common LWRs.

### 2.3.4 CATHARE-2 V2.5

The development of the Cathare2 (Code for Analysis of Thermal-Hydraulics during an Accident of Reactor and safety Evaluation) code was initiated in 1979 thanks to the joint effort of CEA, IRSN, EDF and FRAMATOME-ANP.

The objectives of the code are:

- to perform safety analyses with best estimate calculations of thermal-hydraulic transients in Pressurized Water Reactors for postulated accidents or other incidents, such as LBLOCA, SBLOCA, SGTR, Secondary breaks, Loss of Feed-Water;
- to quantify the conservative analyses margin;
- to investigate Plant Operating and Accident Management Procedures;
- to be used as a plant analyzer, in a full scope training simulator providing real time calculation.

Its applications [15] are limited to transients during which no severe damage occurs to fuel rods. The code is based on a two-fluid six-equation model. The presence of non-condensable gases (such as nitrogen, hydrogen, air and argon) can be modeled by one to four additive transport equations. A non-volatile component (as boron) and activity can be treated by the code.

The code is able to model any kind of experimental facility or PWR (western type and VVER), and is usable for other reactors (fusion reactors, RBMK reactors, BWR reactors and research reactors). Cathare2-V2.5 has also a new operator suitable for gas reactors (High Temperature Reactor "HTR", Gas Turbine Modular Helium Reactor "GT MHR", etc.) capable to model gas turbine or compressor, and for containment building modeling, new objects address to the interaction between primary circuit and containment building and to the containment condensation modeling. Moreover, new low pressure water properties are allowed by the activation of a special directive.

Cathare is widely used for research, safety and design purposes by French institutions (i.e. CEA, EDF, and IRSN) and it has been released also abroad to other institutions, i.e. to University of Pisa. Its applications mainly concern plant system and component designs, definition and verification of emergency operating procedures, investigations for new types of core management, new reactors and system designs, preparation and interpretation of experimental programs. For safety analysis, a methodology has also been developed in order to evaluate uncertainties on the code predictions.

#### 2.3.4.1 Code structure and models

Cathare2 has a modular structure. Several modules can be assembled to represent the primary and secondary circuits of any reactor and of any separate-effect or integral test facility. The modules are:

- the 1-D module to describe pipe flow,



- the 1-D module with tee used to represent a main pipe (1-D module) with a lateral branch (tee-branch); the T module predicts phase separation phenomena, and a specific modeling effort has been paid for cases where the flow is stratified in the main pipe,
- the volume module, a two-node module used to describe large size plena with several connections, such as the pressurizer, the accumulator, the steam generator dome or the lower plenum and upper plenum of a PWR; the volume predicts level swell, total or partial fluid stratification and phase separation phenomena at the junctions;
- the 3-D module to describe multidimensional effects in the vessel.

To complete the modeling of the circuits, sub-modules can be connected to the main modules:

- o the CCFL module which may be connected at any junctions, or at any vector node of the 1-D module, in order to predict the counter current flow limitation in complex geometries such as the upper core plate and the inlet of steam generator tubes;
- o the multi-layer wall module in which radial conduction is calculated;
- o the reflooding model with 2-D heat conduction in the wall or fuel rod for predicting quench front progression: both bottom up quenching and top-down quenching can be predicted;
- o the fuel pin thermo-mechanics sub-module, which can predict fuel cladding deformation, creep, rupture, clad oxidation and thermal exchanges;
- o heat exchangers between two circuits or between two elements of a circuit;
- o the point neutronics module (a 3-D neutronics code can also be coupled to Cathare2);
- o the accumulator sub-module;
- o sources and sinks, breaks, SGTR;
- o 1-node pump;
- o pressurizer sub-module based on Volume module with specific features;
- o valves, safety valves, check valves, flow limiters;
- o boundary conditions.

### ***Physical description***

All modules use the two-fluid model to describe steam-water flows and up to four non-condensable gases may be transported. Both thermal and mechanical non-equilibrium of the two phases are described. All kinds of two-phase flow patterns are modeled. Only two transitions are explicitly written and used in several closure terms of Cathare2:

- the transition between stratified and non-stratified flow, which depends on two criteria: a first criterion is based on Kelvin-Helmholtz instability threshold and the second depends on the relative effects of bubble sedimentation and of bubble turbulent mixing;
- the transition between annular and droplets flows; these two transitions describe the passage from a separate flow to a dispersed flow; co-current and counter-current flows are modeled with prediction of the Counter-Current Flow Limitation.

Heat transfer with wall structures and with fuel rods is calculated taking into account all heat transfer processes:

- natural and forced convection with liquid in both laminar and turbulent regimes;
- natural and forced convection with gas in both laminar and turbulent regimes;
- sub-cooled and saturated nucleate boiling with criteria for onset of nucleate boiling and net vapor generation;
- critical heat flux, dry-out criterion, rewetting temperature and transition boiling;
- film boiling for inverted annular, inverted-slug and dispersed flows;
- film condensation and effect of non-condensable gases;
- radiation to vapor and to liquid;
- enhancement model downstream a quench front.

The interfacial heat and mass transfers describe not only the vaporization due to superheated steam and the direct condensation due to sub-cooled liquid, but also the steam condensation or liquid flashing due to metastable sub-cooled steam or superheated liquid. The range of parameters is rather large: pressure from 0.1 to 25 MPa, gas temperature from 20°C to 2000°C, fluid velocities up to supersonic conditions, duct hydraulic diameter from 0.01 to 0.75 m.

### *System of equations*

Mass, momentum, and energy equations are established for any Cathare2 module. They are written for each phase. They are derived from exact local instantaneous equations, using some simplifications through physical assumptions and using time and space averaging procedures. One up to four transport equations can be added when non condensable gases are present. Fluid scalar properties, like pressure, enthalpy, density and void fraction, are represented by average fluid conditions viewed as being located at the mesh center (scalar point). Fluid vector properties, like velocity, are located at vector points (point between two meshes in axial elements) or at junctions.

### *Closure laws*

Closure relationships concern mass, momentum, and energy exchanges between phases and between each phase and the wall.

- o As far as possible, physical closure laws are developed on an experimental basis. Original correlations are developed when existing models are not satisfactory.
- o In the domain where experimental and theoretical knowledge is missing, extrapolations are adopted by making simple assumptions.
- o Thermal and mechanical transfers are interconnected.

As a first approximation, it is assumed that those mechanical interactions do not strongly depend on thermal exchanges. Mechanical terms are first derived from experiments where thermal non-equilibrium is negligible. Interfacial heat transfer terms are then derived. Finally, wall to fluid heat fluxes are correlated. Each closure law is unique. No choice between several correlations is proposed to the users in order to reduce the user effect.

### ***Differential terms***

- The mass term is added in momentum equations in order to better control the sonic velocity.
- Interfacial pressure difference term is taken into account in momentum equations in order to model level variation effects in stratified flows, and to ensure the hyperbolicity of the model.
- Cross-section area variation term is considered in momentum equations in order to model level effects in stratified flows in area reduction or enlargement.

### ***Wall and interfacial transfers***

Many correlations are original; some of them are listed in the following:

- o the interfacial friction correlations for bubbly-slug-churn flows;
- o the wall friction is mainly derived from a modified Lockhart-Martinelli correlation;
- o the wall heat transfer for dry wall situation; models parameters have been adjusted to fit reflooding data;
- o the flashing model; the correlation is mainly empirical and derived from the analysis of critical flow tests;
- o the direct contact condensation at safety injection; a semi-empirical correlation accounting the local effects of the Injection jet has been developed;
- o the non-condensable gas effect.

The modeling of mass diffusion effects is based on a classical heat and mass transfer analogy. An original procedure was developed in order to avoid the calculation of the interface temperature. The numerical method in the Cathare2 code uses a first order finite volume-finite difference scheme with a staggered mesh and the donor cell principle. Mass and energy equations use a conservative form and are discretized in order to keep a very good mass and energy conservation. The wall conduction is implicitly coupled to hydraulic calculations.

### ***Solution procedure***

A fully implicit numerical scheme was adopted in order to use-time steps as long as possible. The non linear system of equations is solved by a Newton-Raphson iterative method following several steps. At each iteration:

- increments of internal variables of each element are eliminated as function of increments of junction variables;
- increments of all junction variables are calculated.

All variable increments are regenerated and convergence tests are performed.

## 2.3.5 MARS

MARS (Multi-dimensional Analysis of Reactor Safety) code [31] has been developed by KAERI for the realistic multi-dimensional thermal-hydraulic system analysis of light water reactor transients. It is a versatile system analysis code for use in rulemaking, licensing audit calculations, evaluation of operator guidelines, and as a basis for a nuclear plant analyzer. Specific applications of this capability have included simulations of transients in LWR systems and also simulation of a wide variety of hydraulic and thermal transients in both nuclear and non nuclear systems involving steam-water non condensable solute fluid mixtures.

### 2.3.5.1 Development of MARS3.0

MARS development program consisted of three stages of code development [31], the MARS 1.x has been developed as a basic code frame for multi-dimensional thermal-hydraulic system analysis. MARS 2.x has been developed as a consolidated code for coupled analysis of multi-dimensional system thermal-hydraulics, 3-D core kinetics, core CHF and containment. MARS 3.x has been developed as a multi-purpose code for hydraulic analysis of new types of advanced reactors. Development of MARS 1.x has been completed by April, 1999, having as its backbones RELAP5/MOD3.2.1.2 [8] and COBRA-TF [33] codes that provide bases of System Analysis and 3-D Vessel Analysis modules of MARS respectively.

MARS version 1.1 was developed in early 1997, which implicitly coupled the numerical solution scheme of COBRA-TF and RELAP5/MOD3.2. COBRA-TF code was completely merged into RELAP5, including the 3D Vessel Analysis (COBRA-TF) and the System Analysis (RELAP5) modules of MARS. The programming language was converted into standard FORTRAN 90 to enhance the code portability. Next, MARS version 1.2 was developed in September 1997, where the System Analysis module of MARS 1.1 was replaced with RELAP5/MOD3.2.1.2 that possessed the outstanding models of AP600. And the input systems of both the System Analysis and 3D Vessel Analysis modules were unified using INP package, which enhanced user friendliness as well as code maintenance capability.

MARS version 1.3 was released in May 1998. In this occasion, the code was restructured and modernized using the new features of FORTRAN 90 and further unification of code models was carried out. The System Analysis module of the MARS was completely restructured using the modular data structure and the derived type variables of standard FORTRAN 90. This greatly improved the code readability and the code maintenance capability by removing the data management scheme based on the file transfer block (FTB) that used to be an obstacle in modifying the code models and correlations. Then, a dynamic memory management scheme was applied for each module, which enhanced the flexibility of memory requirement and reduced the size of hard disk for restart file storage. Then, the code was modernized to have on-line graphic display of calculated results using Windows graphic. As part of code unification works, the light water property routines of equation-of-state (EOS) were unified such that the light water property routines of the 3D Vessel Analysis module were completely replaced with those of the System Analysis module. Also, the transport properties of light water were improved to represent new ASME '92 water and steam properties.

MARS version 1.4 was released in April 1999 by extending the code modeling capability and enhancing the user friendliness. The point kinetics model was implemented into heat structure models of the 3D Vessel Analysis module to simulate core power transients. Heat structure models of both modules were coupled so that the heat structure models of the System Analysis module can simulate the heat structures facing the hydrodynamic volumes of either the System Analysis or 3D Vessel Analysis modules. The control functions of the System Analysis module were improved for the extended use of 3D Vessel Analysis module variables and the input check function in the 3D Vessel Analysis module was added for user friendliness. The automatic initialization function of the 3D Vessel Analysis module was added in the code, which greatly enhanced the user convenience in the simulation of a full three-dimensional system. Also, new features of RELAP5/MOD3.2.2  $\beta$  version were implemented in the System Analysis module, which included the reflood model, CHF model, the Courant time step control, etc.

Development of MARS version 2.x has been commenced starting from April, 1999. Major scopes of the development were the implementation of coupled analysis capability of three-dimensional reactor kinetics, containment and CHF, the improvement of thermal-hydraulic and numerical models and the enhancement of user friendliness. The dynamic link library (DLL) technique of Windows was used for the coupling of independent kinetics and containment codes. For user-friendliness, both on-line and off-line GUI routines were incorporated using QUICKWIN features of Visual FORTRAN90 compiler. The MARS 2.1 version has been released in March 2002. After the release of MARS 2.1, efforts to extend the code capability to the severe accident analysis and multidimensional turbulence models have been done. The severe accident analysis code, MIDAS was linked and resumes the calculation through data transfer after the completion of MARS calculation. The MULTID component which has a turbulence mixing model and conduction model has been installed as a new component of MARS system module. The new capability for gas cooled reactor analysis was also added by using gas property tables and new heat transfer correlations. The last version of this series is MARS3.0, which was released in 2005.

MARS runs on Windows platform, and can also be connected, by means of dynamic linkage using DLLs, to 3D kinetics codes and containment analysis codes such as MASTER and, CONTAIN and CONTEMPT.T-H modeling capability of the MARS is being improved and extended for application not only to light and heavy water reactors but also to research reactors and many advanced reactor types. Many other models and capabilities were added into the first version and the last version of the development is MARS version 3. Now this version of MARS is currently a popular multi-dimensional thermal-hydraulic tool in use for the analyses of reactor transients, experiment facility simulations and various safety research purposes.

The developmental assessment problems performed using MARS involve the assessment of system analysis module derived from RELAP5/MOD3.2 and that of 3D vessel analysis module derived from COBRA-TF. The problems are divided into four categories: phenomenological problems; separate effects-problems; integral problems; and plant application. Additional assessment activity has been conducted in the framework of cooperative agreement between Korean Institution for Nuclear Safety (KINS) and the University of Pisa specifically focused on

the assessment of 3D capability of the MARS code. During the collaboration both single phase and two phase code performances have been tested and compared against suitable experimental data ([34], [35]).

## 2.4 Sub-channel codes

This class of codes ([36], [37]) is used to analyze the flow distribution inside a fuel assembly and for multi-component modeling in the core. Sub-channel codes can be used to perform pin-by-pin thermo-hydraulic calculations. The simulated volume is divided into several parallel channels. In each channel, properties like temperature, density or pressure, only depend on the axial height. Cylindrical rods and gaps delimit these sub-channels (see Figure 2-7). Gaps can be opened or closed: in the first case, interaction between the channels, called “cross flow”, is possible, in the second case it is not possible. Modern fuel bundle designs with part length rods and large water holes pose new challenges to the sub-channel codes: the proper prediction of the void distribution within the bundle, especially near the non-heated water rods, may require improvements in the so-called lateral void drift modeling [40].

Normally a 3D model for the two-phase flow, 1D models of the different fuel rods and detailed models for the heat transfer between the cladding surface and the coolant are included.

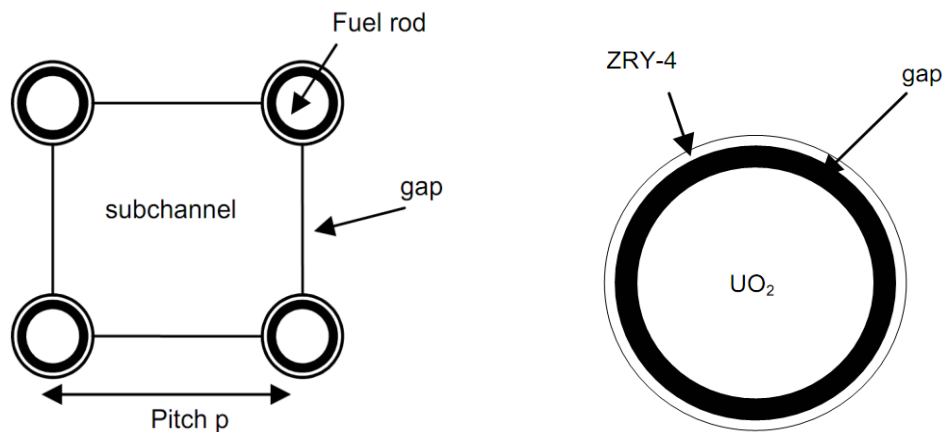


Figure 2-7. Scheme of a sub-channel and fuel rod [37]

### 2.4.1 COBRA-EN

The COBRA-EN code was developed as an upgrade of the COBRA-3C/MIT code [38] in the 80's. It is used for Thermal-Hydraulic Analyses of Light Water Reactor Fuel Assemblies or Cores. After being improved with the VIPRE features and with some EPRI correlations, it was widely used to verify the SBWR and AP600 design in the safety studies relating to the reactivity transient accidents [39]. In COBRA-EN, both transient and steady state analyses are possible. Starting from a steady-state condition in a LWR core or fuel element, the code allows to simulate the thermal-hydraulic transient response to user-supplied changes of the total power, of the outlet pressure and of the inlet enthalpy and mass flow rate.

The underlying principles of this code are related to several theoretical models. A general outline here, whereas [38] presents a more detailed overview. It is based on a Flow Field Model, which describes the mass flux of liquid and vapor through the system and a Heat Transfer Model, treating the heat flux inside the fuel rod and the heat exchange with the coolant.

### ***Flow Field model***

The COBRA-EN Flow Field Model is based on three partial differential equations (i.e. a three-equation model) that, using what is known as "sub-channel approximation", describes the conservation of mass, energy and momentum vector in axial and lateral directions for the water liquid/vapor mixture. Optionally, a fourth equation (resulting in a four-equation model) can be added which tracks the vapor mass separately and which, along with the correlations for vapor generation and slip ratio, replaces the subcooled quality and quality/void fraction correlations, needed to extend the capabilities of the essentially homogeneous three-equation model [39].

If the computational domain is subdivided into a number of axial intervals, the control volume for mass, energy and axial momentum is a segment of sub-channel while the control volume for the lateral momentum is a segment of the somewhat arbitrary region which straddles the two adjoining sub-channels around a lateral gap. In each control volume, the flow equations (as well as the one-dimensional (r) heat conduction equations in the fuel rods) are approximated by finite differences. The resulting equations for the hydrodynamic phenomena form a system of coupled nonlinear equations that are solved either by an implicit iterative scheme based on the calculation of the pressure gradients in the axial direction or by a Newton-Raphson iteration procedure.

The finite-difference mass, energy and momentum balance equations are shown in the following. A detailed description of them can be found in [37] and [38].

#### Mass balance equation:

$$A_i \frac{\Delta X_j}{\Delta t} (\rho_{ij} - \rho_{ij}^n) + m_{ij} - m_{ij-1} + \Delta X_j \sum_{k \in i} e_{ik} w_{kj} = 0 \quad (49)$$

#### Energy balance equation:

$$\begin{aligned} & \frac{A_i}{\Delta t} \left[ \rho_{ij}'' (h_{ij} - h_{ij}^n) + h_{ij} (\rho_{ij} - \rho_{ij}^n) \right] + \frac{1}{\Delta X_j} (m_{ij} h_{ij}^* - m_{ij-1} h_{ij-1}^*) + \sum_{k \in i} e_{ik} w_{kj} h_{kj}^* = \\ & = \sum_{r \in i} P_r \Phi_{ir} q'_{rj} - \sum_{k \in i} w'_{kj} (h_{ij} - h_{nj}) - \sum_{k \in i} C_k s_k (T_{ij} - T_{nj}) + \sum_{r \in i} r_Q \Phi_{ir} q'_{rj} \end{aligned} \quad (50)$$

#### Momentum balance equations:

- Axial momentum balance

$$\begin{aligned} & \frac{\Delta X_j}{\Delta t} (m_{ij} - m_{ij}^n) + m_{ij} U'_{ij} - m_{ij-1} U'_{ij} + \Delta X_j \sum_{k \in i} e_{ik} w_{kj} U'_{kj} = \\ & - A_i (P_{ij} - P_{ij-1}) - g A_i \Delta X_j \rho_{ij} \cos \theta - \frac{1}{2} \left( \frac{\Delta X f \phi^2}{D_h \rho_l} + K v^* \right) \Big|_{ij} \frac{m_{ij}}{A_i} - f_r \Delta X_j \sum_{k \in i} w'_{kj} (U'_{ij} - U'_{nj}) \end{aligned} \quad (51)$$

- Lateral momentum balance

$$\frac{\Delta X_j}{\Delta t} (w_{kj} - w_{kj}^n) + \bar{U}'_{kj} w_{kj}^* - \bar{U}'_{kj-1} w_{kj-1}^* = \frac{s_k}{l_k} \Delta X_j P_{kj-1} - \frac{1}{2} \left( K_G \frac{\Delta X v^*}{sl} \right) \Big|_{kj} w_{kj} \quad (52)$$



## Heat Transfer model

The Heat Transfer Model consists of a model for the heat conduction inside the rod and of a model for the heat exchange between rod and coolant.

By using the fuel rod heat conduction model, the temperature distribution in the cylindrical fuel rod is calculated at each axial level. Axial heat conduction is neglected compared to that in the radial direction. The heat balance equation in radial direction is approximated with the first order finite-difference equation (Eq. (53)).

The fuel rod consists of the fuel pellet, the clad and a gap. Five (or more) nodes are reserved for the fuel pellet, two for the clad (see Figure 2-8).

$$(\rho C_p V)_i \frac{\partial T_i}{\partial t} = Q_{i-1,i} + Q_{i+1,i} + Q_i''' V_i \quad (53)$$

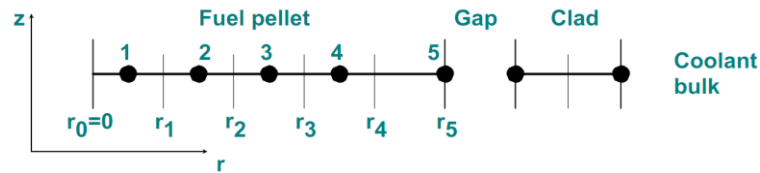


Figure 2-8. Fuel rod mesh [37]

The Surface Heat Transfer model describes the transfer of heat between clad and coolant liquid. The rod-to-coolant heat transfer model is featured by a full boiling curve (see Figure 2-9), comprising the basic heat-transfer regimes (forced convection, nucleate boiling, transition and film boiling), each represented by a set of optional correlations for the heat-transfer coefficient. However, in a PWR only single-phase forced convection and nucleate boiling (Thom correlation) appear, except in case of an accident.

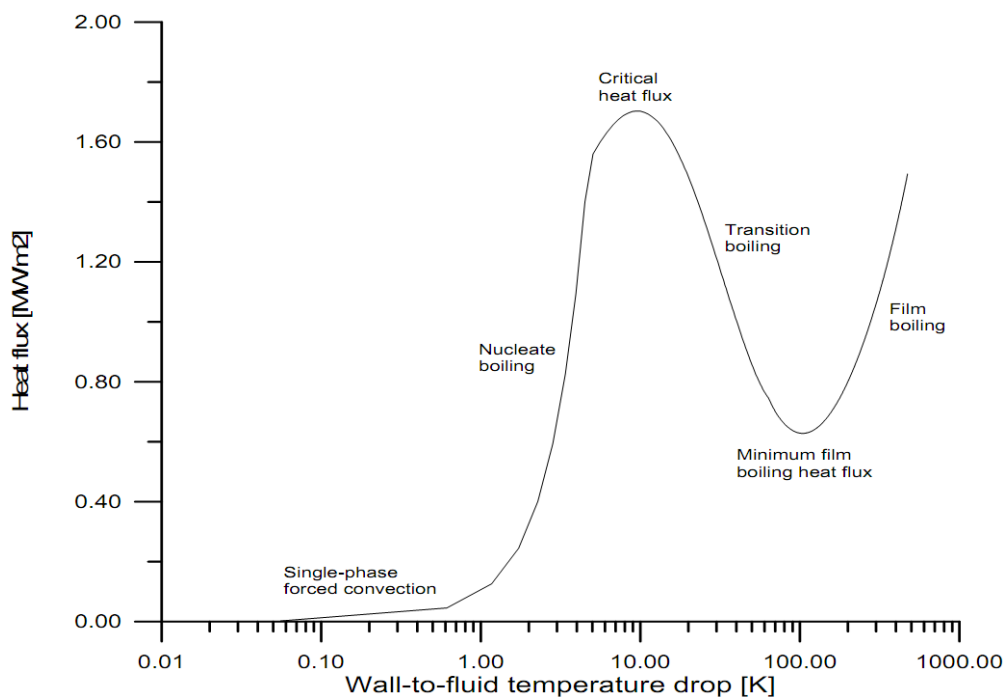


Figure 2-9. Heat flux as function of superheat [37]

The heat transfer coefficient of the liquid phase forced convection is calculated by Dittus-Boelter formula [27], while the heat transfer coefficient for nucleate boiling by (54) the mentioned Thom correlation [41]:

$$H_{T_{\text{hom}}} = \left[ e^{P/1260} \cdot (T_w - T_{\text{sat}}) / 0.072 \right]^2 / (T_w - T_b) \quad (54)$$

## 2.4.2 VIPRE-W

VIPRE-W [42] is Westinghouse's version of the VIPRE-01 code [41] developed under the sponsorship of the Electric Power Research Institute (EPRI). VIPRE-01 was developed based on several versions of the COBRA code by the Battelle Pacific Northwest Laboratories.

The VIPRE-W code is currently used for various core thermal-hydraulic risk and safety analysis calculations, in particular for PWR non-LOCA core thermal-hydraulics safety analysis [43]. With respect to VIPRE-01, VIPRE-W contains additional features and enhancements for reactor core design applications [43]. Some of them include models for post-CHF fuel temperature calculations, fuel boiling duty evaluation at highly subcooled boiling conditions [42] and linkage to software libraries containing proprietary correlations and models. These new features enhance the code capability for PWR core design and licensing applications, without altering the fundamental solution scheme of the VIPRE-01 code. The available VIPRE-01 models are described in detail in [41].

VIPRE-W solves the mass, momentum (axial and lateral) and enthalpy conservation equations for the two-phase mixture (three-equation model) and the void is calculated via a constitutive relation. Alternatively, the mass conservation equation for the vapor phase can also be solved along with a drift flux velocity accounted for in the mixture momentum equation (four-equation drift flux model) [45].

### *Cross-flows*

VIPRE-W code – like most two-phase sub-channel codes – models two types of lateral transport mechanisms, usually referred to as diversion cross-flows and turbulent mixing, respectively [44]. The diversion cross-flow is a net mass-flow from one sub-channel to a neighbor sub-channel driven by a lateral pressure gradient. In VIPRE and most similar codes it is assumed that the enthalpy carried with the diversion cross-flow is the mixture enthalpy of the donor (i.e. upstream) sub-channel.

The turbulent mixing, on the other hand, may be modeled in various ways. In single-phase flow it would typically correspond to the transport of heat from one sub-channel to a neighbor without net mass-transport by heat conduction and by random turbulent motions of the fluid. This concept has been carried over to the VIPRE-W model even though it is not obvious that the mass-transport should be zero (this issue is further discussed by Lahey and Moody [47]) when a net density gradient is present as in two-phase flows [46]. The VIPRE-W model for turbulent mixing assumes no mass-transfer (in addition to the diversion cross-flow) but a net

transport of enthalpy equal to  $w_{TM} \Delta h$ , where  $w_{TM}$  is a virtual mass-exchange rate per unit axial length and  $\Delta h$  is the difference in mixture enthalpies between the two neighbor sub-channels.

### 2.4.3 FLICA-OVAP

The FLICA-OVAP code [48] is being developed at the *Commissariat à l'énergie atomique et aux énergies alternatives* (CEA), France. FLICA-OVAP is an advanced two-phase flow thermal-hydraulics code based on a full 3D sub-channel approach. It can simulate flows in Light Water Reactors cores such as PWRs, BWRs and experimental reactors. To increase its feasibility to multiple industrial applications, the FLICA-OVAP platform [49] contains several models: the Homogeneous Equilibrium model, the drift flux model, the two-fluid model and also a general multi-field model, with a variable number of fields for both vapor and liquid phases. For each of them, an adapted set of closure laws is proposed concerning mass and heat transfer, interfacial and wall forces and turbulence.

Hereafter, the four-equation drift-flux model (for the sake of simplicity without taking into account porosity) and the most important correlations (wall transfer, mass transfer) coming directly from FLICA-4 code [50], are mentioned.

The two phases are assumed to be at the same pressure, while the relative velocity between liquid and vapor phases is taken into account by a kinetic constitutive equation.

Mixture mass conservation:

$$\frac{\partial}{\partial t} \left( \sum_{k=v,\ell} \alpha_k \rho_k \right) + \nabla \cdot \left( \sum_{k=v,\ell} \alpha_k \rho_k \mathbf{u}_k \right) = 0 \quad (55)$$

Mixture momentum balance:

$$\frac{\partial}{\partial t} \left( \sum_{k=v,\ell} \alpha_k \rho_k \mathbf{u}_k \right) + \nabla \cdot \left( \sum_{k=v,\ell} \alpha_k \rho_k \mathbf{u}_k \otimes \mathbf{u}_k \right) + \nabla P - \nabla \cdot \left( \sum_{k=v,\ell} \alpha_k \underline{\underline{\tau}}_k \right) = \rho \mathbf{g} + \mathbf{F}_w \quad (56)$$

Mixture energy balance:

$$\frac{\partial}{\partial t} \left( \sum_{k=v,\ell} \alpha_k \rho_k E_k \right) + \nabla \cdot \left( \sum_{k=v,\ell} \alpha_k \rho_k H_k \mathbf{u}_k \right) - \nabla \cdot \left( \sum_{k=v,\ell} \alpha_k \mathbf{q}_k \right) = q_w + \rho \mathbf{g} \cdot \mathbf{u} \quad (57)$$

Vapor mass conservation:

$$\frac{\partial}{\partial t} (\alpha_v \rho_v) + \nabla \cdot (\alpha_v \rho_v \mathbf{u}_v) - \nabla \cdot (K_c \nabla c) = \Gamma_v \quad (58)$$

this latter is added to take into account the thermal disequilibrium or subcooled boiling flows.

#### *Drift-flux correlations*

FLICA-OVAP includes several Zuber-Findlay type correlations in order to estimate the relative velocity  $\mathbf{u}_r = \mathbf{u}_v - \mathbf{u}_\ell$  between vapor and liquid phases. Chexal-Lellouche correlation [51] and a correlation derived from Ishii [52] are also implemented.

### ***Wall heat transfer***

Nusselt number and bulk temperature are defined according to the heat transfer regime (single-phase convection heat transfer, subcooled nucleate boiling, saturated nucleate boiling, etc.).

For example, the single-phase heat transfer coefficient is obtained by the Dittus-Boelter correlation [27]. The onset of significant void (OSV), that is the transition between single-phase heat transfer and subcooled nucleate boiling (SNB), is predicted according to Jens and Lottes correlation [53], which allows estimating the minimum wall superheating  $\Delta T_{\text{sat}}$  demanded to achieve net vapor generation.

### ***Pressure drops***

The friction  $F_w$  appearing in Eq. (56) is the sum of the singular friction due to the assembly grids or other pressure drops  $F_{\text{sing}}$  and the distributed friction on wall  $F_{\text{frict}}$ . The Darcy-Weisbach friction factor used to compute the distributed friction is the product of the isothermal friction factor, the heating wall correction factor and the two-phase multiplier.

Further details on the numerical methods and the models of the FLICA-OVAP code can be found in [49], [48].

## **2.5 Computational Fluid-Dynamics (CFD) codes**

Computational Fluid Dynamics (CFD) is a well-established industrial design tool for non-nuclear applications, helping to reduce design time scales and to improve processes throughout the engineering world, providing a cost-effective and accurate alternative to scale model testing.

Within the Nuclear Reactor Safety (NRS) framework, the traditionally adopted tools for safety analysis evaluation (i.e. integral thermal-hydraulic codes) are not capable of predicting the effect of inherently three-dimensional flow fields and mixing phenomena in complex geometries. Therefore, the application of CFD techniques is considered to potentially bring real benefits in terms of deeper understanding of involved phenomena and of increased safety.

However, in many statements about the need to further validate CFD codes for nuclear reactor applications, there is an underlying belief that, behind the attractive features of CFD interfaces, there is not a completely reliable predictive tool, at least not reliable enough for being applied to safety related problems. CFD codes are not yet – generally speaking – fully reliable tools: being inherently “three-dimensional” and “local” does not constitute a sufficient condition for assuring that 3D and local phenomena are accurately predicted. On the other hand, intensive CFD codes development and assessment work have been and are being carried out in recent years, made more and more effective by the availability of increasing computing resources.

Such advancements are certainly oriented to obtaining reliable and efficient predictive tools; however, some additional efforts are necessary to meet the quality assurance requirements that would make such tools applicable to the nuclear reactor technology, and in particular to the safety analysis within the licensing process.

### **2.5.1 The Role of CFD Codes in Nuclear Reactor Safety Analyses**

A description of the state-of-the-art in the application of CFD codes to NRS problems [60] has recently been produced by the three “Writing Groups on CFD”. Those groups of experts were created by the CSNI in 2002 with the aims of providing Best Practice Guidelines (BPG), evaluating the existing CFD assessment database and related limitations, and exploring the possibilities of extension to two-phase flows. They have met until the end of 2006, 2007 and 2008 respectively, and the result of their work is summarized in several reports (e.g. [54], [55], [57]).

Moreover, several experimental campaigns and code development and assessment activities have been carried out in the recent years, both in international and national frameworks, as well as international workshops and conferences devoted to the CFD application in the nuclear field.

#### **2.5.1.1 Identification of NRS issues requiring CFD**

An important outcome of the work done by one of the CSNI Writing Groups on CFD has been a sort of classification of a number of NRS problems identified as needing the support of CFD.

Such problems are indicated in Table 2-1 (extracted from [55]), along with the following information:

- related part of the nuclear system (reactor core, primary/secondary circuit, containment);
- relevant to normal operation, Design Basis Accident (DBA) or Beyond Design Basis Accident (BDBA);
- involving single-phase or two-phase flow (or both).

**Table 2-1. NRS issues needing CFD [55]**

<b>NRS problem</b>	<b>System classification</b>	<b>Incident classification</b>	<b>Single- or multi-phase</b>
Erosion, corrosion and deposition	Core, primary and secondary circuits	Operational	Single/Multi
Core instability in BWRs	Core	Operational	Multi
Transition boiling in BWR/determination of MCPR	Core	Operational	Multi
Recriticality in BWRs	Core	BDBA	Multi
Reflooding	Core	DBA	Multi
Lower plenum debris coolability/melt distribution	Core	BDBA	Multi
Boron dilution	Primary circuit	DBA	Single
Mixing: stratification/hot-leg heterogeneities	Primary circuit	Operational	Single/Multi
Heterogeneous flow distribution (e.g. in SG inlet plenum causing vibrations, HDR experiments, etc.)	Primary circuit	Operational	Single
BWR/ABWR lower plenum flow	Primary circuit	Operational	Single/Multi
Water-hammer condensation	Primary circuit	Operational	Multi
Pressurised Thermal Shock (PTS)	Primary circuit	DBA	Single/Multi
Pipe break – in-vessel mechanical load	Primary circuit	DBA	Multi
Induced break	Primary circuit	DBA	Single
Thermal fatigue (e.g. T-junction)	Primary circuit	Operational	Single
Hydrogen distribution	Containment	BDBA	Single/Multi
Chemical reactions/combustion/detonation	Containment	BDBA	Single/Multi
Aerosol deposition/atmospheric transport (source term)	Containment	BDBA	Multi
Direct-contact condensation	Containment/Primary	DBA	Multi
Bubble dynamics in suppression pools	Containment	DBA	Multi
Behavior of gas/liquid surfaces	Containment/Primary	Operational	Multi
Special considerations for advanced (including Gas-Cooled) reactors	Containment/Primary	DBA/BDBA	Single/Multi

### 2.5.1.2 State-of-the-art in CFD Quality Assurance

The application of numerical analysis tools to problems connected to nuclear technology should be performed so as to reduce the related uncertainties and inaccuracies as far as possible, to collect all the necessary information to assess the degree of reliability of the results, and to optimize the exploitation of the available computational resources. This is what, in other terms, can be referred to as the “quality assurance” of the analyses.

An efficient means to implement a quality-oriented approach in the use of codes consists in providing the user with written guidance on the “best practice” to follow when addressing given problems, where the “best practice” is the synthesis of all the experience achieved by the most advanced users on those problems and of the common knowledge about capabilities and limitations of the tools.

In 2002, the “BPGs for the CFD Code Validation for Reactor-Safety Applications” were produced as the first deliverable of the ECORA Project [57]: these are the first official guidelines for CFD oriented to nuclear applications, even though they are quite general and do not address specific problems.

The need of establishing BPG was then recognized by the CSNI: a group composed by 15-20 experts of CFD and nuclear reactor technology came out with the “Best Practice Guidelines for the use of CFD in Nuclear Reactor Safety Applications” [54], which represent a further milestone in the process of quality assurance establishment. Again, also this latter document is incomplete and not exhaustive. It provides useful guidance for a range of single phase applications to a relatively general level of detail; however, a deeper level of specificity is envisaged for each application, but not covered by the document, which is thus intended as the preliminary part of a wider set of (future) guidelines addressing thoroughly many specific problems.

It is worth recalling the IAEA/NEA Technical Meeting on the “Use of CFD codes for safety analysis of reactor systems”, which was hosted by the University of Pisa in 2002, and which provided a comprehensive view of the current state-of-the-art (see [58]). The recommendation to establish BPG for the application of CFD codes to nuclear reactor safety problems was one of the main outcomes of the meeting.

The topics covered by the CSNI BPGs are reported in the list below, which also indicates the structure of the BPG report.

1) Problem definition:

- a) isolation of the problem;
- b) Phenomena Identification and Ranking Table (PIRT);
- c) considerations on special phenomena.

2) Selection of appropriate simulation tool:

- a) classical thermal-hydraulic system code;
- b) component code;

- c) CFD code;
  - d) potential complementary approaches (e.g. CFD-1D coupling).
- 3) User selection of physical models:
- a) guidelines for turbulence modeling in NRS applications;
  - b) buoyancy model;
  - c) heat transfer;
  - d) free surface modeling;
  - e) fluid-structure Interaction.
- 4) User control of the numerical model:
- a) transient or steady-state model;
  - b) grid requirements;
  - c) discretization schemes;
  - d) convergence control;
  - e) free surface consideration.
- 5) Assessment strategy:
- a) demonstration of capabilities;
  - b) interpretation of results.
- 6) Verification of the calculation and numerical model:
- a) error hierarchy;
  - b) round-off errors;
  - c) spatial discretization errors;
  - d) time discretization errors;
  - e) software and user errors.
- 7) Validation of results:
- a) validation methodology;
  - b) target variable and metrics;
  - c) treatment of uncertainties.
- 8) Documentation.

A detailed discussion of the above topics is not presented here. However it is worth underlying the fact that each single step of the analysis, from the definition of the problem through the meshing, the simulation set-up and the result post processing and comparison to the final documentation, is identified and considered analytically.

In particular, a special effort is required to assess the errors affecting the results, which implies that a large number of sensitivity analyses have to be performed. This aspect makes the systematic application of the BPGs a huge task, since the computational cost to be allocated can easily grow by orders of magnitude (e.g., grid sensitivity studies are often missing in published works and demonstrations of the achievement of grid-independence of the results are very rare). Nevertheless, the efforts to follow this quality-oriented approach as far as allowed by the available resources appear to be rapidly growing. The idea that demonstrating the quality of the



performed CFD analysis is an essential step of the analysis itself is becoming more and more widely accepted.

## **2.5.2 Introduction to CFD Techniques**

CFD is a computer-based tool for simulating the behavior of systems involving fluid flow, heat transfer, and other related physical processes. It works by solving the equations of fluid flow (accounting in detail for turbulence effects) over a region of interest, with specified boundary conditions.

For many years numerous programs have been written to solve either specific fluid flow problems or specific classes of fluid flow problems. From the mid-1970's, the complex mathematics required to generalize the algorithms began to be understood, and general purpose CFD solvers were developed. These began to appear in the early 1980's and required what were then very powerful computers, as well as an in-depth knowledge of fluid dynamics, and large effort to set up simulations. Consequently, CFD was a tool used almost exclusively in research.

Recent advances in computing power, together with powerful graphics and interactive 3D manipulation of models have made the process of setting up a CFD model and analyzing results much less labor intensive, reducing time and, hence, cost. Advanced solvers contain algorithms which enable robust solutions of the flow field in a reasonable time. As a result of these developments, CFD is now an established industrial design tool, helping to reduce design time scales and improve processes throughout the engineering world. CFD provides nowadays a cost-effective and accurate alternative to scale model testing, with variations on the simulation being performed quickly, offering obvious advantages.

### **2.5.2.1 Numerical Models**

The set of equations that describe the processes of momentum, mass and heat transfer are known as the Navier-Stokes equations. These partial differential equations were derived in the early nineteenth century and have no known general analytical solution (except for simple problems in extremely simple geometry) but can be discretized and solved numerically.

There is a number of different solution methods which are used in CFD codes; the most widely used is known as the finite volume technique. In this technique, the region of interest is divided into small sub-regions, called control volumes. The equations are then discretized and solved iteratively for each control volume. As a result, an approximation of the value of each variable at specific points throughout the domain can be obtained. Other possible solving approaches would be the "finite difference method" and the "finite element method", which however are not commonly used in CFD-type codes.

Equations describing other processes, such as combustion, chemical reactions or particle transport, can also be solved in conjunction with the Navier-Stokes equations. Usually, an approximating model is used to derive these additional equations, turbulence models being a particularly important example.

A brief definition of the most common approaches in turbulence modeling are provided here as part of basic CFD terminology. Distinctions between the approaches are based on the standard view of turbulence as a superposition of eddies with a continuous distribution of sizes. Selecting a modeling approach is a question of how much of this eddy spectrum is resolved in the direct solution of the Navier-Stokes equations and how much is relegated to special auxiliary models.

#### Reynolds Averaged Navier Stokes (RANS)

RANS is most clearly defined in simulations of “steady” flow. The time independent mean flow field is obtained from Navier-Stokes equations, and mean effects of all turbulence are captured in a separate model. In transient simulations, the time averaging imposed on the Navier-Stokes equations is on a large enough scale that everything recognized as turbulence is filtered, and must be modeled separately.

#### Direct Numerical Simulation (DNS)

DNS takes advantage of the fact that turbulence is part of any detailed solution of the Navier-Stokes equation. In this approach a fine enough computational mesh is introduced to resolve all significant scales of turbulence and no special turbulence models are needed. Unfortunately, turbulence theory tells us that the smallest persistent eddy diameter is roughly proportional to the Reynolds number to the minus three-quarters power ( $1/Re^{3/4}$ ). This means that the number of mesh points in 3D DNS is in the scale of  $Re^{9/4}$ , and only a very limited range of problems can be solved with DNS on current computers.

#### Large Eddy Simulation (LES)

LES is a family of methods that compromise between RANS and DNS. Large-scale eddies are resolved in the flow equation solution, and effects of small-scale eddies are obtained from a special model. This implies a cut-off size in the LES model separating the two scales. This cut-off is small enough that turbulence models for smaller scales can be significantly simpler than those required for good results with RANS.

#### Detached Eddy Simulation (DES)

DES is a further compromise between RANS and LES, to capture key physical phenomena in the lowest possible amount of computer time. A decision is made on spatial regions that are adequately modeled by RANS and those requiring LES. An example is simulation of vortex shedding from the trailing edge of some solid structure. Boundary layers and more far-field flows can be simulated well with RANS. However, the region downstream of the structure would require a finer mesh, and a flag activating LES.

### **2.5.2.2 Examples of Reynolds-Averaged Navier-Stokes equations**

When dealing with a single-phase, non compressible, turbulent flow problem, the continuity equation (59) and the Navier-Stokes equation are solved, “coupled” with further equations

associated to turbulence modeling (except when Direct Numerical Simulation – DNS, is performed), to energy conservation (if relevant) and transport of scalars (if relevant). For further details on turbulence modeling see Ref. [59].

The most common approach to turbulence modeling for “industrial” applications consists of solving Reynolds-Averaged Navier-Stokes (RANS) equations (60) coupled with a two-equation turbulence model derived from the “eddy viscosity” (or Boussinesq’s) hypothesis. Two-equation models are the  $k$ - $\varepsilon$  and the  $k$ - $\omega$  models, and several variants stemming from them. For example, the  $k$ - $\varepsilon$  model requires solving Eq. (61) and (62) for the turbulent kinetic energy ( $k$ ) and the rate of dissipation of turbulent kinetic energy ( $\varepsilon$ ) respectively.

$$\frac{\partial \rho}{\partial t} + \nabla \cdot (\rho \mathbf{U}) = 0 \quad (59)$$

$$\frac{\partial \rho \mathbf{U}}{\partial t} + \nabla \cdot (\rho \mathbf{U} \otimes \mathbf{U}) - \nabla \cdot (\mu_{eff} \nabla \mathbf{U}) = \nabla p' + \nabla \cdot (\mu_{eff} \nabla \mathbf{U})^T + \mathbf{B} \quad (60)$$

$$\frac{\partial (\rho k)}{\partial t} + \nabla \cdot (\rho \mathbf{U} k) = \nabla \cdot \left[ \left( \mu + \frac{\mu_t}{\sigma_k} \right) \nabla k \right] + P_k - \rho \varepsilon \quad (61)$$

$$\frac{\partial (\rho \varepsilon)}{\partial t} + \nabla \cdot (\rho \mathbf{U} \varepsilon) = \nabla \cdot \left[ \left( \mu + \frac{\mu_t}{\sigma_\varepsilon} \right) \nabla \varepsilon \right] + \frac{\varepsilon}{k} (C_{\varepsilon 1} P_k - C_{\varepsilon 2} \rho \varepsilon) \quad (62)$$

The values calculated for  $k$  and  $\varepsilon$  are used to evaluate the eddy (or turbulent) viscosity  $\mu_t$  (Eq. (63)) and then the effective viscosity  $\mu_{eff}$  (Eq. (64)).

$$\mu_t = C_\mu \rho \frac{k^2}{\varepsilon} \quad (63)$$

$$\mu_{eff} = \mu + \mu_t \quad (64)$$

Note that Eq. (60) contains a modified pressure term which is related to the turbulent kinetic energy as the following

$$p' = p + \frac{2}{3} \rho k \quad (65)$$

The above mentioned energy conservation equation may be formulated in terms of enthalpy:

$$\frac{\partial (\rho h_{tot})}{\partial t} - \frac{\partial p}{\partial t} + \nabla \cdot (\rho \mathbf{U} h_{tot}) = \nabla \cdot (\lambda \nabla T) + S_E \quad (66)$$

where the “total” enthalpy  $h_{tot}$  is defined as

$$h_{tot} = h + \frac{1}{2} U^2 \quad (67)$$

Finally, a transport equation for a scalar (such as a chemical species transported by the flow) can be expressed as:

$$\left(\frac{\partial \phi}{\partial t} + \nabla \cdot (U\phi)\right) = \nabla \cdot \left( \left( \rho D_\phi + \frac{\mu_t}{Sc_t} \right) \nabla \cdot \left( \frac{\phi}{\rho} \right) \right) + S_\phi \quad (68)$$

### 2.5.2.3 Discretization

The balance equations described in the previous section have to be “discretized” over the computational domain, so as to permit solving them by means of some numerical iterative computer-solved method. With that purpose, the domain itself is discretized, i.e. the continuum is ideally replaced by a number of discrete “nodes”. Adjacent nodes define the so-called “cells” or “elements”, which in a 3D domain usually have the shapes show in Figure 2-10. In addition, to the classical shapes represented in the figure, polyhedral cells are now used for discretization in some of the adopted codes.

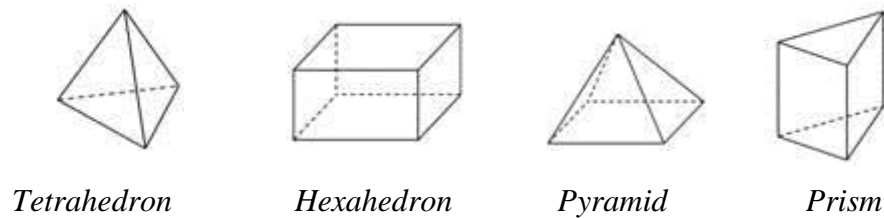


**Figure 2-10. Types of elements**

### 2.5.3 ANSYS CFX Code

ANSYS CFX is a general purpose commercial CFD code, among the most used codes (of the same kind) all over the world, combining an advanced solver with pre- and post-processing capabilities. An exhaustive description of the code capabilities and features can be found in Ref. [61].

CFX features the following modeling capabilities:

- Steady-state and transient flows
- Laminar and turbulent flows
- Subsonic, transonic and supersonic flows
- Heat transfer and thermal radiation
- Buoyancy
- Non-Newtonian flows
- Transport of non-reacting scalar components
- Multiphase flows
- Combustion
- Flows in multiple frames of reference
- Particle tracking

The CFX solver is based on a “finite volume” approach, i.e. the balance equations are solved in a integral, discretized form forcing the conservation of the mass, momentum and energy over control volumes in which the computational domain is subdivided, which do not coincide with the elements, but are automatically defined from the combination of portions of adjacent elements, according to the criterion depicted in Figure 2-11. For further details see Ref. [61].

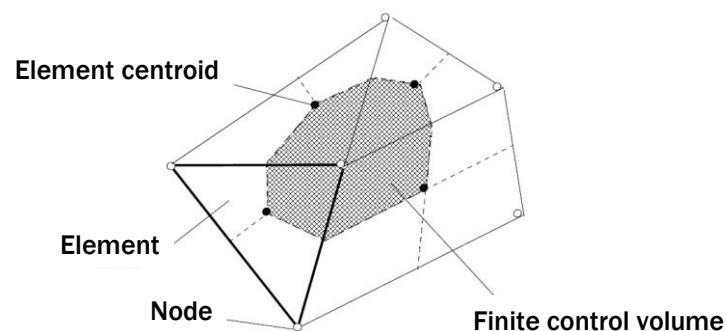


**Figure 2-11. Definition of finite control volumes from nodes and elements (2D example)**

Almost all the computational grids adopted for CFX analyses have been generated using the meshing tool ANSYS ICEM-CFD. An exhaustive description of the software capabilities and features can be found in [62].

The package allows performing the following tasks:

1. Generating solid models of the computational domains to be meshed (i.e. creating the “geometry”).
2. Importing geometries created with other tools (e.g. CAD packages).
3. Discretizing the computational domain by defining meshes of three-dimensional “elements” of various type, each one identified by a number of “nodes”:
  - o Tetrahedra (4 nodes)
  - o Hexahedra (8 nodes)
  - o Prisms (6 nodes)
  - o Pyramids (5 nodes)
4. Controlling the local grid refinement.
5. Performing a block-structuring of the domain to obtain high-quality body-fitted hexa grids on complex geometries.
6. Handling hybrid grids, i.e. meshes based on the use of more than one element type.
7. Creating prisms layers to enhance the turbulence treatment close to the walls in CFD calculations.
8. Checking the grids for possible errors and inconsistencies.
9. “Smoothing” the grids to improve their quality.
10. Exporting the created grids onto several available formats, which can be handled by most common CFD and FEM solvers.

The simpler way to obtain a suitable mesh is the Tetra grid generator, which quite automatically creates unstructured grids. The Hexa grid generator can only create “structured” grids, i.e. grids made up with hexahedra arranged according to a Cartesian pattern (or to a pattern topologically equivalent to a Cartesian one), so that an “i, j, k” notation is sufficient for identifying each node. On the other hand, when dealing with a complex geometry it is usually impossible to establish a topological equivalence with a Cartesian domain, thus it is impossible to create a structured, body-fitted mesh. However, such limitations can be bypassed by subdividing the domain into several Cartesian sub-parts (blocks), and creating a structured grid on each block. The resulting hexahedral mesh will thus be globally unstructured (which does not represent a limitation for most CFD solver, including CFX), and body-fitted. However, it has to be remarked that block-structuring of very complex geometries with many items and discontinuities to be modeled requires huge efforts, skill and expertise and may not be achievable in some cases.

When dealing with computational domains which include sub-parts featured by different levels of geometric complexity, a more practical approach may be the generation of “hybrid” grids, i.e. grid based both on tetra and hexa cells.

## 2.5.4 ANSYS FLUENT Code

ANSYS FLUENT is a general purpose commercial CFD code, among the most used codes in conventional industry all over the world. It has been successfully applied to industrial applications ranging from flow over an aircraft wing to combustion in a furnace, from blood flow to wastewater treatment plants.

Following the acquisition of FLUENT by ANSYS Inc., the CFD code has been included in the framework of the ANSYS WorkBench, so as to take advantage from the direct interface with CAD and structural mechanics tools, e.g. for fluid-structure interaction analyses. ANSYS FLUENT provides modeling capabilities for a broad range of incompressible and compressible, laminar and turbulent fluid flow problems. A wide range of mathematical models for transport phenomena is combined with the ability to model complex geometries. Examples of applications include laminar non-Newtonian flows in process equipment; conjugate heat transfer in turbomachinery and automotive engine components; pulverized coal combustion in utility boilers; external aerodynamics; flow through compressors, pumps, and fans; and multiphase flows in bubble columns and fluidized beds.

In order to allow modeling flows in special processes and equipment, several dedicated features have been implemented in FLUENT, such as porous media, lumped parameter models for fans and heat exchangers, periodic flow and heat transfer, swirl, moving reference frame models, free surface and multiphase flow models. The latter can be used for analysis of gas-liquid, gas-solid, liquid-solid, and gas-liquid-solid flows. For these types of problems, ANSYS FLUENT provides the volume-of-fluid (VOF), mixture, and Eulerian models, as well as the discrete phase model (DPM). The DPM performs Lagrangian trajectory calculations for dispersed phases (particles, droplets, bubbles), including coupling with the continuous phase. Examples of multiphase flows include channel flows, sprays, sedimentation, separation, and cavitation.

The turbulence models provided (Standard, RNG and Realizable  $k-\epsilon$ , Spalart-Allmaras Model, Standard and SST  $k-\omega$  Model, Reynolds Stress Model, DES and LES) may include the effects of other physical phenomena, such as buoyancy and compressibility. Particular care has been devoted to addressing issues of near-wall accuracy via the use of extended wall functions and zonal models.

Various modes of heat transfer can be modeled, including natural, forced, and mixed convection with or without conjugate heat transfer, porous media, etc. The set of radiation models and related sub-models for modeling participating media can take into account the effect of combustion. A host of other models useful for reacting flow applications are also available, including coal and droplet combustion, surface reaction and pollutant formation models.

The ANSYS FLUENT solver has the following features and modeling capabilities:

- quadrilateral, triangular, hexahedral (brick), tetrahedral, prism (wedge), pyramid, polyhedral, and mixed element meshes;
- pressure-based coupled solver, fully segregated pressure-based solver and two density-based solver formulations;

- parallel processing numerics to utilize multiple multi-core processors in a single machine and in multiple machines on a network;
- automatic dynamic load balancing to distribute computational cells among the processors in parallel calculations;
- incompressible or compressible flows, including all speed regimes (low subsonic, transonic, supersonic, and hypersonic flows);
- Newtonian or non-Newtonian flows;
- ideal or real gases;
- heat transfer, including forced, natural, and mixed convection, conjugate (solid/fluid) heat transfer, and radiation;
- chemical species mixing and reaction, including homogeneous and heterogeneous combustion models and surface deposition/reaction models;
- free surface and multiphase models for gas-liquid, gas-solid, and liquid-solid flows;
- Lagrangian trajectory calculation for dispersed phase (particles/droplets/bubbles), including coupling with continuous phase and spray modeling;
- cavitation model;
- phase change model for melting/solidification applications;
- porous media with non-isotropic permeability, inertial resistance, solid heat conduction, and porous-face pressure jump conditions;
- lumped parameter models for fans, pumps, radiators, and heat exchangers;
- acoustic models for predicting flow-induced noise;
- inertial (stationary) or non-inertial (rotating or accelerating) reference frames;
- multiple reference frame (MRF) and sliding mesh options for modeling multiple moving frames;
- mixing-plane model for modeling rotor-stator interactions, torque converters, and similar turbomachinery applications with options for mass conservation and swirl conservation;
- dynamic mesh model for modeling domains with moving and deforming mesh;
- dynamic (two-way) coupling with GT-Power and WAVE;
- Magnetohydrodynamics (MHD) module;
- continuous fibre module;
- fuel cell modules

An exhaustive description of the code capabilities and features can be found in [63].



### 2.5.5 Cd-Adapco STAR-CCM+

STAR-CCM+ [64] is the latest product of Cd-Adapco CFD code series, that also included the STAR-CD code [65].

STAR-CCM+ is presently being developed as a multi-physics computational tool able to cope with different physical problems already integrated in its structure or which can be integrated with it with an external coupling. The following relevant characteristics are possessed by the code in relation to different relevant aspects [64]:

- Time: Steady-state, Unsteady Implicit/Explicit, Harmonic Balance;
- Motion: Stationary, Moving Reference Frame, Rigid Body Motion, Mesh Morphing, Multiple Superimposed Motions;
- Material: Single, Multiphase and Multi-Component Fluids, Non-Newtonian Fluids, Incompressible, Ideal gas, Real Gas & User Defined Compressibility;
- Multiphase: Free surface (VOF) with Boiling or Cavitation, Lagrangian, Eulerian and Discrete Element Modeling (DEM), Wave profile generation for Flat, First and Fifth Order Stokes, Irregular, Superimposed Waves;
- Flow: Segregated or Coupled Flow and Energy;
- Regime: Inviscid, Laminar, Turbulent (RANS, LES, DES), Gamma-Re Theta and User Defined Transition Modeling;
- Multi-Domain: Porous Media (volumetric and baffle), Fan and Heat Exchanger models, Conjugate Heat Transfer;
- Heat Transfer: Conduction, Convection, Solar, Thermal, Multi-Band and Specular Radiation (Discrete ordinates or surface-to-surface);
- Combustion and Chemical Reaction: PPDF, CFM, PCFM, EBU, Coal Combustion, Soot & NOx prediction and DARS CFD complex Chemistry Coupling;
- Dynamic Fluid Body Interaction (DFBI): Fluid Induced Motion in 6 Degrees of Freedom including Propulsion and Maneuvering, multi-Body Interactions Including Body-Body Linear and Catenary Couplings;
- Aeroacoustic Analysis: Fast Fourier Transform (FFT) Spectral Analysis, Inverse FFT, Broadband noise sources, Ffowcs-Williams Hawkins (FWH) model, Signal Processing;
- Finite Volume Stress Modeling: Linear thermo-elastic, small and large deformation modeling, linear and non-linear contacts, fully coupled fluid-structure interaction;
- Electrical Field Simulation: Electro-thermal Lithium-Ion Battery Simulation, Electrodynamics and Electrostatics: Joule (Ohmic) Heating and Electrostatic Coating;
- CAE Integration: Co-simulation and bi-directional mapping between STAR-CCM+ and 1D/3D codes.

As it can be noted from the previous list, the code includes many classical models for turbulent flows, that can be used coupled with wall functions or low-Re approaches. RANS models, in particular, include the standard  $k-\varepsilon$  and  $k-\omega$  models, together with their well known advanced variants, offering flexibility to tackle with more challenging problems than in usual

applications, as required for some Generation IV reactors for which considerable model assessment and development is needed.

It can be also noted that the code features a built-in finite volume stress analysis model and that it provides allowance for its coupling with external programs also owing to the adoption of java routines or user codes. In particular, the STAR-CD code has been coupled in the past with the Monte Carlo code MCNP, addressing the analysis of PWR sub-channels [66]. The coupling requires an external management of variables from and to the CFD code and the Monte Carlo neutronic program.

STAR-CCM+ was also coupled with the deterministic neutronic code DeCart in a recent work by Westinghouse [67]. The work addressed in detail the coupled neutronic and thermal-hydraulic effects, taking into account also the complex structure of spacer grids and their effect on local fuel temperature. The coupling strategy made use of tables for exchanging data between the codes and of java routines. Though this kind of coupling is presently limited to small portions of the core, the increasing computing power will allow for more and more extended applications of this technique.

STAR-CCM+ was also coupled with RELAP5-3D in the frame of the development of licensing tools for New Generation Nuclear Plants (NGNP) [68]. This represents an example of the multi-physics and multi-scale approaches that are considered nowadays for nuclear power plant analyses.

## 2.5.6 NEPTUNE CFD Code

NEPTUNE CFD is a code mainly developed for two-phase flow thermal-hydraulics[70]. It is being jointly developed by EDF and CEA and co-funded by IRSN and AREVA NP as part of the NEPTUNE EDF/CEA joint research and development program for nuclear reactor advanced simulation tools. The project aims at developing industrial two-phase flow codes covering the whole range of modeling scales and to build a platform allowing easy multi-scale and multidisciplinary coupling in a shared environment. The project covers the fields of software development together with research in physical modeling and numerical methods, development of instrumentation techniques and performance of new experimental programs.

NEPTUNE CFD is based on a fully unstructured finite volume approach. The adopted models and Eulerian transport equations represent an extension of the classical two-phase flow model developed for the codes Astrid 3.4 and Code\_Saturne. It provides physical models for two-fluid or multi-field flows combined with interfacial area transport and two-phase turbulence; for further details see Ref. [69] and [70].

NEPTUNE\_CFD is one of the reference codes adopted in the framework of FP6 NURESIM Integrated Project (2005 – 2007) and its follow-up NURISP Collaborative Project (2009 – to date). In such context (see for example Refs. [71] and [72]), the code has benefited from huge development and validation efforts, especially dealing with the modeling and simulation of the complex phenomenology involved in convective boiling flows and in Pressurized Thermal Shock (PTS) scenarios. Moreover, the code was integrated into the free open source platform SALOME, along with other codes, in order to allow the numerical simulation of coupled multi-scale and multi-physics problems.

The software has the following main characteristics and functions, grouped by themes:

- flow systems:
  - o 1 to 20 fluid fields (phases or fields);
  - o processing of water/steam flows with actual thermodynamic laws;
- numerical methods:
  - o meshes with all types of cell (element), non-conforming connections;
  - o “cell-center” type Finite Volume method;
  - o calculation of co-localized gradients with reconstruction methods;
  - o distributed-memory parallelism by domain splitting;
- physical models:
  - o interfacial momentum transfer terms;
  - o interfacial energy and mass transfer terms;
  - o different turbulence models;
  - o head losses and porosity;

- architecture:
  - o interfacing with the Code\_Saturne Envelope module for management of the pre-processing operations, of the parallelism and of the post-processing;
  - o coding in Fortran 77 (the majority) and C (ANSI 1989) (procedural programming);
  - o ported on LINUX and UNIX systems.

The adopted transport equations and the associated closure laws are described in Ref [73]. The solving algorithm, based on the "elliptic fractional-step" method [74] focuses on mass conservation with original pressure step actualization assuring the local volume conservation.

### 2.5.7 Code\_Saturne

Code\_Saturne is the EDF's general purpose CFD code [75]. Developed since 1997, it is based on a co-located Finite Volume approach that accepts meshes with any type of cell (tetrahedral, hexahedral, prismatic, pyramidal, polyhedral) and any type of grid structure (unstructured, block structured, hybrid, conforming or with hanging nodes).

The basic capabilities of Code\_Saturne enable the handling of either incompressible or compressible flows including heat transfer and turbulence modeling. Dedicated modules are available for specific physics such as radiative heat transfer, combustion, magneto-hydrodynamics, two-phase flows (Euler-Lagrange approach with two-way coupling) as well as extensions to specific applications (e.g. for atmospheric environment: code Mercure\_Saturne).

It is portable on all Linux and UNIX platforms. Parallel code coupling capabilities are provided by the "Finite Volume Mesh" library. Compatible mesh generators include I-DEAS, GMSH, Gambit, Simail, Salomé, Harpoon and ICEM. Post-processing output is available in EnSight, CGNS and MED\_fichier formats.

Code\_Saturne can be coupled to EDF's thermal software SYRTHES (conjugate heat transfer); it can also be used jointly with EDF's structural analysis software Code\_Aster. Examples of application of Code\_Saturne to nuclear reactor safety related problems can be found in Ref. [76] and [77].

Like NEPTUNE\_CFD, also Code\_Saturne has been integrated into the SALOME platform. Moreover, it is available in the free Linux distribution CAELinux: <http://www.caelinux.com/CMS/>. More information on the code can be found on the dedicated EDF webpage: <http://research.edf.com/research-and-the-scientific-community/software/code-saturne/introduction-code-saturne-80058.html>, from which it can also be downloaded.

## 2.5.8 OpenFoam Code

The OpenFOAM (Open Field Operation and Manipulation) CFD Toolbox is a free, open source CFD software package produced by OpenCFD Ltd. It has a large user base across most areas of engineering and research, from both commercial and academic organizations. OpenFOAM has an extensive range of features to handle complex fluid flows involving chemical reactions, turbulence and heat transfer, solid dynamics and electromagnetics. It includes tools for meshing, notably snappy HexMesh, a parallelized mesher for complex CAD geometries, and for pre- and post-processing. It runs in parallel as standard, including meshing, and pre- and post-processing.

By being open, OpenFOAM offers users complete freedom to customize and extend its existing functionality, either by themselves or through support from OpenCFD. It follows a highly modular code design in which a set of precompiled libraries are dynamically linked during compilation of the solvers and utilities. Libraries such as those for physical models are supplied as source code so that users may conveniently add their own models to the libraries.

OpenFOAM is a C++ library, used primarily to create executables, known as applications. It is distributed with a large set of precompiled applications but users also have the freedom to create their own or modify existing ones with some pre-requisite knowledge of the underlying method, physics and programming techniques involved. Applications are split into two main categories:

- Solvers: that are each designed to solve a specific problem in computational continuum mechanics;
- Utilities: that perform simple pre- and post-processing tasks, mainly involving data manipulation and algebraic calculations.

The OpenFOAM distribution contains numerous solvers and utilities covering a wide range of problems; it includes over 80 solver applications that simulate specific problems in engineering mechanics and over 170 utility applications that perform pre- and post-processing tasks, e.g. meshing, data visualization, etc.,

OpenFOAM is supplied with pre- and post-processing environments, e.g. paraFoam, a post-processing utility that uses ParaView, an open source visualization application. Other methods of post-processing are offered, including EnSight, Fieldview and the post-processing supplied with Fluent.

The interface to the pre- and post-processing are themselves OpenFOAM utilities, thereby ensuring consistent data handling across all environments. Like Code\_Saturne, also OpenFOAM is available in CAELinux. More information on the code can be found on the webpage: <http://www.openfoam.com/features/>, from which it can also be downloaded.



### 3. Coupling with neutronic and thermal-mechanic codes

As previously mentioned, the safety analysis is mainly based on the application of analytical simulation methods. Important fields of safety analysis are static and transient reactor core and whole plant transient behavior. The latter is tackled by T-H system codes, the former by 3D neutronics models.

Nowadays, both these kinds of codes have achieved a high degree of realistic modeling. Nevertheless, the separate analysis of the reactor core by 3D neutronic models and the whole plant system using simplified neutronic models needs additional assumptions on the interfacing conditions if a strong coupling between the neutronics in the reactor core and the fluid-dynamics in the primary circuit exists. Therefore, in the last decades, great efforts were made to develop coupled code systems directly integrating 3D neutronics models into system codes. Although, most of the system codes have the capability of describing reactor core through point and sometimes 1D neutronics models, their application needs attention to determine correctly the reactivity feedback functions.

On the other hand, a more detailed analysis of reactor core behavior can be achieved by 3D neutronic codes. Most of them, i.e., diffusion codes, solve the neutron diffusion equation including the reactivity feedback effects caused by changes of coolant flow conditions and changes of the fuel rod temperatures. Once the neutron flux is obtained, the power distribution is computed. For reactor core calculations the boundary conditions have to be defined, e.g. the mass flow and temperature distribution of the coolant at the core inlet together with the time-functions for pressure. Actually, these boundary conditions will be affected by the power generation in the reactor core, and this limits the application to fast transients like a control rod ejection or transients with a weak coupling between fluid-dynamics in the primary circuit and the nuclear power generation in the reactor core. These problems of separated analysis can only be avoided by directly coupling 3D neutronic codes with system codes.

Coupling 3D neutronics model to system code can improve significantly the accuracy of the following analyses [92]:

- the local boron dilution accident in PWR, which was identified as a potential reactivity initiated accident even in shutdown conditions when all control rods are inserted;
- the cool-down transients with strongly negative moderator temperature reactivity coefficient in PWR; the occurrence of a recriticality during cool-down and its consequences have to be analyzed;
- ATWS analyses which are strongly affected by feedback reactivity coefficients;
- the BWR instability in plant conditions beyond the stability threshold.

In the framework of this research effort for the coupling among codes, it is worth to mention the relevant on-going activities: CASL and SALOME.

CASL (Consortium for Advanced Simulation of LWRs) [78] is a DOE platform for the modeling and the simulation of Nuclear Reactors. It is an integrated partnership of government, academia and industry: EPRI, INL, Los Alamos National Laboratory, MIT, ORNL and Westinghouse are some of the core partners. CASL is aimed at applying existing modeling and simulation capabilities and developing advanced capabilities to create a usable environment for predictive simulation of LWR. The virtual reactor (VR) simulation capability, known as the Virtual Environment for Reactor Applications (VERA), will incorporate science-based models, state-of-the-art numerical methods, modern computational science and engineering practices, and uncertainty quantification and validation against data from operating PWRs. It will couple state-of-the-art fuel performance, neutronics, thermal-hydraulics, and structural models with existing tools for systems and safety analysis.

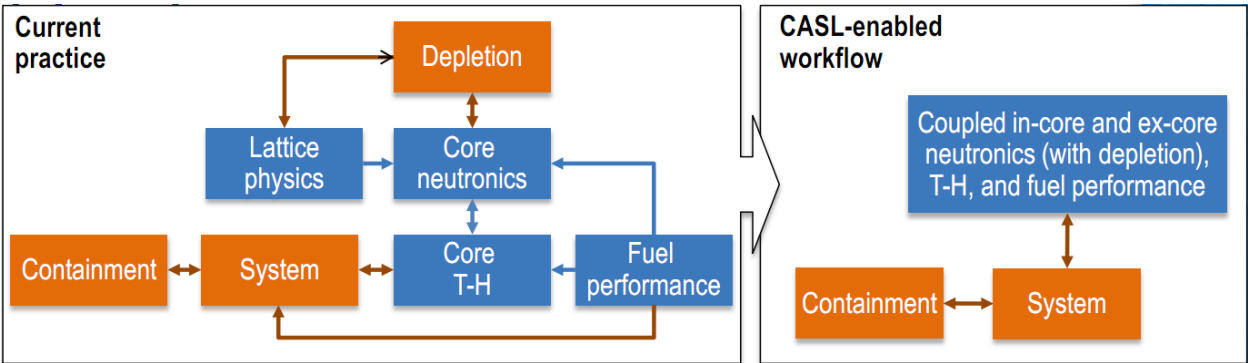


Figure 3-1. CASL Virtual Reactor vision [79]

SALOME is an open-source software that provides a generic platform for Pre- and Post-Processing of numerical simulations. SALOME can be used as standalone application for generation of CAD models, their preparation for numerical calculations and post-processing of the calculation results, but also as a platform for integration of the external third-party numerical codes to produce a new application for the full life-cycle management of CAD models. An exhaustive description of SALOME can be found in [80].



### 3.1 Some considerations related to the coupling between thermal-hydraulic and neutronic nodes

Performing accurate neutronic/thermal-hydraulic calculations in a reasonable amount of CPU time in coupled simulations is strongly dependent by the following six key topics:

- 1) coupling approach – integration algorithm or parallel processing;
- 2) ways of coupling – internal, external or parallel coupling;
- 3) spatial mesh overlays;
- 4) coupled time-step algorithms;
- 5) coupling numerics – explicit, semi-implicit and implicit schemes;
- 6) coupled convergence schemes.

Two different approaches are generally utilized to couple 3-D kinetics models with system codes: serial integration coupling and parallel processing coupling. Serial integration requires modifications of the codes usually performed by implementing a neutronics subroutine into the T-H system code. Parallel processing allows the codes to be run separately, with only minor modifications, while the exchange data between the two codes (see Figure 3-2) in carefully and properly selected time sequences becomes a crucial issue. The data exchange is usually performed using Multi-Processor Interaction (MPI) or a Parallel Virtual Machine (PVM) environment.

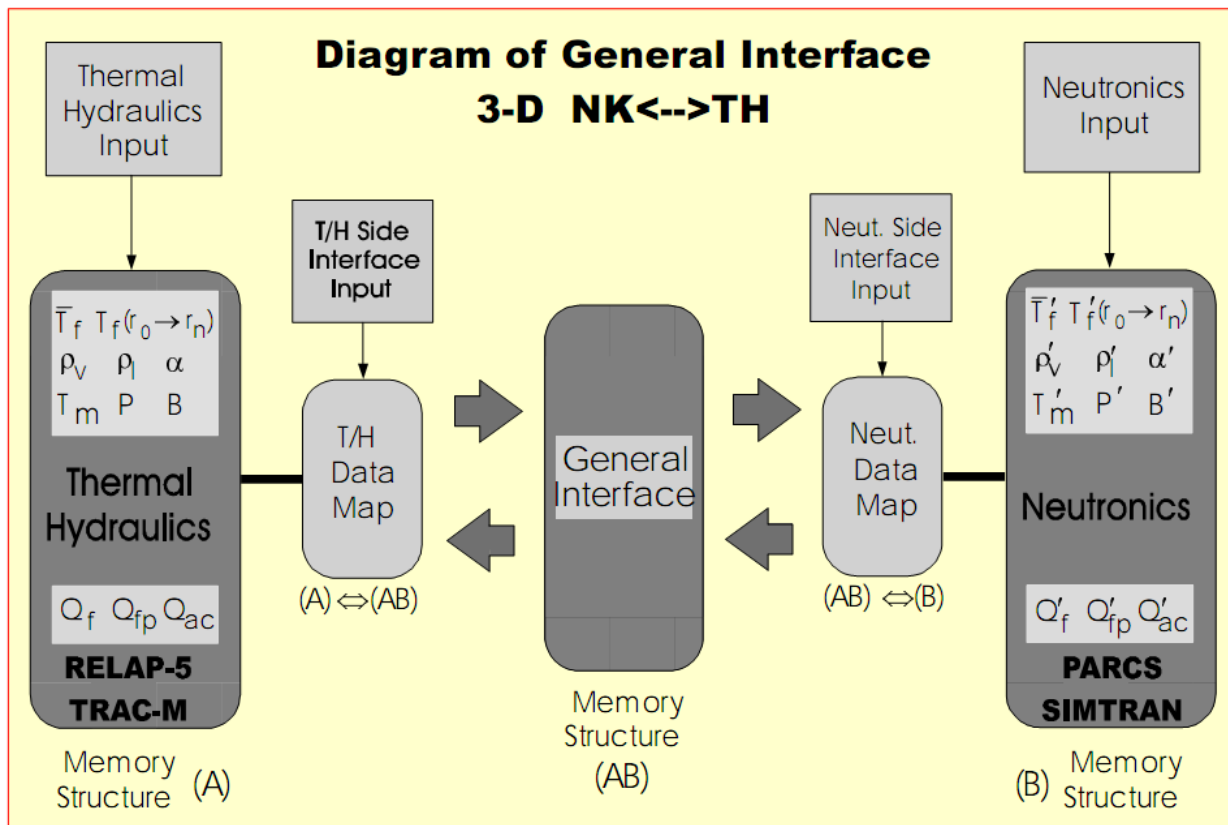


Figure 3-2. Scheme of the coupling between PARCS and RELAP5 [3]

With regard to the way of coupling [91], three kinds can be achieved: internal, external and parallel coupling (see Figure 3-3).

- *Internal coupling:*  
coupling of the 3D neutronics model to the system code, which models completely the thermal-fluid-dynamics in the primary circuit including the core region;
- *External coupling:*  
coupling of the 3D neutronics model including the fuel rod and the fluid-dynamic model of the core region to the system code, which models only the thermal-fluid-dynamics in the primary circuit excluding the core region;
- *Parallel coupling:*  
the 3D neutronics model including the fuel rod model and the fluid-dynamic model represents the reactor core; the system code models the thermal-fluid-dynamic in the primary circuit and the core region in a simplified manner; the calculated boundary conditions of the system code are transferred as time-dependent boundary conditions of the more detailed core calculation performed in parallel.

These coupling approaches maintain the capabilities of the separated codes and provide the necessary exchange of the main physical parameters. These are:

- o the power density distribution, which is the result of the neutronics calculation and which must be transferred to the fluid-dynamics;
- o the distribution of fuel temperature, coolant density and coolant temperature as well as boron concentration, which are the result of the fluid-dynamic model including the boron transport model and which must be transferred to the neutronics as feedback parameters.

Another challenging task to be fulfilled for obtaining a satisfying coupling is the choice of an appropriate spatial mesh overlays. Exact, detailed mapping provides better spatial resolution in coupled calculations, but requires also significant computational resources. Especially for transients with coupled core/system interactions, the computer requirements become enormous. Furthermore, careful consideration has to be given to expected possible asymmetric and local core behavior conditions, as the nodalization of the core in the two models and their interrelationship have a great influence in determining the local core parameters and hence the power distribution during the simulated transient.

The available T-H system codes have the option to model the core by means of several parallel channels, with possible additions of cross-flow radial connections (as in the RELAP5 code), or by using a 3-D T-H component, included for instance in the TRAC-PF1 and TRACE codes. In the latter case, another option is whether to use cylindrical or Cartesian geometry. The Cartesian option has a provision for a better geometrical correspondence between the T-H core layout and the neutronics core model. The nodes of the latter model (the default core layout being divided assembly-wise) can be directly coupled to a T-H cell and heat structure in both the radial and axial directions. The exact detailed mapping in that case is more easily perceived and provides improved spatial resolution in the coupled calculations.

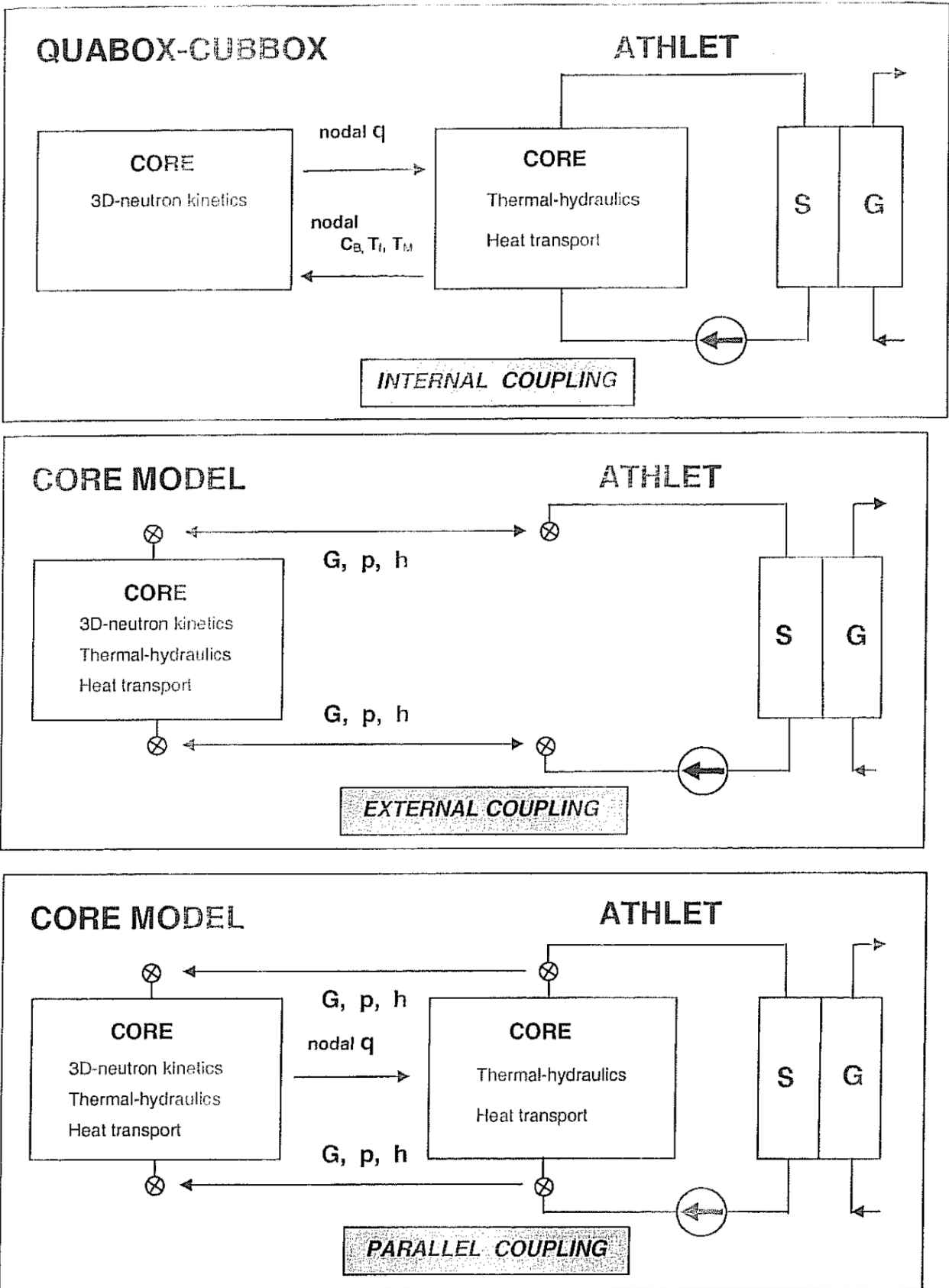


Figure 3-3. Exchange of parameters for internal, external and parallel coupling [91]

Sensitivity studies on spatial mesh mappings for the analysis of PWR control rod ejection accident (REA) [94] suggested that the local refinement of the Doppler feedback model does not necessarily improve the accuracy of the results. It was shown that the REA simulations are also

sensitive to the spatial coupling schemes, particularly in the radial direction. While the impact of neutronics mesh refinement is well known, it has recently been found that the local predictions (and the global predictions) are very sensitive to thermal-hydraulic refinement. The obtained results indicate that the T-H feedback phenomenon is non-linear and cannot be separated even in REA analysis, where the Doppler feedback plays a dominant role.

These conclusions have been emphasized through a comparative analysis of MSLB results with the 3-D core T-H models [96]. The results obtained indicated that the detail and geometry approximation of the core T-H can be an important source of deviations for local parameters, especially for the relative power and fuel temperature distribution in the vicinity of a stuck control rod. During the course of the MSLB transient, a power spike was seen at the position of the stuck rod. However, in the coarse mesh model this assembly was averaged with several of the surrounding assemblies while mapping the neutronics model to the T-H model. This had a significant effect in underestimating the feedback in this part of the core. On the other hand, the detailed model did more accurately predict the feedback (as a result of a better spatial feedback resolution), and therefore also the relative power shape and local safety parameters, near the stuck rod.

The next section is devoted to make a concise review of the neutronic codes currently used.

## 3.2 Neutron kinetics codes

### 3.2.1 DYN3D

DYN3D, developed at FZ Rossendorf [81], is used to investigate reactivity transients in the cores of thermal power reactors with hexagonal or quadratic fuel assemblies. The three-dimensional neutron kinetics model HEXDYN3D of the code is based on the nodal expansion method for solving the two-group neutron diffusion equation. If it is supposed that the reactor core consists of hexagonal fuel assemblies divided into a number of slices, then the nodes are the parts of the fuel assemblies in each slice. The neutron group constants are assumed to be spatially constant in each node. The solving of the time-dependent neutron diffusion equations, including the equations for delayed neutrons for all nodes, is used for transient processes calculation.

Through the thermal-hydraulic component, FLOCAL, including a two-phase flow model for describing coolant behavior, and a fuel rod model, additionally, some hot channels with power-peaking factors belonging to chosen fuel elements can be considered. Several safety parameters such as temperature, DNBR and fuel enthalpy are evaluated.

Macroscopic cross-sections depending on thermal-hydraulic parameters and boron concentration are the input data of the code, while the flow model is based on four differential balance equations for mass, energy and momentum of the mixture and mass balance of the vapor phase.

In transient calculations, the following perturbations can be treated:

- 1) movements of single control rods or a control rod bank;
- 2) variation of core coolant inlet temperature;
- 3) variation of boron acid concentration;
- 4) changes of core pressure drop or total mass flow rate;
- 5) changes of pressure.

Hereafter, the main features of the present version of the code DYN3D-2000/M1 are pointed out:

- implementation of burn-up calculations;
- input and output of fission product poison distributions;
- better handling of input data for fuel distribution (input of core load maps);
- simpler definition of control rods and control rod motion;
- improved control rod model for VVER-440 (control assemblies);
- damping of cusping effects during slower control rod motion through an improved flux weighting procedure;

Notwithstanding, a deterministic model of fuel rod failure during accidents is not included in DYN3D2000/M1, some parameters for diagnostics of possible fuel rod failure are given, such as fuel enthalpy for each axial node of the rod, cladding oxide thickness, signalization of possible cladding rupture when the cladding stress is positive (inner pressure is larger than outer pressure) and exceeds the yield point.

### **3.2.2 NEM**

NEM ([82], [83]) is a 3-D multi-group nodal code developed and used at The Pennsylvania State University (PSU). It can model both steady-state and transient core conditions, in 3-D Cartesian, cylindrical and hexagonal geometry. Its source is the nodal expansion method for solving the nodal equations in three dimensions. It utilizes a transverse integration procedure and is based on the partial current formulation of the nodal balance equations.

The leakage term in the one-dimensional transverse integrated equations is approximated with a standard parabolic expansion using the transverse leakages in three neighbor nodes; the nodal coupling relationships are expressed in partial current formulation and the time dependence of the neutron flux is approximated by a first order, fully explicit, finite difference scheme. This method, although it lacks the precision of the advanced nodal codes, has been shown to be very efficient. An upgrade of the method has recently been completed, replacing the fourth-order polynomial expansion with a semi-analytical expression which contains a more accurate approximation of the transverse leakage.

### **3.2.3 NESTLE**

NESTLE [84] is a multi-dimensional neutron kinetics code developed at North Carolina State University. It solves the two- or four-group neutron diffusion equations in either Cartesian or hexagonal geometry using the Nodal Expansion Method (NEM) and the non-linear iteration technique. Three-, two-, or one-dimensional models may be used. Several different core symmetry options are available including quarter, half and full core options for Cartesian geometry and 1/6, 1/3 and full core options for hexagonal geometry. Zero flux, non-re-entrant current, reflective and cyclic boundary conditions are available. The steady-state eigenvalue and time-dependent neutron flux problems can be solved by the NESTLE code.

### **3.2.4 PARCS**

PARCS ([85], [86]) is a three-dimensional reactor core simulator developed at Purdue University. It solves the steady-state and time-dependent neutron diffusion equation to predict the dynamic response of the reactor to reactivity perturbations such as control rod movements or changes in the temperature/fluid conditions in the reactor core. The code is applicable to both PWR and BWR cores loaded with either rectangular or hexagonal fuel assemblies.

The neutron diffusion equation is solved with two energy groups for the rectangular geometry option, while any number of energy groups can be used for the hexagonal geometry option. PARCS is coupled directly to the thermal-hydraulics systems codes TRACE and RELAP5, which provide the temperature and flow field information to PARCS during the transient. The thermal-hydraulic solution is incorporated into PARCS as feedback into the few-group cross-sections.

Numerous sophisticated spatial kinetics calculation methods have been incorporated into PARCS so as to achieve the various tasks with high accuracy and efficiency. The Coarse Mesh Finite Difference (CMFD) formulation, for example, is employed in PARCS to solve for the neutron fluxes in the homogenized nodes. It provides a means of performing a fast transient calculation while avoiding expensive nodal calculations at times in the transient when there is no strong variation in the neutron flux spatial distribution. Specifically, a conditional update scheme is employed so that the higher-order nodal update is performed only when there are substantial changes in the core condition to require such an update.

In rectangular geometry, the Analytic Nodal Method (ANM) is used to solve the two-node problems for accurate resolution of coupling between nodes in the core, and the Triangle-based Polynomial Expansion Nodal (TPEN) method is used for the same purpose in hexagonal geometry.

### **3.2.5 QUABOX**

QUABOX ([87], [91]) is a neutron kinetics code developed in the 70s at Gesellschaft für Anlagen und Reaktorsicherheit (GRS) in Germany for 3-D core neutron flux and power calculations in steady-state and transient conditions. It solves the neutron energy diffusion equation with two prompt neutron groups and up to six of delayed neutron precursors. The coarse mesh method is based on a polynomial expansion of neutron flux in each energy group. The time integration is performed by a matrix-splitting method which decomposes the solution into implicit one dimensional steps for each spatial direction. The reactivity feedback is taken into account by dependence of homogenized cross-section on feedback parameters, the functional dependence can be defined in a very general and flexible manner [91].

### **3.2.6 Transport codes**

Transport codes are most commonly based on the discrete ordinates method. They solve the Boltzmann transport equation for the average particle behavior to calculate the neutron flux. With discrete ordinate methods, the phase space is divided into many small boxes and particles are moved from one box to another. If this approach is to be used for modeling a fuel assembly, the guide tubes, the coolant sub-channels, and fuel rods will be homogenized and the medium is discretized to solve the transport equation. Therefore, this type of geometry modeling does not accurately represent the important design details essential for the fuel assembly. Transport codes use macroscopic cross section data, which are processed from multi-group energies. Processed macroscopic cross section data from microscopic scale are required for different parts in the geometry. For complicated geometries with varying parameters such as coolant and moderator density, preparation of the macroscopic cross section data would also require a lot of effort. Therefore deterministic codes need to be homogenized for complex geometries. Computer codes based on transport methods include DORT, two dimensional (X-Y, and R-Z) geometries, TORT,

a three-dimensional discrete transport code and DORT-TD, a transient neutron transport code [36].

### **3.2.7 Monte Carlo Method**

A Monte Carlo method does not solve an explicit equation like the deterministic codes, but rather obtains the answers by simulating individual particles and recording some aspects (tallies) of their average behavior. Monte Carlo codes use a continuous energy scale to represent the variation of cross section data. They are widely used because of the capability of complex geometries modeling and accurate solution produced with the continuous energy scale used to represent the cross section data. Computer codes based on the Monte-Carlo methods include the MCNP (Monte Carlo N-Particle), that is a general-purpose, continuous-energy, generalized-geometry, coupled neutron/photon/electron transport code. The application of the Monte Carlo codes in nuclear energy is increasing for fuel assembly and core design analysis typically in BWR where the density varies in the core [36].



### 3.3 Results and experiences of coupled neutronic/T-H codes

Below, an overview of 3-D coupled neutronics/thermal-hydraulics calculations available from a recent interesting literature paper [36] is shown.

**Table 3-1. Overview of 3-D coupled neutronics/thermal-hydraulics calculations available from the literature [36]**

No.	Title and authors	Coupled codes	NPP	Transient type ef.
1	<i>Coupling of the Thermal-hydraulics Code TRAC with 3-D Neutron Kinetics Code SKETCH-N</i> H. Asaka, V.G. Zimin, T. Iguchi, Y. Anoda	J-TRAC TRAC-BF1 Sketch-N	PWR	RIA
			BWR (Ringhals-1)	Stability benchmark cases
			BWR	Instabilities
2	<i>Core-wide DNBR Calculation for NPP Krško MSLB</i> I-A. Jurkovića, D. Grgić, N. Debrecin	RELAP5/ MOD3.2 COBRA III C QUABOX/CUBBOX	PWR (NPP Krško)	MSLB
3	<i>MSLB Coupled 3-D Neutronics/Thermal-hydraulics Analysis of a Large PWR Using RELAP5-3-D</i> F. D'Auria, A. Lo Nigro, G. Saiu, A. Spadoni	RELAP5/MOD3.2 NESTLE	PWR B&W TMI-1	MSLB
			AP-1000	
4	<i>TMI-1 MSLB Coupled 3-D Neutronics/Thermal-hydraulics Analysis: Application of RELAP5-3-D and Comparison with Different Codes</i> R. Bovalini, F. D'Auria, G.M. Galassi, A. Spadoni, Y. Hassan	RELAP5/MOD3.2.2 PARCS	PWR (B&W TMI-1)	MSLB
		RELAP5/MOD3.2.2 QUABBOX		
		RELAP5/3-D NESTLE		
5	<i>PWR REA Sensitivity Analysis of TRAC-PF1/NEM Coupling Schemes</i> N. Todorova, K. Ivanov	TRAC PF1 NEM	PWR (B&W) TM-1	REA
6	<i>Coupled 3-D Neutronic/Thermal-hydraulics Codes Applied to Peach Bottom Unit 2</i> A. M <sup>a</sup> Sánchez, G. Verdú , A. Gómez		BWR (Peach Bottom Unit 2)	TT
7	<i>Study of the Asymmetric Steam Line Break Problem by the Coupled Code System KIKO3D/ATHLET</i> Gy. Hegyi, A. Keresztúri, I. Trosztel	ATHLET KIKO3D	VVER 440	MSLB
8	<i>Development of Coupled Systems of 3-D Neutronics and Fluid-dynamic System Codes and their Application for Safety Analysis</i> S. Langenbuch, K. Velkov, S. Kliem U. Rohde, M. Lizorkin, G. Hegyi, A. Kereszturi	ATHLET DYN3D BIPR-8	VVER-1000	LOFW
				Station black out
				MCP stop
9	<i>VIPRE-02 Subchannel Validation Against NUPEC BWR Void Fraction Data</i> Y. Aounallah, P. Coddington	VIPRE-02 ARROTTA	BWR	Void fraction validation study
10	<i>High Local Power Densities Permissible at Siemens Pressurised Water Reactors</i> K. Kuehnel, K.D. Richter, G Drescher, I. Endrizzi	PANBOX	PWR	Maximum local heat flux investigation

ATWS: Anticipated Transient without Scram; RIA: Reactivity Induced Accident;  
REA: Rod Ejection Accident; MCP: Main Coolant Pump; LOFW: Loss Of proper Feed Water

No.	Title and authors	Coupled codes	NPP	Transient type ef.
11	<i>Analysis of a Boron Dilution Accident for VVER-440 Combining the Use of the Codes DYN3D and SiTap</i> U. Rohde, I. Elkin, V. Kalinenko	SiTap DYN3D	VVER 440	RIA
12	<i>RELAP5-PANTHER Coupled Code Transient Analysis</i> B.J. Holmes, G.R. Kimber, J.N. Lillington, M.R. Parkes	RELAP5 PANTHER	PWR (Sizewell-B)	Grid frequency error injection test Single turbine trip event
13	<i>TACIS R2.30/94 Project Transient Analysis for RBMK Reactors</i> H. Schoels, Yu. M. Nikitin Nikiet	FLICA GIDRA SADC DINAO CRONOS QUABOX/CUBOX	RBMK (Smolensk 3)	RIA
14	<i>PWR Anticipated Transients Without SCRAM Analyses Using PVM Coupled RETRAN and STAR 3-D Kinetics Codes</i> M. Feltus, K. Labowski	RETRAN STAR 3-D	PWR	ATWS
15	<i>Development and First Results of Coupled Neutronic and Thermal-hydraulics Calculations for the High-performance LWR</i> C.H.M. Broeders, V. Sanchez-Espinoza, A. Travleev	RELAP5 KAPROS	HPLWR	FA tests
16	<i>Analysis and Calculation of an Accident with Delayed Scram on NPP Greifswald using the Coupled Code DYN3D-ATHLET</i> S. Kliem	ATHLET DYN3D	VVER-440 (Greifswald)	Delayed scram
17	<i>Multi-dimensional TMI-1 Main Steam Line Break Analysis Methodology using TRAC-PF/NEM</i> K. Ivanov, T. Beam, A. Baratta, A. Irani, N. Trikouros	TRAC-PF NEM	PWR (B&W TMI-1)	MSLB
18	<i>Realistic and Conservative Rod Ejection Simulation in a PWR Core at HZP, EOC with Coupled PARCS and RELAP Codes</i> J. Riverola, T. Núñez, J. Vicente	RELAP PARCS	Three-loop PWR	Peripheral rod ejection
19	<i>OECD/NRC BWR Benchmark 3<sup>rd</sup> Workshop</i>	ATHLET QUABOX/CUBOX	BWR Peach Bottom	TT
ATWS: Anticipated Transient without Scram; RIA: Reactivity Induced Accident; REA: Rod Ejection Accident; MCP: Main Coolant Pump; LOFW: Loss Of proper Feed Water				

Hereafter, two specific investigations on coupled codes performed for the PWR MSLB Benchmark issued by OECD/NEA [90] are presented. The benchmark refers to the Three Mile Island-Unit 1 (TMI-1) nuclear power plant configuration, including the geometric data and the operational conditions of the plant. It was defined to validate the coupled code systems with 3D neutronics by comparing solutions of different codes (code-to-code comparison). Among the three phases defined for the benchmark: first phase analyzing the plant transient through system codes using point kinetics, second phase analysis of the 3D reactor core behavior with specified

boundary conditions, and third phase analysis by the coupled codes, we will focus on the last one.

The transient analyzed was a main steam line break at hot full power. This causes the worst case of overcooling because the steam generator liquid inventory corresponds to the maximum possible value. A stuck rod condition of the most effective rod was assumed for the reactor trip, which was initiated at 114% of nominal power. The accident was initiated by a double-ended rupture of the main steam line upstream of the isolation valve. The break was simulated by two discharge valves opening within 0.1 s, one at the steam line and the other at the cross connecting pipe (see Figure 3-4). The break flow was simulated following the specification by the Moody discharge flow model.

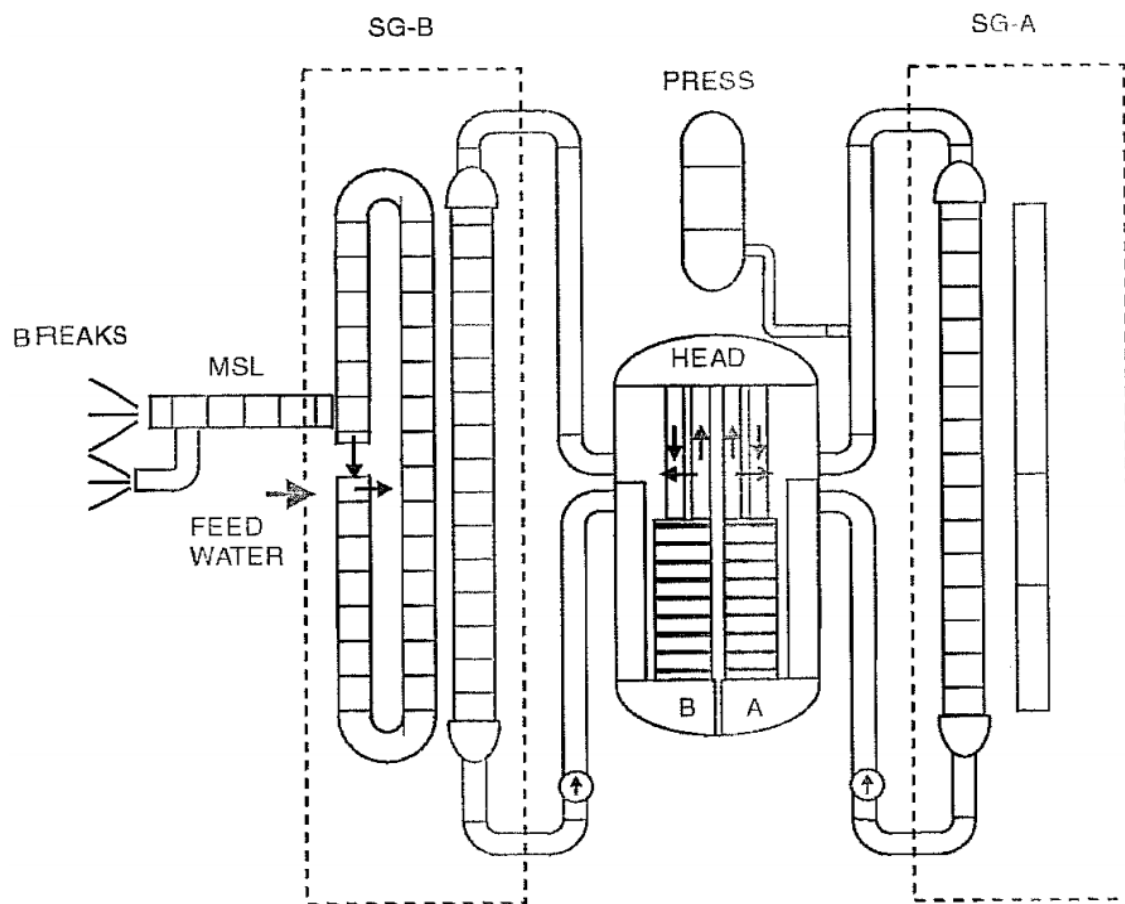


Figure 3-4. ATHLET nodalization scheme for MSLB Benchmark [93]

The main physical phenomena of the MSLB transient evolution are the following:

- the break of the main steam line causes a pressure decrease on the steam generator secondary side; this is affected by the break mass-flow, dependent on the ratio of water and steam discharge, and the feed water supply;
- the pressure on the secondary side determines the saturation temperature of the coolant in the steam generator and consequently the heat removal from the primary side; an efficient heat-transfer exists as long as the steam generator contains sufficient liquid; therefore, the temperature in the cold leg follows directly the decrease of the saturation temperature on the secondary side;
- the cool-down of primary circuit is terminated when the steam generator becomes dry;

- the coolant temperature in the reactor core, which determines the criticality condition after reactor trip, is dependent on the mixing phenomena between the coolant flows from the affected and intact primary loop as well as the mixing in the core region.

### **3.3.1 ATHLET-QUABOX/CUBBOX [93]**

The GRS made the calculations for the OECD Benchmark [90] by means of the coupled code system ATHLET-QUABOX/CUBBOX. The coupling approach implemented in ATHLET was based on a general interface, which separated data structures from neutronics and thermo-fluid dynamic code and performed the data exchange in both directions. The internal coupling carried out had the following features: the fluid-dynamic equations for the primary circuit and the flow channels in the reactor core region were completely modeled and numerical solved by ATHLET methods. The time integration in the neutronics code QUABOX/CUBBOX was performed separately. Therefore, both codes kept their capabilities. The time step size was synchronized during the transient, whereby the accuracy control was preferably done by the fluid-dynamic code [91].

#### ***Description of the ATHLET plant model***

The primary circuit of TMI-1 PWR NPP consists of the reactor vessel with the core and two symmetric loops with a hot leg, a once-through steam generator (OTSG) and a cold leg. The coolant flow through the reactor vessel and core is modeled by two equal parallel flow paths by splitting the down-comer, the lower plenum, the reactor core and the upper plenum. These parallel flow paths behave independently, except for flow connections in the upper plenum.

The secondary side of the steam generator consists of the feed water supply, the down-comer, the riser region and the steam line with the main safety valves.

#### ***MSLB transient performed and results***

Performing calculations with the coupled code ATHLET-QUABOX/CUBBOX was done stepwise:

1. study of the T-H system response and initialization of the system models (performance of point kinetics calculation with the stand-alone version of ATHLET);
2. generation and qualification of the reactor cross sections;
3. initialization of the 3D core neutronics model (performance of calculations with the stand-alone version of QUABOX/CUBBOX with constant feedback distributions);
4. modeling of the mixing phenomena at core entrance depending on the scenario of the transient;
5. selecting a mapping scheme for fuel assemblies and THC (1:1, optimal or any other);
6. performing a zero-transient with the coupled code at nominal power to prove the stability of the whole modeled system and to tune some T-H core parameters;
7. complete simulation of the transient by the coupled code.

For the OECD Benchmark, the analysis of the MSLB transient was performed by using three different mapping schemes:

- o a 1:1 modeling of the core with 178 thermal-hydraulic channels (THCs), that means that each fuel assembly corresponds to a single THC and a single fuel rod;
- o a mapping proposed in the specification with 19 THCs;
- o a mapping with 15 THCs taking into account the features of the core loading and the core configuration.

The effect of using different numbers of THCs and fuel rods with mappings tot the fuel assemblies of the core loading was studied in detail because it was important to know this effect of mapping for a proper application of coupled codes.

The results showed the following:

- the simulation of the MSLB transient with all three mapping schemes results in good agreement for the integral parameters as power history, primary and secondary pressure, cold and hot leg coolant temperatures on the primary side;
- deviations are observed for  $k_{\text{eff}}$ -values using different schemes. In comparison with the model using a 1:1 mapping, the optimized model with 15 THCs obtains a better agreement than the 19 THCs model as specified;
- relevant differences are observed for the local parameters of the core: comparing the results of different mapping schemes for the maximum fuel temperature (Figure 3-5), it is seen that the difference for the optimized model with 15 THCs in only 18 K, but for the 19 THCs model already 135 K, probably because the neighborhood of the stuck-rod with high local power peaking is not correctly taken into account by this scheme.

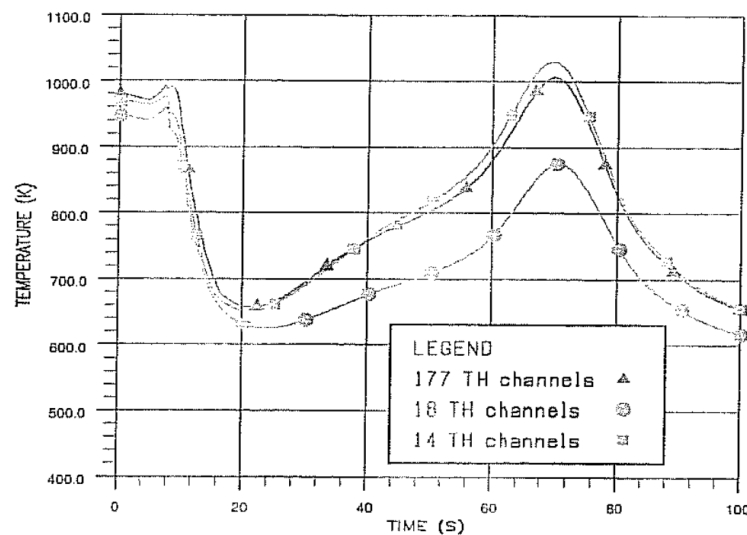
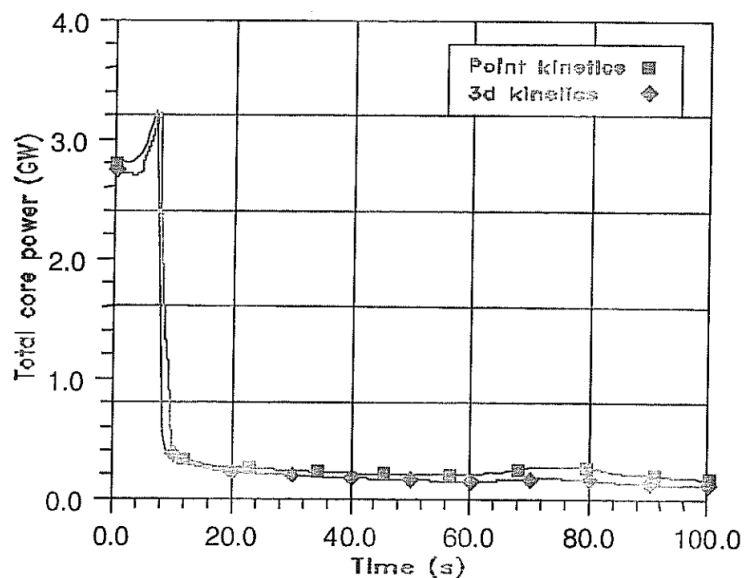


Figure 3-5. Comparison of maximum fuel temperature for different mapping schemes [93]

Simulation results obtained by point kinetic and ATHLET-QUABBOX/CUBBOX model were also compared (see Figure 3-6). The deviations between the two solutions were small - less than 3.9%. Differences are to be seen in the time-period before reaching 114% nominal power, when the reactor trip is initiated, and also in the maximum value of power during the phase of return to power. Approximately, similar good agreement were obtained for all integral parameters.

Nevertheless, the great advantage of the coupled code using the 3D neutronic solution is the consistent calculation of reactivity changes and the direct calculation for local core parameters. In conclusion, a good agreement of point-kinetics and 3D neutronics solution is achieved, because the reactivity feedback coefficients and the reactivity effect of the reactor trip used for point-kinetics were carefully determined by 3D neutronics calculations.



**Figure 3-6. Comparison of ATHLET-QUABBOX/CUBBOX calculation with respect to point kinetics transient [93]**

### 3.3.2 RELAP5/PANBOX [97]

The coupling of RELAP5 with PANBOX has been made by Forschungszentrum Karlsruhe and Framatome Advanced Nuclear Power Erlangen in the frame of the PWR MSLB Benchmark issued by OECD/NEA [90].

PANBOX is a 3D neutron kinetics code with multidimensional core thermal hydraulics model, developed by Siemens/KWU to perform PWR safety analysis and all kinds of transient in which the power distribution is significantly affected. It solves the time-dependent few-group diffusion equation in Cartesian geometry using a semi-analytical nodal expansion method (NEM).

The coupling between RELAP5 and PANBOX was realized via the general interface package EUMOD. It consists of a set of subroutines that allows external codes to be explicitly linked to RELAP5. The main functions of EUMOD are the transfer of data from RELAP5 to the external code, the call for execution of that code and the appropriate transfer of its results back to RELAP5. This process is repeated after each RELAP5-time step. Since no iteration is carried out between the neutron kinetics solution and RELAP5, the EUMOD interface affects neither the integration algorithm nor the physical models of RELAP5. Reduction of the time step is performed by the RELAP5 stability criteria, though, the RELAP5-time step can be also reduced by PANBOX.

In Figure 3-7, the logic of the coupling is depicted. After each RELAP5-time step thermal hydraulic data are passed to PANBOX, where the 3D power distribution is calculated and if necessary the safety related parameters are evaluated. Then PANBOX data are adapted and transferred back to RELAP5, where the next time step is determined based on new power distribution.

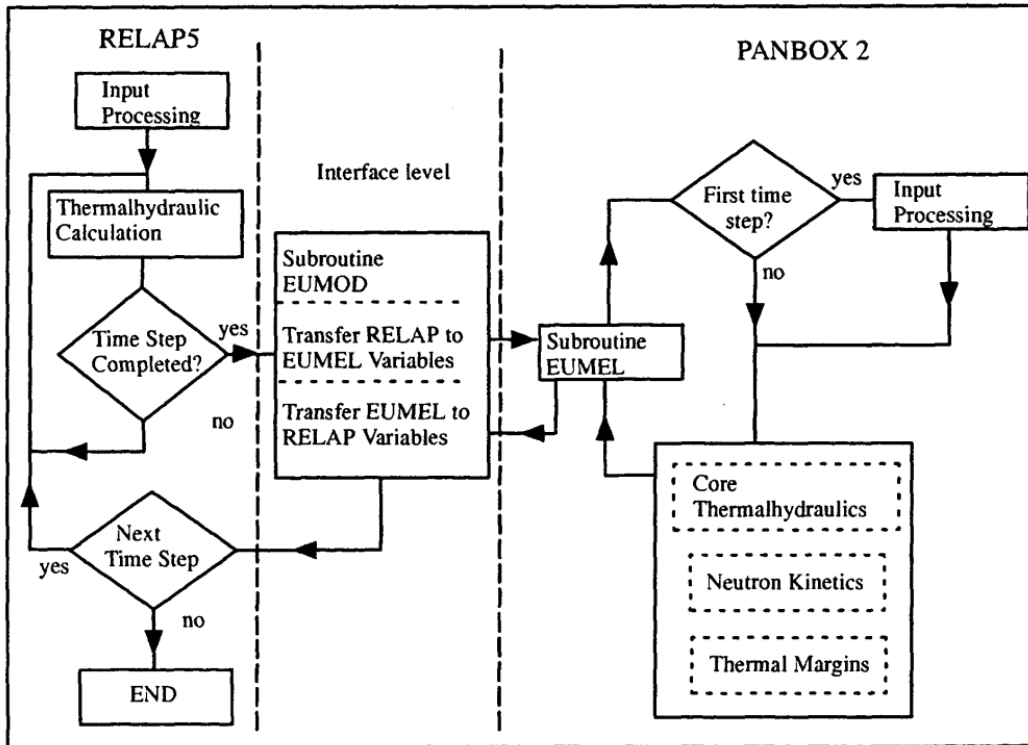


Figure 3-7. Flow logic for coupling of RELAP5 with PANBOX using EUMOD[97]

For the multi-dimensional analysis of the core behavior in interaction with the plant thermal hydraulics two scenarios were addressed:

- a) best-estimate scenario (BE);
- b) return-to-power scenario (RP), which was specified to better test the coupling of 3D kinetics model with the plant T-H models.

In Figure 3-8 and Figure 3-9 the average moderator temperature and the core power predictions are showed. In Figure 3-10 and Figure 3-11, respectively, the 2D coolant temperature distributions for BE and RP cases at two different times ( $t=6.1$  s and  $t=66$ s) are showed. As it can be seen, at problem time 6.1 s (just after scram) the asymmetrical cool-down of the core is already noticeable, but at the time of 66 s the non-symmetrical coolant temperature distribution gets even worse. Furthermore, in contrast to the results of BE scenario, the RP results showed a more pronounced temperature distortion.

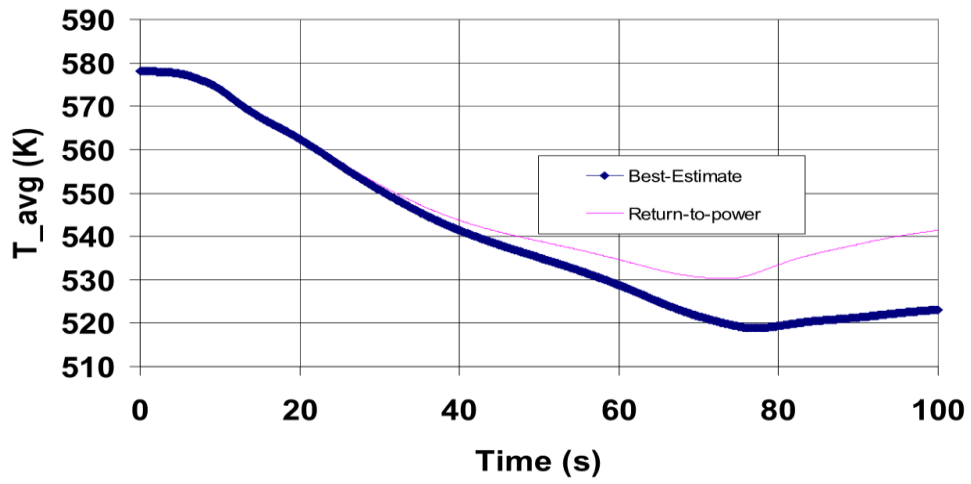


Figure 3-8. Core average moderator temperature (BE and RP case) 119[97]

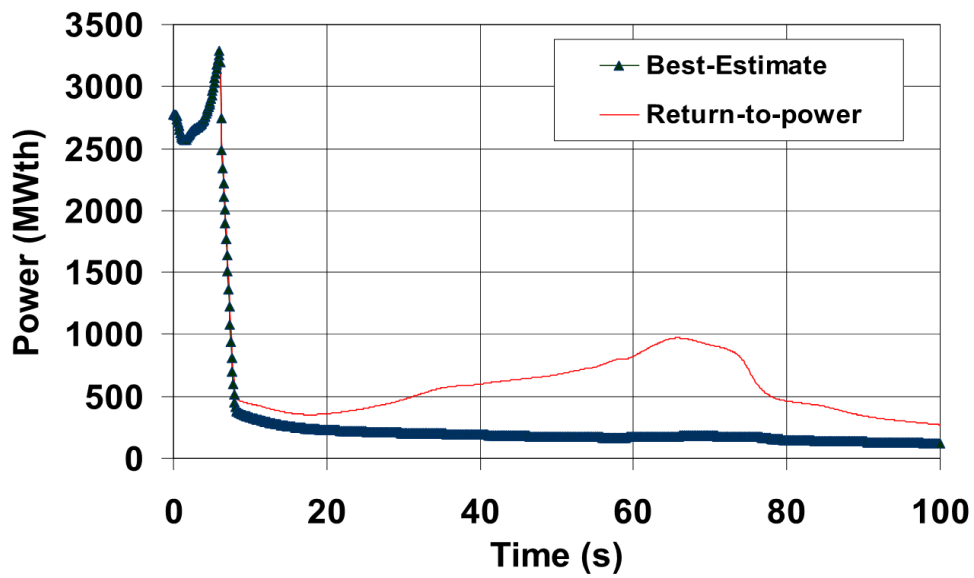


Figure 3-9. Predicted total core power (BE and RP case) 119[97]

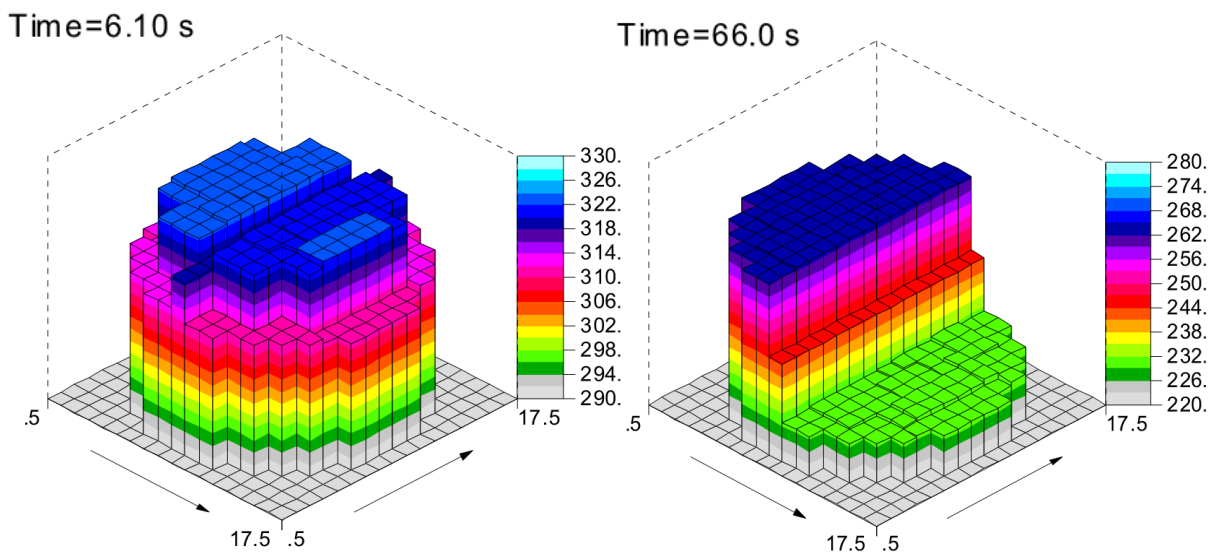
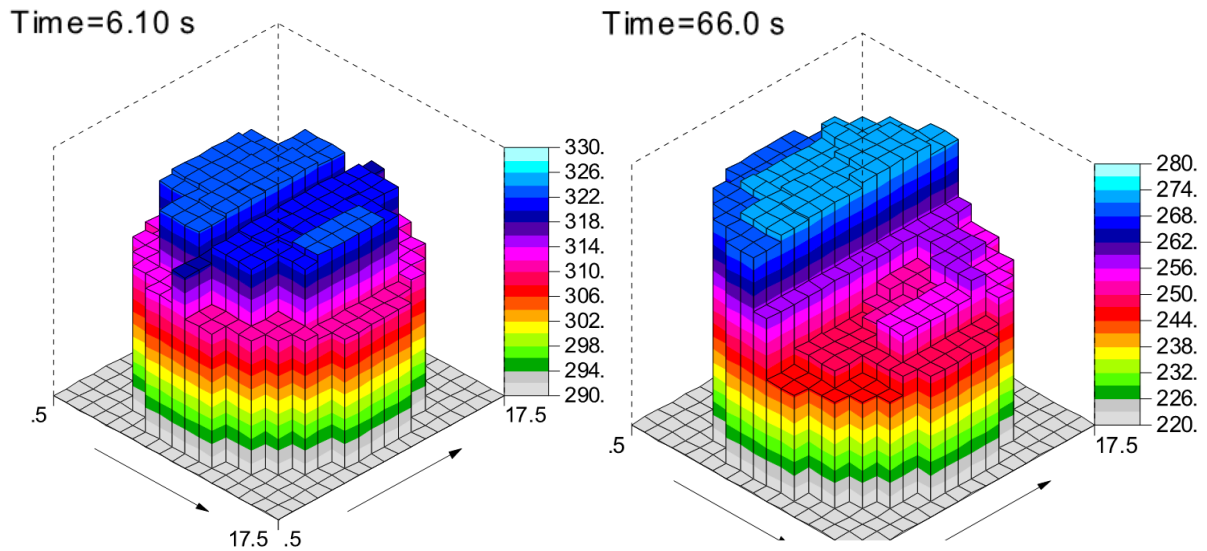


Figure 3-10. 2D coolant temperature distribution at plane  $z=3.14$  m for BE case [97]





**Figure 3-11. 2D coolant temperature distribution at plane  $z=3.14$  (node=27) for RP-case [97]**

In Figure 3-12 the total power predicted with point and spatial kinetics are shown. At transient beginning, the total power is the same for both calculations. Then the power of the point kinetics calculation increases while that of the spatial kinetics decreases firstly due to the different treatment of the feedback mechanisms. Around scram time both calculations predict the same power up to about 20 s transient time. Later on, the power predicted by the point kinetics starts to continuously increase faster with a larger gradient than the one of the spatial kinetics. The discrepancies become larger at the time when the cold leg coolant temperature reaches the minimum value. The point kinetics calculates a considerable power increase of about 20.3 % while RELAP5/PANBOX predicts only a small power peak of 6.5%.

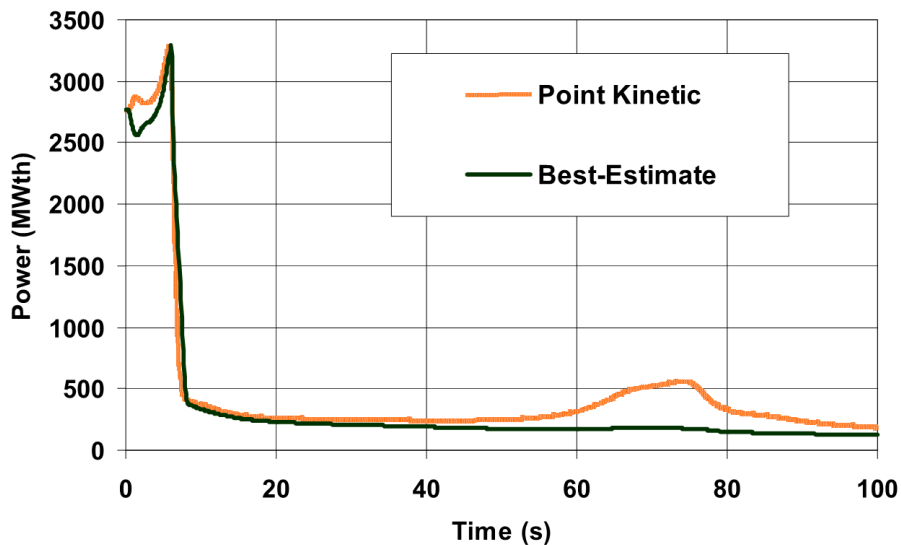


**Figure 3-12. Comparison of total power as predicted by point kinetic of RELAP5 and the coupled code RELAP5/PANBOX [97]**

### 3.3.3 Code-to-code comparison for the PWR MSLB Benchmark [90]

In this section a code-to-code comparison of different coupled codes results is provided. The case-study investigated refers to the PWR MSLB Benchmark issued by OECD/NEA [90]. The aim was to highlight similarities and deviations among the different coupled codes. In Table 3-2 a list of participants and coupling codes adopted is shown.

**Table 3-2. List of participants in Phase III of the PWR MSLB Benchmark [90]**

Participant number	Company name	Country	Code
1	BE/Tractebel (1)	UK/Belgium	RELAP5/PANTHER
2	CEA (1)	France	CATHARE/FLICA4/CRONOS2
3	CEA (2)	France	CATHARE/FLICA4/CRONOS2
4	CSA/GPUN	USA	RETRAN-3-D
5	FRAMATOME ANP/FZK	Germany	RELAP5/PANBOX
6	FZR	Germany	DYN3-D/R-AHTLET
7	GRS	Germany	Q-C/ATHLET
8	JAERI	Japan	THYDE-NEU
9	KAERI	Korea	MARS/MASTER
10	PSU	USA	TRAC-PF1/NEM
11	Purdue/NRC	USA	RELAP5/PARCS
12	UP/UZ	Italy/Croatia	RELAP5/PARCS
13	UP/UZ	Italy/Croatia	RELAP5/QUABOX
14	UPC	Spain	RELAP5/PARCS
15	UPM	Spain	SIMTRAN/RELAP5
16	UPV	Spain	TRAC-PF1/NEM
17	VTT	Finland	TRAB-3-D/SMABRE

Among the several results obtained, hereafter only a code-to-code comparison concerning the coolant temperature is presented. In Figure 3-13, Figure 3-14 and Figure 3-15, the coolant core averaged, broken loop hot leg and broken loop cold leg temperature, are respectively shown.

When the steam line break occurs, the pressure in the broken steam generator (SG) decreases rapidly and causes an increase of the flow rate within the SG. The increased flow rate results in an increase in the heat transfer and overcooling of the reactor coolant system fluid. The cold leg temperature plot shows an immediate temperature decrease as a result of the broken SG depressurization; however, the hot leg temperature plots show a more gradual decline. The reason is that the decreasing reactor coolant system temperature results in an increase in the core power, which initially offsets the broken SG's cooling effect.

In the second half of the transient, there is an increase in the core power, and the overcooling effect from the broken SG becomes secondary. In addition to the increase in power, the broken SG loses its cooling capacity throughout the transient as it blows dry. The broken loop sees an increase in reactor coolant system temperature as a result of this power increase. The deviations for the broken loop are fairly low for both the hot and cold legs. Any local deviations in the temperature behavior throughout the transient are caused by modeling differences in the reactor coolant system, the modeling assumptions and the code correlations. Overall, also the deviations for the average moderator temperature are relatively small.

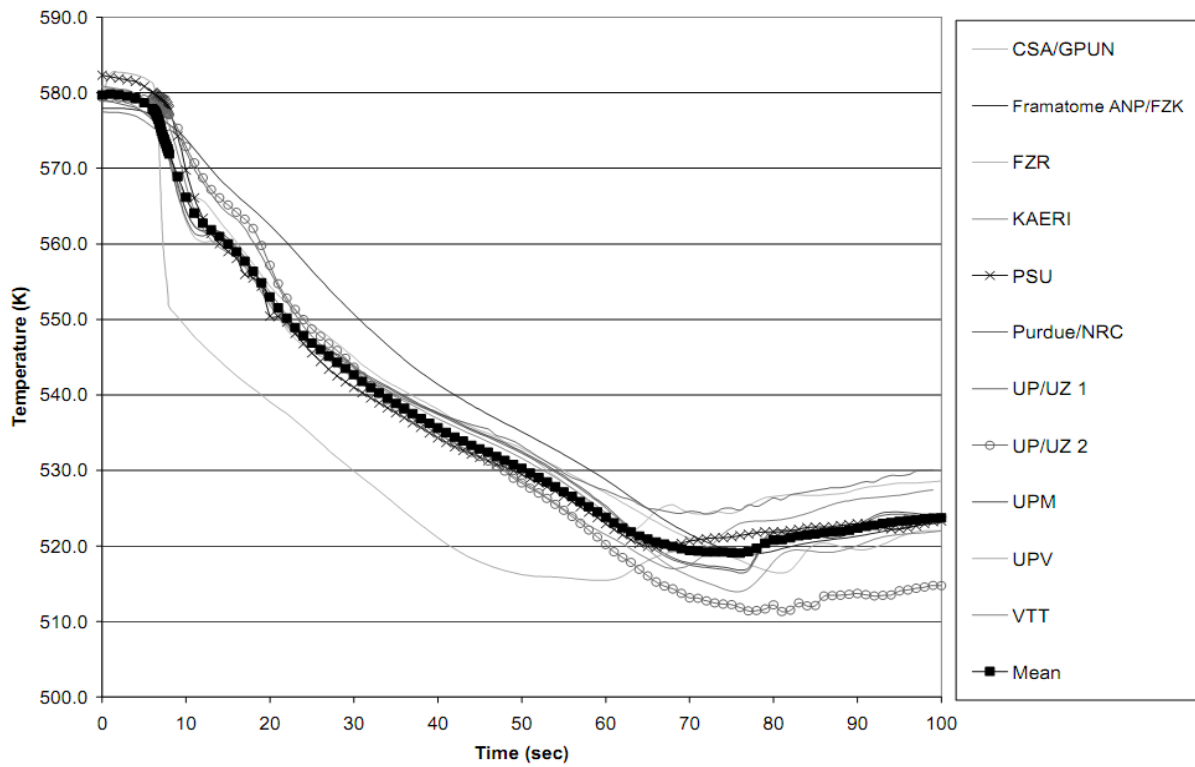


**Figure 3-13. Code-to-code comparison for the average coolant temperature for BE scenario [90]**

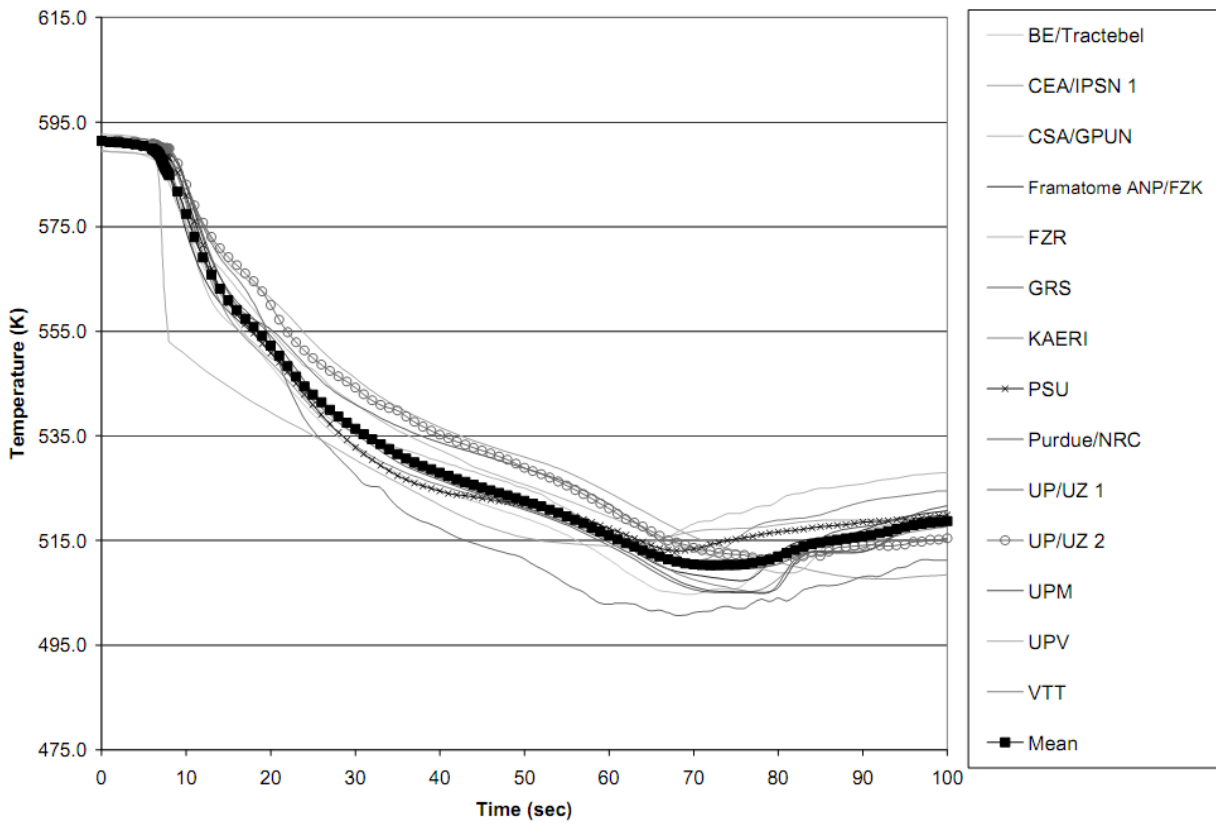


**Figure 3-14. Code-to-code comparison for the broken loop hot leg temperature for BE scenario [90]**

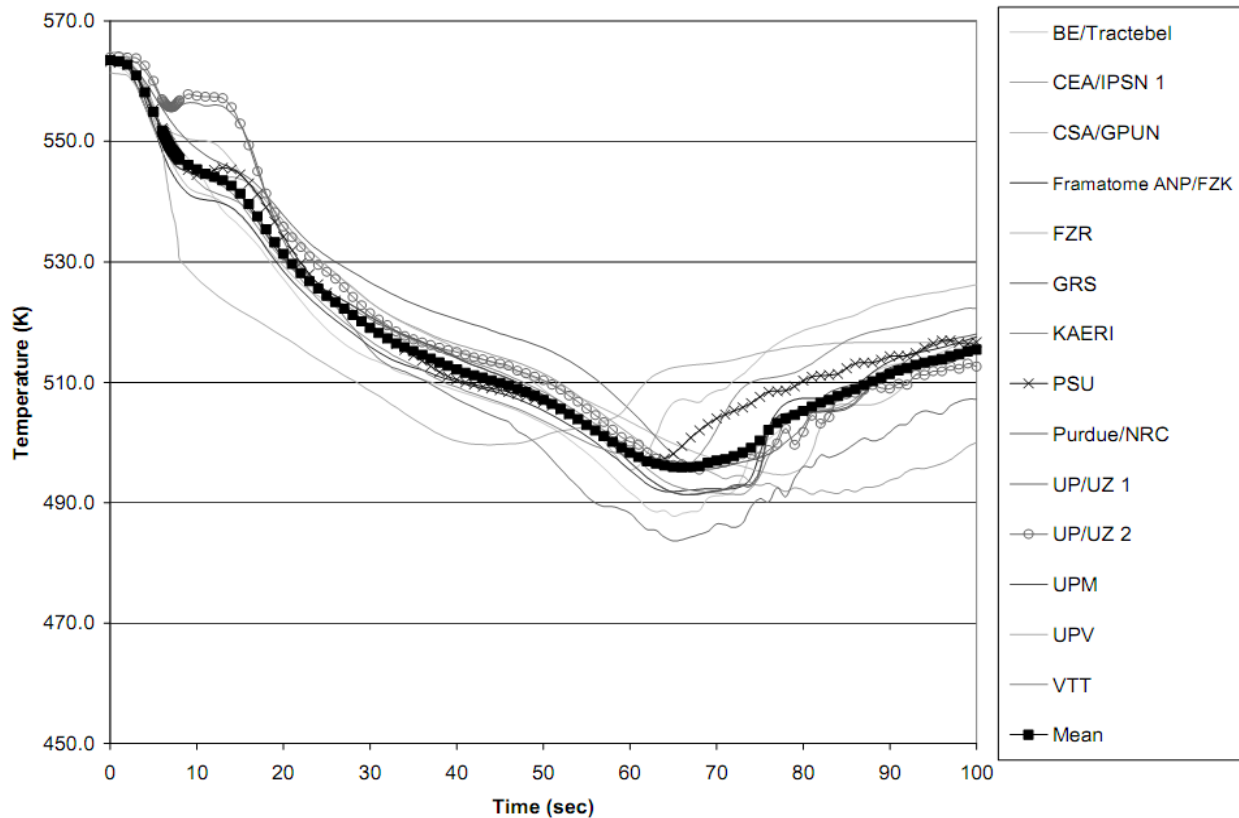


**Figure 3-15. Code-to-code comparison for the broken cold leg temperature for BE scenario [90]**

### 3.3.4 TRAC-PF1/NEM [94]

In this research activity, Todorova and Ivanov [94] have performed a sensitivity analysis of the coupled code TRAC-PF1/NEM results to the spatial mesh overlays used for modeling a PWR rod ejection accident (REA).

#### *Rod ejection accident*

REA simulations were based on TMI-1 REA Benchmark [95]. The postulated REA event assumes physical failure of a control rod drive mechanism housing such that the reactor coolant system pressure ejects the control rod (CR) assembly to a fully withdrawn position. As a consequence of the mechanical failure there is a rapid positive reactivity insertion that results in a core power excursion with a large localized power increase. If the reactivity insertion is large enough, the reactor may momentarily achieve prompt criticality, which may in turn lead to localized Departure from Nucleate Boiling (DNB) and fuel rod damage.

It is assumed that the highest worth CR is originally inserted 100% into the core and the ejection begins at time zero of the transient with constant rate of 2380.8 cm/s. No scram is simulated to permit a better understanding of the feedback effects, and two core initial conditions are evaluated: hot zero power (HZP) and hot full power (HFP).

### Coupling approach and results

NEM was integrated as a subroutine into TRAC-PF1. At the beginning of a time step, TRAC-PF1 first performed its prepass stage, where fluid-state dependent material properties and heat transfer coefficients were calculated based on T-H conditions at the end of the previous time step. In the outer iteration stage, the multidimensional fluid-dynamics equations were solved using the previous time-step fuel-rod heat fluxes. The 3D transient NEM model calculated the present time step nodal power distribution using cross section-dependent feedback parameters based on present fluid conditions and previous time-step fuel-rod temperatures. Finally, in the postpass stage, the new nodal power distribution was used in the numerical solution of the heat-conduction equations. Three different models for the core have been developed to analyze the effect of the spatial noding and coupling schemes:

- a) a cylindrical geometry with 18 radial T-H cells and 6 axial layers, as well as for the heat structure nodalization;
- b) a cylindrical geometry model with a more detailed heat structure nodalization, 67 fuel rods radially; in the quadrant where the ejected rod (N12 cell in Figure 3-16) was located each assembly was neutronics node coupled to separate fuel rod;
- c) a very detailed Cartesian nodalization: 241 T-H radial cells (including 64 reflector cells) and 26 layers axially; here each neutronics node was coupled to a different T-H cell in both radial and axial directions; the heat-structure model had 177 rods corresponding to the number of fuel assemblies in the core.

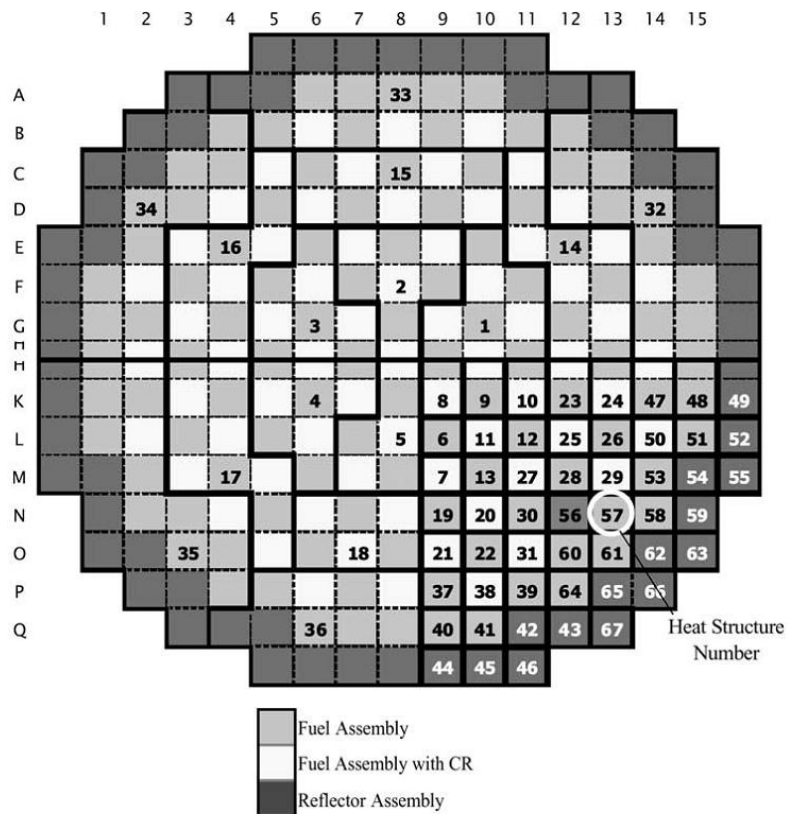


Figure 3-16. Radial thermal-hydraulic/heat structure coupling scheme for TRAC-PF1/NEM core model with 67 rods [94]

It is worth to notice that a coarse cylindrical nodalization (like that of model a) ) leads to two approximations: first, several neutronics nodes are mapped to a T–H cell in both radial and axial directions, second, the neutronics nodes are not mapped to the T–H cells exactly because of the difference in the geometry models.

The behavior of the three models was compared in four core conditions – at beginning of cycle (BOC) and at end of cycle (EOC), at hot zero power (HZP) and at hot full power (HFP) conditions. After specifying the initial conditions (see Todorova and Ivanov [94]) both steady-state and transient calculations have been performed using the three different meshes described above.

The obtained results for  $k_{eff}$  and subsequently the evaluated static control rod worth (RW) for the ejected rod at position N12 have been compared in Table 3-3. While predicted RW values for HZP cases with different models at REA are in good agreement (the difference is below 1%), for the HFP case using the detail Cartesian T–H model results in much higher RW deviations (above 30%). The total power evolution predicted for HFP at EOC (see Figure 3-17) has shown, unlike the HZP simulation, significant differences between the 3 models from the very beginning of the transient, because, at the initial steady state, the thermal-hydraulic feedback has spatial dependence. As it can be seen in Figure 3-17, the bounding result comes from the detailed 3D Cartesian model.

**Table 3-3. Comparison of the ejected rod worth predicted by the three models [94]**

Model	Cylindrical 18 rods		Cylindrical 67 rods		Cartesian	
	$\Delta k/k$ (%)	Rod worth (\$)	$\Delta k/k$ (%)	Rod worth (\$)	$\Delta k/k$ (%)	Rod worth (\$)
HZP BOC	0.4953	0.7832	0.4914	0.7771	0.4913	0.7770
HFP BOC	0.2475	0.3914	0.2456	0.3884	0.3411	0.5395
HZP EOC	0.3573	0.6856	0.3533	0.6780	0.3572	0.6855
HFP EOC	0.1157	0.1830	0.1069	0.1690	0.1719	0.2718

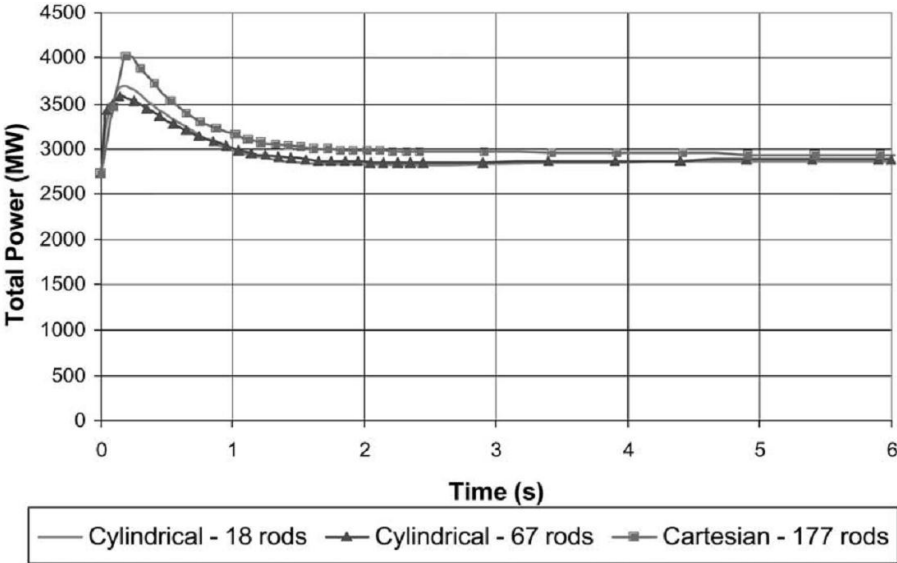


**Figure 3-17. Power evolution during REA transient for HFP at EOC predicted by TRAC-PF1/NEM [94]**

Hereafter, the software platforms adopted in the framework of the Final Safety Analysis Report of Atucha II NPP [98] by GRNSPG/UNIPI are mentioned. The platform is a coupling technique that involves different specialized codes able to solve parts of a complex problem and to exchange data with the other codes involved in the analysis.

The platforms were developed for coupling:

- HELIOS-NESTLE for the two-groups homogenized cross section libraries derivation and for the reactor core steady-states and transients simulations;
- CFX for the calculation of the boron distribution during boron injection into the moderator as input for the NK analysis;
- RELAP5/3D for the calculation of the fluid temperatures in the downcomer to be used as input for the ANSYS FE code for structural mechanics analysis during PTS scenarios;
- RELAP5/3D for calculating the boundary conditions for a more detailed analysis of the fluid temperature distribution in the downcomer by means of the CFX code to be transferred to ANSYS FE code for PTS analysis.

An exhaustive description of the platforms can be found in [104].

### **3.3.5 HELIOS-NESTLE**

A procedure was developed by GRNSPG/UNIPI for the coupling of the HELIOS lattice physics code [99] with the NESTLE [100] three dimensional neutron kinetic code.

HELIOS is a generalized-geometry lattice physics code capable of analyzing nuclear fuel designs for hexagonal VVER reactors, non-LWR lattices (CANDU, PHWR, Magnox, RBMK), and experimental reactor designs (like MTR and TRIGA).

The coupling is a off-line type coupling, i.e., results of HELIOS code calculations (the two group homogenized cross section libraries) are implemented into the NESTLE code via the NESTLE input deck. Then the NESTLE code is run for steady-state and transients simulations.

#### ***HELIOS Cross Section Libraries Structure***

The HELIOS Cross Section Libraries for the Atucha-2 core at Equilibrium Burn-up (BEQ) are contained in 5 different ASCII files, one for the unrodded libraries and the remaining four for the rodded libraries. Each library is composed by 780 different compositions, representing the burnup distribution for each of the 4510 neutronic node in which the core was discretized. More information about the HELIOS libraries and the procedure for cross section derivation can be found in [101].

#### ***The Coupling Routine***

Cross Section libraries are implemented into the NESTLE code input deck by the “ATUCHACROSS v.8” code, a software developed by the GRSNGP/UNIPI. The program is written in FORTRAN90 language, using IMSL libraries for mathematical routines and flexible

memory allocation. The user has to set-up via a on-the-screen procedure the dimensions of the cross section libraries being read and interpolated.

The main functions of the code are:

- setting up of dynamic arrays;
- read the 5 HELIOS cross section libraries and store it into the dynamic arrays;
- read the auxiliary files for the rodded cross sections “correction” (see [102]);
- set-up of the physical parameter values for the interpolation;
- perform the interpolation;
- print the results on dedicated ASCII files, performing the “corrections” for the reference and the cross section variation coefficients parameters;
- print on the screen the process status.

### 3.3.6 CFX – Relap5/3D (Nestle)

A procedure was developed by UNIPI for coupling the CFD analysis of boron injection into the moderator with the Neutron Kinetics analysis (both 1D and 3D). NESTLE code was embedded as a sub-routine in the RELAP5/3D© system code.

The procedure consisted of the following steps:

1. Data extraction from CFD results. The boron concentration calculated with CFD, for several selected instants and for each control volume of the computational grid, is extracted onto text files in table format;
2. CFD data processing. Special routines read and process the above results. Given a particular discretization of the moderator domain into “macro-cells” (i.e. the 3D-NK mesh), the routines calculate at each instant the mass of boron contained in each macro-cell, and output the related boron mass time history.

Further details on the two steps above are provided in the following.

#### *Step 1: data extraction from CFD results*

The first step is easily achieved with the GUI of CFX-Post [103], with the help of some user-defined Power Syntax routines (i.e. routines written in a special language which is based on Perl language and is directly interpreted by CFX-Post).

First of all an ASCII file is generated which contains the coordinates of the centroid of each control volume (CV) of the CFD model, and the corresponding volume. Secondly, an ASCII file with CFD results is generated for each selected instant. Such a file contains the values of the mixing scalar MS (i.e. the normalized boron concentration), of the fluid temperature and, optionally, of the fluid density, for each control volume (see Figure 3-18).



```

1
2 [Name]
3 Moderator
4
5 [Data]
6 MS.Temperature [ K ],Density [ kg m^-3 ]
7 0.0000e+00,4.4078e+02,9.9801e+02
8 0.0000e+00,4.2781e+02,1.0125e+03
9 1.4435e-20,4.4078e+02,9.9800e+02
10 0.0000e+00,4.4441e+02,9.9380e+02
11 0.0000e+00,4.4292e+02,9.9553e+02
12 0.0000e+00,4.4078e+02,9.9800e+02
13 0.0000e+00,4.4281e+02,9.9565e+02
14 0.0000e+00,4.4078e+02,9.9800e+02
15 0.0000e+00,4.4078e+02,9.9800e+02
16 0.0000e+00,4.4354e+02,9.9481e+02
17 0.0000e+00,4.4078e+02,9.9800e+02
18 0.0000e+00,4.4413e+02,9.9412e+02
19 4.7149e-27,4.4078e+02,9.9800e+02
20 0.0000e+00,4.4423e+02,9.9401e+02
21 1.2257e-24,4.4078e+02,9.9800e+02
22 0.0000e+00,4.4380e+02,9.9450e+02
23 4.2222e-30,4.4078e+02,9.9801e+02

```

---

```

1600121 1.0000e+00,3.0315e+02,1.1048e+03
1600122 1.0000e+00,3.0315e+02,1.1048e+03
1600123 1.0000e+00,3.0315e+02,1.1048e+03
1600124 1.0000e+00,3.0315e+02,1.1048e+03
1600125 1.0000e+00,3.0315e+02,1.1048e+03
1600126 1.0000e+00,3.0315e+02,1.1048e+03
1600127 1.0000e+00,3.0315e+02,1.1048e+03
1600128 1.0000e+00,3.0315e+02,1.1048e+03
1600129 1.0000e+00,3.0315e+02,1.1048e+03
1600130 1.0000e+00,3.0315e+02,1.1048e+03
1600131

```

Figure 3-18. Text file containing CFD results for a given instant [104]

### Step 2: CFD data processing

The CFD data processing is performed by means of Visual Basic 6.0 routine developed on purpose. The front-end graphical user interfaces (GUIs) of a routine is shown in Figure 3-19.

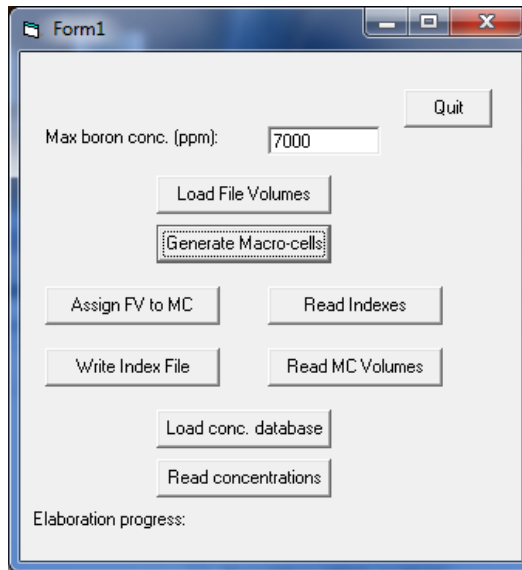


Figure 3-19. GUI of the VB routine [104]

The routine performs the following operations:

1. Reading the ASCII file with information on CVs
2. Generating the MCs  
The macro-cells (MC) that define the NK discretization are generated by a subroutine, based on algebraic criteria. The total “gross” volume of MCs and the number of MCs are output.
3. Assigning each CV to the NK macro-cell to which it belongs  
When the button “Assign CV to MC” is pushed, a subroutine scans all CVs and assign

them to the MCs. A matrix is filled containing the identification number of the macro-cell (MC) to which each CV belongs. Its content can also be written on an ASCII file.

4. Reading indexes

If necessary, the index file written in the previous step is read, in order to fill a matrix containing the identification number of the macro-cell to which each CV belongs.

5. Reading the MC volumes

6. Loading the database of CFD results

An ASCII file, properly filled by the user, and containing a list of transient result files to be read, is loaded.

7. Reading CFD results

This is the most time consuming operation (up to several hours, depending on the number of transient result files to be read). A subroutine scans the i-th file and performs the necessary data processing before jumping to the next file. So, after reading each file, the routine calculates the mass of boron in each CV (as the product of the boron mass concentration times the fluid mass contained in the CV, which in turn is obtained from volume times local density), then sums up all the contributions over each MC, using for this purposes the matrix of indexes previously defined.

8. Writing results

The time history of the boron mass calculated for each MC is written onto an ASCII file (see Figure 3-20), in which each line corresponds to a MC and each column to a time value.

1 Mass of boron contained in each of 7140 macro-cells											
2 Maximum boron concentration = 7000 ppm											
3 Time values in the first row											
4	1.5	1.505	1.51	1.515	1.52	1.525	1.53	1.535	1.54	1.545	1.5
5	0	0	0	0	0	0	0	0	0	0	0
6	0	0	0	0	0	0	0	0	0	0	0
7	0	0	0	0	0	0	0	0	0	0	0
8	0	0	0	0	0	0	0	0	0	0	0
9	0	0	0	0	0	0	0	0	0	0	0
10	0	0	0	0	0	0	0	0	0	0	0
11	0	0	0	0	0	0	0	0	0	0	0
12	0	0	0	0	0	0	0	0	0	0	0
13	0	0	0	0	0	0	0	0	0	0	0
14	0	0	0	0	0	0	0	0	0	0	0
15	0	0	0	0	0	0	0	0	0	0	0
16	0	0	0	0	0	0	0	0	0	0	0
17	0	0	0	0	0	0	0	0	0	0	0
18	0	0	0	0	0	0	0	0	0	0	0
19	0	0	0	0	0	0	0	0	0	0	0
20	0	0	0	0	0	0	0	0	0	0	0
21	0	0	0	0	0	0	0	0	0	0	0
22	0	0	0	0	0	0	0	0	0	0	0
23	0	0	0	0	0	0	0	0	0	0	0
-----											
7124	7.07288085124178E-20		7.6082649743573E-20		8.17999041452662E-20		8.79026945274883E-20				
7125	1.92020306158828E-19		2.06426521741483E-19		2.21792664837151E-19		2.38196971926847E-19				
7126	5.51573922625552E-20		5.94708692491866E-20		6.4089562447354E-20		6.90357194781979E-20				
7127	2.83574696646558E-21		3.04866587216251E-21		3.27619071501761E-21		3.51908703781613E-21				
7128	1.06390755303336E-22		1.15655404460143E-22		1.25669730867891E-22		1.36494534870105E-22				
7129	3.79440691048427E-24		4.12658664845723E-24		4.48571456237718E-24		4.87401681390526E-24				
7130	1.82714512979468E-21		1.9676262385411E-21		2.1178616800825E-21		2.27849382544921E-21				
7131	1.61341799099431E-19		1.72636034196789E-19		1.84630178841396E-19		1.97370521272941E-19				
7132	1.73505796699364E-18		1.85539657558154E-18		1.98310894816492E-18		2.11863413572078E-18				
7133	1.6396301234257E-17		1.74477314731141E-17		1.85578664890347E-17		1.97309107394699E-17				
7134	4.14663629405943E-18		4.42602770029435E-18		4.72200283631749E-18		5.03523570082245E-18				
7135	1.21298836183874E-20		1.31282672796207E-20		1.420085850184E-20		1.53521928914742E-20				
7136	0	0	0	0	0	0	0	0	0	0	0
7137	1.13607105064228E-21		1.22525352576002E-21		1.32087559358844E-21		1.42331477094839E-21				
7138	2.70025161771015E-24		2.93278007195604E-24		3.18401397002088E-24		3.45527318601756E-24				
7139	4.90699853341371E-24		5.35958468268018E-24		5.85125642066704E-24		6.38505936706172E-24				
7140	2.73999937879902E-25		2.98358660803707E-25		3.24701645095694E-25		3.53185313558809E-25				
7141	1.03129946628436E-21		1.11702612928461E-21		1.20922688330655E-21		1.30833505280801E-21				
7142	2.34601368440431E-19		2.51474340978521E-19		2.69430685561305E-19		2.88528866936846E-19				
7143	4.17440378785772E-20		4.47511952817292E-20		4.79526732504042E-20		5.13604559820497E-20				
7144	0	0	0	0	0	0	0	0	0	0	0
7145	0	0	0	0	0	0	0	0	0	0	0

Figure 3-20. Output file from CFD data processing, containing time history of boron mass in each macro-cell [104]

The final text file (boron mass in macro-cells) can either be directly used for the definition of neutron absorption cross section in setting up 3D NK analyses, or be further processed to calculate the boron mass or the boron average concentration over collapsed regions.

In any case, the described procedure allows only a one-way, external coupling, since the data transfer is from CFD to NK (and not viceversa), and is not made automatically during the parallel execution of both CFD and NK analyses, but rather it is made off-line after the completion of CFD calculations.

### 3.3.7 Relap5/3D – ANSYS

The platform described hereafter is based on a one-way coupling between the system thermal hydraulic code RELAP5/3D and ANSYS Finite Element (FE) code. It has been set-up for the Pressurized Thermal Shock (PTS) analysis, as it is a multidisciplinary field involving the thermal hydraulic, the structural mechanics and the fracture mechanics. Its aim is to evaluate the Reactor Pressure Vessel (RPV) material behavior under the pressure and thermal loads generated by a PTS scenario. RELAP5/3D calculates the fluid-wall heat transfer coefficient, the fluid temperature and pressure time trend on the inner RPV surface wall during the transient evolution. Then, these variables become the boundary conditions for the ANSYS simulation that gives as result the stress profile in the RPV inner wall.

An additional coordinate system in the multi-D component, compatible with FE model has also been implemented. This step was needed to transfer the data calculated in each point by RELAP5/3-D to the correspondent point of the FE model. Since the number of nodes in the FE model was lower than the nodes in RELAP5/3D multi-D component, a subroutine was also developed to transfer the RELAP/3D nodes temperature to the FE model nodes on the basis of the 4 closest nodes of the multi-D component (see Figure 3-21). It calculated the temperature to be assigned to FE mesh node using a weighted means of distances between nodes. In Figure 3-22 an example of the result of such subroutine is shown.

An exhaustive description of the coupling can be found in [104].

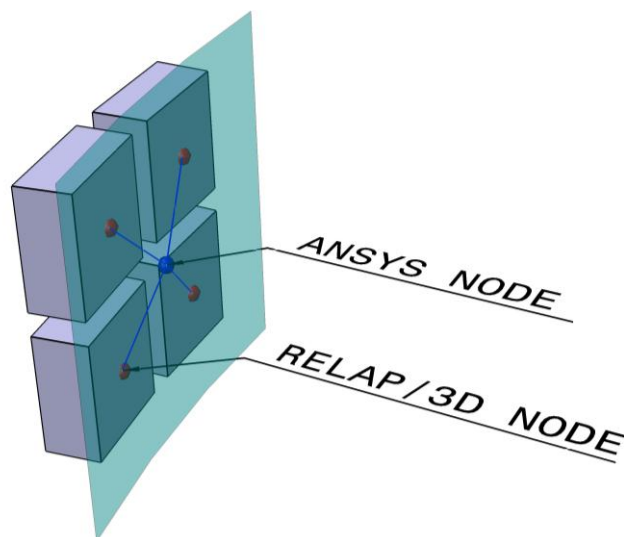


Figure 3-21. RELAP/3D to ANSYS temperature transfer [104]

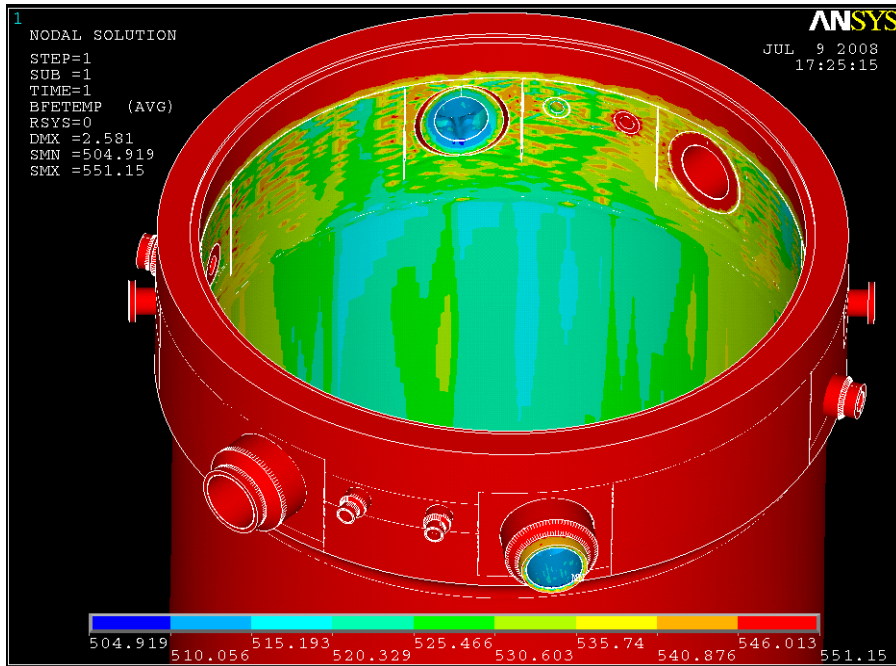


Figure 3-22. Temperature transfer in FE model [104]

### 3.3.8 Relap5/3D – CFX – Ansys

In this paragraph a more sophisticated coupling technique adopted for PTS analysis involving a system code such as RELAP5/3D, a CFD and a Structural Mechanics code such as ANSYS FE is mentioned.

In this case, Relap5/3D calculated the following parameters needed for the CFX calculation:

1. mass flow rates in both CL1 and CL2 taken before the emergency point injection;
2. fluid temperatures in both CL1 and CL2 measured before the emergency injection point;
3. emergency mass flow rates in both CL1 and CL2 and in the two injection points in the down-comer;
4. emergency fluid temperatures (measured in the same positions as in item 3).

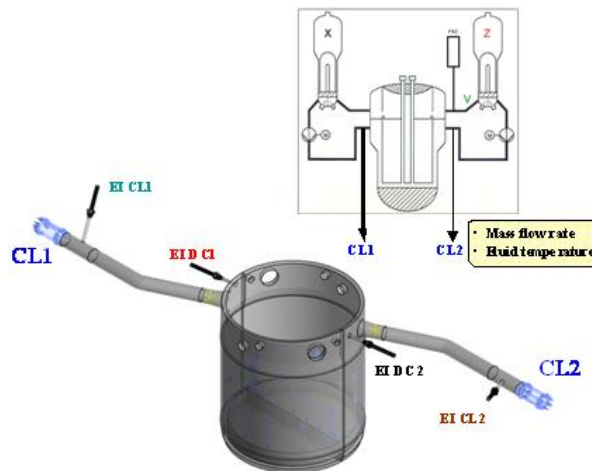
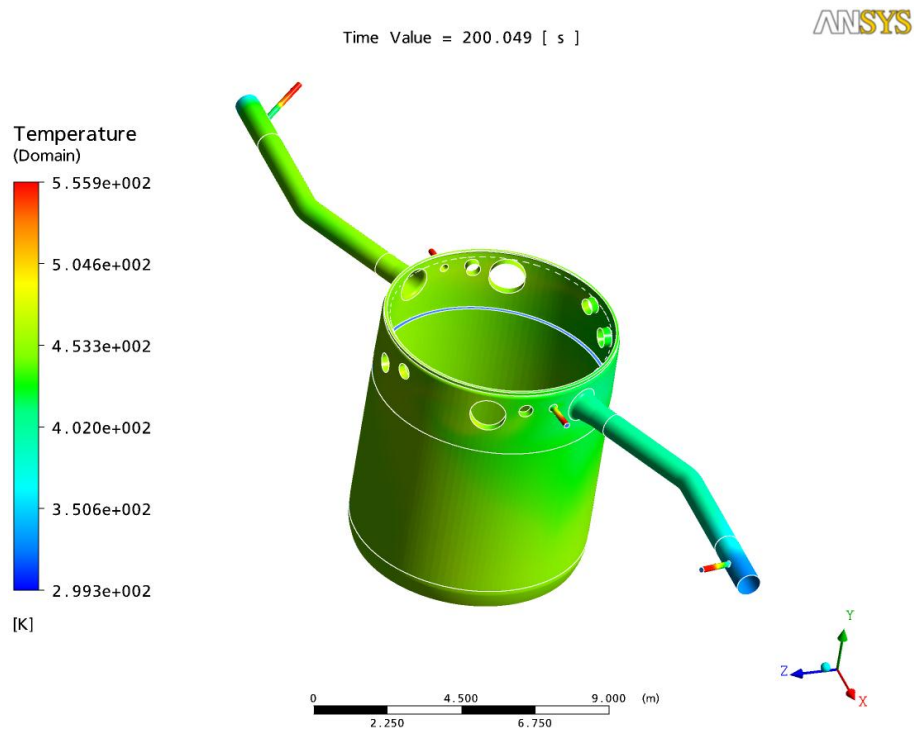


Figure 3-23. RELAP5/3D - CFX coupling technique [104]

Next, these parameters were taken and transferred to the CFX model. By adopting this approach, it was possible to simulate with CFX the mixing phenomena occurring when the emergency cold water was injected in both CL and down-comer.

Finally, from the CFX calculations, the time trend of the fluid temperature in the nodes at the interface RPV wall-downcomer, and from RELAP/3D-Dynetz calculation, the pressure acting on the internal RPV wall, were exported as boundary condition for the structural mechanics analysis by means of Ansys.



**Figure 3-24. Temperature distribution at the wall-fluid interface at t = 200 s [104]**

### 3.3.9 Relap5/3D – TRANSURANUS

TRANSURANUS [105] is a computer program for the thermal and mechanical analysis of fuel rods in nuclear reactors. It was developed at the Institute for Transuranium Elements (ITU). The TRANSURANUS code consists of a clearly defined mechanical–mathematical framework into which physical models can easily be incorporated. The mechanical–mathematical concept consists of a superposition of a one-dimensional radial and axial description (the so called quasi two-dimensional or 1 ½ D model), the code was specifically designed for the analysis of a whole rod. TRANSURANUS code incorporates physical models of thermal and radiation densification of the fuel, models of fuel swelling, fuel cracking and relocation, a model of generation of fission gases, a model of redistribution of oxygen and plutonium, and some other physical models.

TRANSURANUS can be used in connection with other codes, with the aim of investigating the behavior of the fuel and evaluating the performance.

### *Procedure for safety analysis*

The results from the T-H coupled 3D-NK calculations, are used to provide the boundary and initial conditions for the analysis performed by fuel behavior codes such as TRANSURANUS code. A “transferring map” is usually necessary to provide the correspondences among the NPP core configuration, the TH and the NK representations.

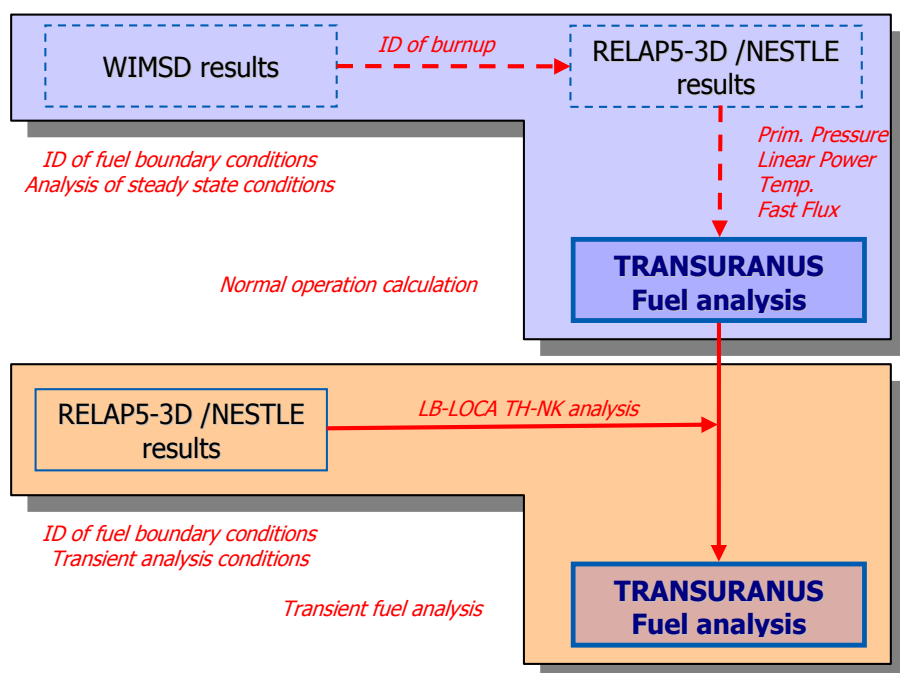
The fuel analysis requires two separate calculation steps performed by the code fuel behavior code and the T-H-3DNK coupled nodalization, see

Figure 3-25 as an example. The interface software utilized for actuating the sketch in this figure constitutes the “platform Relap5/3D – TRANSURANUS” adopted for the analysis of the Chapter 15 of the FSAR of Atucha-II NPP [98]. The first step aims at the evaluation of the initial conditions of the fuel rods at beginning of the LB-LOCA, whereas the second step calculations simulate the transient (blue and orange boxes of

Figure 3-25, respectively). Each step implies the execution of 451 calculations or 451 multiplied by the number of the radial power peaking factors available from the NK analysis (4 for the current example).

The methodology was developed at the GRNSPG and applied for the analysis of the fuel behavior during accident conditions such as LOCA and RIA to the licensing of Atucha-II NPP in construction in Argentina (FSAR Chapter 15 “Accident Analysis”).

It should be finally highlighted the importance of the validation activities of the code and the coupling against experimental data available, to prove its capabilities and to evaluate the reliability of the results.



**Figure 3-25. Roadmap of code connections for the TRANSURANUS code [106]**

### ***Assumed Initial and Boundary Conditions***

The boundary conditions required for the fuel performance analyses for each individual channel are:

- the channel pressure;
- the linear heat rate;
- the fast neutron flux;
- the cladding temperature.

The values of the boundary conditions assumed in the fuel performance calculations are the results of the T-H-coupled NK analysis. Several analyses [106] were performed using the coupled nodalization.

### ***MATLAB transfer program***

The number of cases to be analyzed and the variety of the boundary conditions needed for the analysis calls for the use of programs to perform the analysis and post-processing the results. The boundary conditions for the fuel analysis are extracted from the T-H-3DNK analysis and implemented in the TRANSURANUS MACRO part for the subsequent run with the aid of “ad hoc” written MATLAB scripts. The boundary conditions selected for the fuel analysis to be implemented in the MACRO part of the input are:

- linear heat rate;
- fast neutron flux;
- rod surface temperature;
- pressure.

### ***Code interactions***

RELAP5-3D© provides:

- o power in [W], for 451 hydraulic channels, 10 axial positions;
- o fast neutron flux [ $n/m^2s$ ], for 451 hydraulic channels, 10 axial positions;
- o cladding temperature in [K], for 280 hydraulic channels, 10 axial positions;
- o pressure in [Pa]; for 280 hydraulic channels, 1 axial positions.

The information needed as input in the TRANSURANUS MACRO part are:

- linear heat rate;
- fast neutron flux;
- cladding temperature;
- pressure.





## 4. Concluding remarks

The current report provides a review on the state-of-the-art of the most important codes used for the safety analysis of nuclear power plants.

An overall look at the proposed material suggests an increasing role of CFD techniques in providing detailed descriptions of reactor phenomena that are otherwise impossible to be achieved by system codes. Anyway it should be highlighted the qualification issue of the CFD codes and the current licensing issues, that does not envisage such approach for the safety analysis but only in support to that.

A growing tendency to couple differently scaled thermal-hydraulic codes with programs conceived for the deterministic or probabilistic analysis of neutronic behavior is a well known additional feature of ongoing developments, aiming to set up an integrated representation of interacting phenomena that can be hardly represented separately.

All these developments seem quite promising, though they are conditioned by the availability of powerful computing machines. Compromise solution are anyway proposed at an engineering level, choosing different detail in the description of different plant components, e.g., by coupling system codes and CFD codes. The development of such solutions seems to represent a field of very active research for the years to come.



## References

- [1] D'Auria F., et al. *DEGB LBLOCA (2 X 100% Break in CL) in Atucha-2 NPP*, Contract NA-SA UNIPI 01 - Atucha II, University of Pisa Report, DIMNP NT 628(08) - rev. 1, Pisa, March 2008.
- [2] <https://domino.grs.de/ecora/ecora.nsf>.
- [3] *Neutronics/Thermal-hydraulics Coupling in LWR Technology: State-of-the-art Report (REAC-SOAR)*, CRISSUE-S – WP2, OECD 2004 NEA No. 5436.
- [4] <http://www.ist-world.org/ProjectDetails.aspx?ProjectId=f0197bfd89134ed4ba4befc2aee163ad>.
- [5] <http://www.nuresim.com/www/nurisp/index.php>.
- [6] EUROFASTNET –European Project for Future Advances in Sciences and Technology for Nuclear Engineering Thermal-Hydraulics, Final Synthesis Report, 5<sup>th</sup> Framework Programme (1998-2002).
- [7] *Neutronics/Thermal-hydraulics Coupling in LWR Technology, Vol. 1*, CRISSUE-S – WP1: Data Requirements and Databases Needed for Transient Simulations and Qualification, 5<sup>th</sup> EURATOM Framework Programme (1998-2002).
- [8] *RELAP5/MOD3 Code Manual Volume I: Code structure, system models, and solution methods*. Thermal Hydraulics Group, Idaho, June 1995.
- [9] *RELAP5/MOD3.3 Code Manual, Volume VI: Validation of Numerical Techniques in RELAP5/MOD3.0*, Nuclear Safety Analysis Division, Information Systems Laboratories, Inc., Rockville, Maryland, Idaho Falls, Idaho, Oct. 1994 (revised version Dec. 2001).
- [10] *RELAP5/MOD3.3 Code Manual. Volume II: User's Guide and Input Requirements*, Nuclear Safety Analysis Division, Information Systems Laboratories, Inc., Rockville, Maryland, Idaho Falls, Idaho, Dec. 2001.
- [11] *RELAP5/MOD3.3 Code Manual. Volume V: User's Guidelines*, Nuclear Safety Analysis Division, Information Systems Laboratories, Inc., Rockville, Maryland, Idaho Falls, Idaho, Dec. 2001.
- [12] *TRACE V5.0 Theory Manuals - Field Equations, Solution Methods, and Physical Models*. U.S. Nuclear Regulatory Commission, October 2008.
- [13] *ATHLET Mod 1.2 Cycle A, User's Manual*, Lerchl, G., H. Austregesilo, Gesellschaft für Anlagen und Reaktorsicherheit (GRS) mbH, GRS-P-1/Vol. 1, Rev.1, March 1998.
- [14] *ATHLET Mod 2.2 Cycle A, Program Overview*, Gesellschaft für Anlagen und Reaktorsicherheit (GRS) mbH, July 2009.

- [15] Bestion, D. and G. Geffraye, “*The CATHARE Code*”, in Operational Practice of Nuclear Power Plants of University of Budapest, CEA Report DTP/SMTHL/LMDS/EM/2001-063, Grenoble, France, April 2002.
- [16] E. Coscarelli - *Lecture [03a] FONESYS: MOTIVATION AND OBJECTIVES*, Seminar on: Advanced Modelling and Numerical Strategies for Two-Phase Flow in Nuclear Systems San Piero a Grado Nuclear Research Group (GRSNPG), 5-7 July, 2011, Pisa, Italy.
- [17] *CSNI Integral Test Facility Matrix for the Assessment of Thermal-hydraulic Codes for LWR LOCA and Transients*, NEA/CSNI/R(96)17, July 1996.
- [18] *Separate Effects Test Matrix for Thermal-hydraulic Code Validation*, Volume I, NEA/CSNI/R(93)14/Part.1/Rev., Volume II, NEA/CSNI/R(93)14/Part.2/Rev., Sept. 1993.
- [19] V. H. Ransom and D. L. Hicks, “*Hyperbolic Two-Pressure Models for Two-Phase Flow*,” *Journal of Computational Physics*, 53, 1984, pp. 124-151.
- [20] V. H. Ransom and M. P. Scofield, *Two-Pressure Hydrodynamic Model for Two-Phase Separate Flow*, INEL Report SRD-50-76, 1976.
- [21] P. S. Anderson, P. Astrup, L. Eget, and O. Rathman, “*Numerical Experience with the Two Fluid Model RISQUE*,” Proceedings from Topical Meeting on Thermal Reactor Safety, Sun Valley, ID, July 31-August 4, 1977.
- [22] K. T. Chaxton, J. G. Collier, and J. A. Ward, *H.T.F.S. Correlation for Two-Phase Pressure Drop and Void Fraction in Tubes*, AERE-R7162, 1972.
- [23] D. Chisholm, “*A Theoretical Basis for the Lockhart-Martinelli Correlation for Two-Phase Flow*,” *Journal of Heat-Mass Transfer*, 10, 1967, pp. 1767-1778.
- [24] J. C. Chen, “*A Correlation for Boiling Heat Transfer to Saturated Fluids in Convective Flow*,” *Process Design and Development*, 5, 1966, pp. 322-327.
- [25] J. C. Chen, R. K. Sundaram, and F. T. Ozkaynak, *A Phenomenological Correlation for Post-CHF Heat Transfer*, NUREG-0237, June 1977.
- [26] L. A. Bromley, “*Heat Transfer in Stable Film Boiling*,” *Chemical Engineering Progress*, 46, 1950, pp. 221-227.
- [27] F. W. Dittus and L. M. K. Boelter, “*Heat Transfer in Automobile Radiators of the Tubular Type*,” *Publications in Engineering*, 2, University of California, Berkeley, 1930, pp. 443-461.
- [28] W. M. Kays, “*Numerical Solution for Laminar Flow Heat Transfer in Circular Tubes*,” *Transactions, American Society of Mechanical Engineers*, 77, 1955, pp. 1265-1274.
- [29] S. W. Churchill and H. H. S. Chu, “*Correlating Equations for Laminar and Turbulent Free Convection From a Vertical Plate*,” *International Journal of Heat and Mass Transfer*, 18, 1975, pp. 1323-1329.

- [30] W. Ambrosini, *PHYSICAL MODELS IN THE RELAP5 CODE Part B – Closure relationships and other models*, Seminar and Training on scaling uncertainty and 3D coupled calculations in nuclear technology, 18 October - 5 November, 2010 – Petten, The Netherlands.
- [31] MARS *Input Manual* – KAERI/TR-2812/2004.
- [32] MARS – KAERI/TR-3042/2005.
- [33] M.J.Thurgood et al., *COBRA/TRAC - A Thermal-Hydraulics Code for Transient Analysis of Nuclear Reactor Vessels and Primary Coolant Systems Volume 1*, NUREG/CR-3046 PNL-4385, March 1983.
- [34] M. Cherubini, F. Moretti, F. D’Auria “*Independent Assessment of Multidimensional Features of the MARS Code*” KINS/RR-669, RETAS-MARS-CA-03, February 2009.
- [35] M. Cherubini, W. Giannotti, F. D’Auria “*Independent Assessment of Multidimensional Features of the MARS Code: PSB-VVER 11% UP break experiment*” KINS/RR-732, RETAS-MARS-CA-04, March 2010.
- [36] Farshad Faghihi, H. Khalafi, and S. M. Mirvakili, *A Literature Survey of Neutronics and Thermal-Hydraulics Codes for Investigating Reactor Core Parameters; Artificial Neural Networks as the VVER-1000 Core Predictor*, 2011.
- [37] Bjorn Becker, Ecole Nationale Supérieure de Physique de Grenoble ENSPG, *Investigations of COBRA-EN and COBRA-TF for core and assembly simulations and coupling of COBRA-TF and KARBUS*, FZKA Technical Report, 2005.
- [38] D. Basile, R. Chierici, M. Beghi, E. Salina and E. Brega: *COBRA-EN, an Updated Version of the COBRA-3C/MIT Code for Thermal-Hydraulic Transient Analysis of Light Water Reactor Fuel Assemblies and Cores*, Report 1010/1, ENEL-CRTN. Milano.
- [39] NEA Data Bank. <http://www.oecd-nea.org/tools/abstract/detail/nea-1614>.
- [40] NEA, Technical Review. *Nuclear Fuel Safety Criteria*, OECD Publishing, 2001.
- [41] EPRI NP-2511-CCM, Volume 1, Revision2; RP-1584-1: Computer Code Manual July 1985; “*VIPRE01: A Thermal-Hydraulic Code for Reactor Cores, Volume 1: Mathematical models*”.
- [42] Sung Y.X. et al., *Westinghouse VIPRE-01 Applications for PWR Core Analyses*, NURETH-9, San Francisco, California, U.S.A., October 1999.
- [43] Y. X. Sung, P. Schueren and A. Meliksetian, *VIPRE-01 Modeling and Qualification for Pressurized Water Reactor Non-LOCA Thermal-Hydraulic Safety Analysis*, WCAP-15306-NP-A, Westinghouse Electric Company LLC (1999).
- [44] M. Glück, “*Validation of the sub-channel code F-COBRA-TF: Part II. Recalculation of void measurements,*” Nucl. Eng. Des., 238, 9, pp. 2317-2327 (2008).

- [45] J. M. Le Corre, C. Adamsson and P. Alvarez, *Transient void, pressure drop and critical power BFBT Benchmark analysis and results with VIPRE-W / MEFISTO-T*. NURETH14. Toronto, Ontario, Canada, September 25-30, 2011.
- [46] Carl Adamsson and Jean-Marie Le Corre, *VIPRE-W / MEFISTO-T – A mechanistic tool for transient prediction of dryout in BWR fuel*. NURETH-14. Toronto, Ontario, Canada, September 25-30, 2011.
- [47] R. T. Lahey and F. J. Moody, *The Thermal-hydraulics of a Boiling Water Nuclear Reactor*. American Nuclear Society, 1993.
- [48] P. Fillion, A. Chanoine, S. Dellacherie, and A. Kumbaro, “*FLICA-OVAP: a New Platform for Core Thermal-hydraulic Studies*,” in Proceedings of NURETH-13, Kanazawa, Japan, Sep. 26 - Oct. 2 (2009).
- [49] Philippe Fillion and Matteo Bucci, *Analysis of the NUPEC PSBT Tests with FLICA-OVAP. Part 1: Void distribution Benchmark*, NURETH-14. Toronto, Ontario, Canada, September 25-30, 2011.
- [50] E. Royer, S. Aniel, A. Bergeron, P. Fillion, D. Gallo, F. Gaudier, O. Grégoire, M. Martin, E. Richebois, P. Salvadore, S. Zimmer, T. Chataing, P. Clément, and F. François, “*FLICA4: Status of numerical and physical models and overview of applications*,” in Proceedings of NURETH-11, Avignon, France, October 2-6 (2005).
- [51] B. Chexal, G. Lellouche, J. Horowitz, and J. Healzer, “*A Void Fraction Correlation for Generalized Applications*,” *Progress In Nuclear Research*, 27, no. 4, pp. 255–295, (1992).
- [52] M. Ishii, “*One dimensional drift-flux model and constitutive equations for relative motion between phases in various two-phase flow*,” Tech. Rep. ANL-77-27, ANL, (1977).
- [53] W. Jens and P. Lottes, “*Analysis of heat transfer burnout, pressure drop and density data for high pressure water*,” Tech. Rep. ANL-4627, ANL, (1951).
- [54] Mahaffy J. et al., “*Best practice guidelines for the use of CFD in nuclear reactor safety applications*”, NEA/CSNI/R(2007)5, May 2007.
- [55] Smith B. et al., “*Assessment of CFD for Nuclear Reactor Safety Problems*”, NEA/CSNI/R(2007)13, January 2008.
- [56] Bestion et al., “*Extension of CFD codes to two-phase flow safety problems*”, NEA/SEN/SIN/AMA(2006)2, August 2006.
- [57] Menter F., “*CFD Best Practice Guidelines for CFD Code Validation for Reactor-Safety Applications*”, EU/FP5 ECORA Project “Evaluation of computational fluid dynamic methods for reactor safety analysis”, EVOL-ECORA-D01, Germany, February 2002.

- [58] *“Use of computational fluid dynamics codes for safety analysis of reactor systems”*, Joint IAEA/NEA technical meeting, Pisa, Italy, November 11-13, 2002, IAEA-TECDOC-1379, IAEA, Vienna, 2003.
- [59] D. Wilcox, *Turbulence Modelling for CFD*, DCW Industries, Inc., Griffin printing, California, 2000.
- [60] F. Terzuoli, *Role of CFD Analysis in Nuclear Reactor Licensing and Design*, PhD Thesis in Nuclear Engineering, Pisa, June 2011.
- [61] *ANSYS CFX Release 13.0 - User Manual*, November 2010 (embedded in the software package).
- [62] *ANSYS ICEM-CFD Release 13.0 - User Manual*, November 2010 (embedded in the software package).
- [63] *ANSYS FLUENT Release 13.0 - User Manual*, November 2010 (embedded in the software package).
- [64] [http://www.cd-adapco.com/products/star\\_ccm\\_plus/index.html](http://www.cd-adapco.com/products/star_ccm_plus/index.html).
- [65] [http://www.cd-adapco.com/products/star\\_cd/index.html](http://www.cd-adapco.com/products/star_cd/index.html).
- [66] Volkan Seker, Justin W. Thomas and Thomas J. Downar, *Reactor Physics Simulations with Coupled Monte Carlo Calculation and Computational Fluid Dynamics*, International Conference on Emerging Nuclear Energy Systems (ICENES-2007), Istanbul, TURKEY, June 3 – 8 2007.
- [67] Jin Yan, Brendan Kochunas, Mathieu Hursin, Thomas Downar, Zeses Karoutas, Emilio Baglietto, *Coupled Computational Fluid Dynamics and MOC Neutronic Simulations of Westinghouse PWR Fuel Assemblies with Grid Spacers*, NURETH-14.Toronto, Ontario, Canada, September 25-30, 2011.
- [68] Richard Schultz, *NGNP Methods: Summary of Approach and Plans*, kindly provided by Dr. Emilio Baglietto, CD-ADAPCO.
- [69] P. Muehlbauer et al., *“Review of two-phase modelling capabilities of CFD computer codes and feasibility of transient simulations”*, EVOL/ECORA/D04, February 2004.
- [70] A. Guelfi et al., *“NEPTUNE: A new software platform for advanced nuclear thermal hydraulics”*, Nuclear Science and Engineering, vol. 156, no3, pp. 281-324, 2007.
- [71] P. Coste, J. Laviéville, J. Pouvreau, C. Baudry, M. Guingo, A. Douce, *“Validation of the Large Interface Method of NEPTUNE CFD 1.0.8 for Pressurized Thermal Shock (PTS) applications”*, Nuclear Engineering and Design (2011), doi:10.1016/j.nucengdes.2011.08.066.
- [72] C. Chauliac, J.M. Aragonés, D. Bestion, D.G. Cacuci, N. Crouzet, F.P. Weiss, M.A. Zimmermann, *“NURESIM – A European simulation platform for nuclear reactor safety:*

- Multi-scale and multi-physics calculations, sensitivity and uncertainty analysis*”, Nuclear Engineering and Design 241 (2011) 3416-3426.
- [73] J. Lavieville et al., “*NEPTUNE CFD V1.0: theory manual*”, 2006.
- [74] N. Mèchitoua et al., “*An unstructured finite volume solver for two-phase water/vapour flows modelling based on elliptic oriented fractional step method*”, NURETH 10, Seoul, South Korea, 2003.
- [75] F. Archambeau, N. Mechitoua, M. Sakiz, “*Code\_Saturne: a Finite Volume Code for the Computation of Turbulent Incompressible Flows*”, International Journal on Finite Volumes, Vol. 1, 2004.
- [76] Y. Fournier, C. Vurpillot, C. Béchaud, “*Evaluation of fluid flow in the lower core of a PWR with Code Saturne*”, Nuclear Engineering and Design 237 (2007) 1729–1744.
- [77] J.M. Ndombo, R.J.A. Howard, “*Large Eddy Simulation and the effect of the turbulent inlet conditions in the mixing Tee*”, Nuclear Engineering and Design 241 (2011) 2172–2183.
- [78] <http://www.casl.gov/index.shtml>
- [79] CASL: *The Consortium for Advanced Simulation of Light Water Reactors- A DOE Energy Innovation Hub for Modeling & Simulation for Nuclear Reactors*, Enlarged Halden Program Group Meeting, Norway, October 2-7, 2011.
- [80] <http://www.salome-platform.org/>.
- [81] Grundmann, U., S. Mittag, U. Rohde, *DYN3D2000/M1 for the Calculation of Reactivity Initiated Transients in LWR with Hexagonal and Quadratic Fuel Elements, Code Manual and Input Data Description*, 3<sup>rd</sup> Edition, Research Center Rossendorf, Inc., September 2001.
- [82] Bandini, R., *A Three-dimensional Transient Neutronics Routine for the TRAC-PF1 Reactor Thermal-hydraulic Computer Code*, PhD Thesis, The Pennsylvania State University (1990).
- [83] Ivanov, K., et al., “*Nodal Kinetic Model Upgrade in The Penn State Coupled TRAC/NEM Codes*”, Annl. Nucl. Ener., 26, 1205 (1999).
- [84] Turinsky, P.J., et al., *NESTLE: A Few-group Neutron Diffusion Equation Solver Utilizing the Nodal Expansion Method for Eigenvalue, Adjoint, Fixed-source Steady State and Transient Problems*, EGG-NRE-11406, Idaho National Engineering Laboratory, June 1994.
- [85] Joo, H.G., D.A. Barber, G. Jiang and T.J. Downar, *PARCS: A Multidimensional Two-group Reactor Kinetic Code Based on the Non-linear Analytical Nodal Method*, University of Purdue Report PU/NE-98-26 (1998).
- [86] Barber, D.A., T.J. Downar and W. Wang, *Final Completion Report for the Coupled Relap5/Parcs Code*, University of Purdue Report PU/NE-98-31 (1998).



- [87] Langenbuch, S., *QUABBOX/CUBBOX-HYCA, Ein Dreidimensionales Kernmodell mit parallelen Kühlkanälen für Leichtwasser-reaktoren*, GRS-A-926, Garching, Germany (1984).
- [88] Grundmann, U., S. Kliem, D. Lucas and U. Rohde, “*Coupling of the Thermohydraulic Code ATHLET with the 3-D Neutron Kinetic Core Model DYN3D*”, Proceedings of the 6th AER Symposium on VVER Reactor Physics and Safety, pp. 179-191, Kirkkonummi, Finland (1996).
- [89] Langenbuch, S., Austregesilo, P., Fomitichenko, P., Rohde, U., Velkov, K.: *Interface Requirements to Couple Thermal-Hydraulics Codes to 3D Neutronic Code*, OCED/CSNI Workshop on Transient Thermal-hydraulics and Neutronic Codes Requirements, Annapolis, United State, 1996.
- [90] NEA/NSC/DOC(2003) 21, *PRESSURISED WATER REACTOR MAIN STEAM LINE BREAK (MSLB) BENCHMARK - Volume IV: Results of Phase III on Coupled Core-plant Transient Modelling*
- [91] Langenbuch, S, K., Velkov,,: *Capability of the coupled code system ATHLET-QUABOX/CUBBOX for safety analysis*. Gesellschaft für Anlagen- und Reaktorsicherheit (GRS) mbH.
- [92] Langenbuch, S., Velkov, K., Kliem, S., Rohde, U., Lizorkin, M., Hegyi, G., Kereszturi, A. : *Development of coupled systems of 3D neutronics and fluid-dynamic system codes and their application for safety analysis*. Gesellschaft für Anlagen- und Reaktorsicherheit (GRS) mbH.
- [93] Langenbuch, S., Velkov: *Results and experiences from the analysis of the OECD PWR MSLB and BWR TT Benchmarks by the coupled code system ATHLET-QUABOX/CUBBOX*. Gesellschaft für Anlagen- und Reaktorsicherheit (GRS) mbH.
- [94] Todorova, N., K. Ivanov, “*Investigation of spatial coupling aspects for coupled code application in PWR safety analysis*”, Annals of Nuclear Energy 30 (2003) 189–209.
- [95] Ivanov K., Watson J., Beam T., 1997. *PWR Reactivity Insertion Accident Methodology Based on TRAC-PF1/NEM, ICONES-2012*, Electronic Publication: CD-Rom.
- [96] Todorova, N., et al., *Pressurised Water Reactor Main Steam Line Break (MSLB) Benchmark. Volume 3: Results of Phase II on 3-D Core Boundary Condition Model*, OECD/NEA Nuclear Science Committee, US Nuclear Regulatory Commission, NEA/NSC/DOC(2002)12 (2002).
- [97] Sanchez-Espinoza, V. H., Hering, W., Knoll, A., Böer, R.: *Analysis of the OECD/NEA PWR Main Steam Line Break (MSLB) Benchmark Exercise 3 with the Coupled Code System RELAP5/PANBOX*, Forschungszentrum Karlsruhe, FZKA 6518.
- [98] NASA, *Final Safety Analysis Report – Chapter 15 “Accident Analysis”*, 2011.
- [99] Studsvik™ ScandPower, “*HELIOS Methods*”, 2006.
- [100] Idaho National Lab, *RELAP5-3D© Code Manual, Volume I: Code Structure*.

- [101] C. Parisi, K. Ivanov “*Atucha-2 XSec Libraries development for BEQ core*”, SIR 2.2 Report, June 2007.
- [102] C. Parisi, M. Pecchia, G. Kotev “*Autcha-2 Control Rod Modelling by NESTLE code*”, NEU E.4.1.d Report, December 2009.
- [103] F. Moretti, F. Terzuoli, D. Melideo, “*Creation of 3 CFD models of Atucha-II RPV and Execution of Steady-state calculations, Final Report of Task 3 (Agreement Atucha-II – UNUPI 01)*”, TFR-3 Rev.0, October 2007.
- [104] D. Araneo, et al. *Documentation for Platform Software Development and Qualification*. NASA-UNUPI 3<sup>rd</sup> Agreement. Task E1/Subtask E1.1.1a (E1.3) [R8].
- [105] Lassmann K., A. Schubert, P. Van Uffelen, Cs. Gyory, J. van de Laar, *Transuranus Handbook version “v1m1j06”* JRC, EC, ITU, July 2006.
- [106] M. Adorni, *Methodology for the Analysis of Fuel Behavior during LOCA and RIA*, PhD Thesis in Nuclear Engineering, Pisa, June 2011.
- [107] Adorni M., A. Del Nevo, F. D’Auria, O. Mazzantini, *A procedure to address the fuel rod failures during LB-LOCA transient in Atucha-2 NPP*, Science and Technology of Nuclear Installations, Article ID 929358, doi:10.1155/2011/929358, 2011.